BELLCOMM, INC.
1100 SEVENTEENTH STREET, N.W. WASHINGTON, D.C. 20036

COVER SHEET FOR TECHNICAL MEMORANDUM

TITLE- LM-Earth S-Band Communications for Powered Descent and Ascent Phases of the Lunar Mission

TM- 67-2013-3

DATE- May 15, 1967

FILING CASE NO(S)- 310

AUTHOR(S)- A. C. Merritt

FILING SUBJECT(S)- (ASSIGNED BY AUTHOR(S)- LM Descent and Ascent
LM Communications

LM-Earth communications cannot be maintained in a real-time, high-bit-rate mode without a period of beam interference for some of the lunar landing sites and dates now contemplated. This memorandum presents a parametric analysis of this beam interference problem and discusses the major interfaces involved. Best and worst case conditions are selected and scanned within estimated parameter limits. Variations in the lunar parking orbit plane, the lunar libration conditions, the lunar landing site location, and the LM yaw attitude were considered in the analysis.

The severity of this problem is shown to be such that in the worst case, communications could be lost more than half the time during either LM powered descent or ascent. Of the eight candidate sites for the first lunar landing, only the Sinus Medii site would be accessible without beam interference, for all landing dates.

It is shown that the most viable solution to this problem centers on re-orienting the LM in yaw attitude within landing radar constraints and/or changing the lunar parking orbit plane within SPS fuel constraints. In considering the interface with landing radar operation, a yaw solution is found possible for all of the candidate landing sites. A nonoptimal lunar orbit plane cannot be chosen in order to avoid beam interference in all cases; the SPS fuel reserve is seen to vary widely over the various launch opportunities. In addition, communications losses due to antenna gimbal stop encounter are discussed, and it is shown that for worst case conditions, the lunar surface may not be viewed from a "face-down" attitude during LM descent to landing sites east of -4° longitude, without gimbal stop encounter upon return to a "face-out" attitude.

SEE REVERSE SIDE FOR DISTRIBUTION LIST

DISTRIBUTION

COMPLETE MEMORANDUM TO

CORRESPONDENCE FILES:

OFFICIAL FILE COPY
plus one white copy for each additional case referenced

TECHNICAL LIBRARY (4)

NASA HEADQUARTERS

Messrs. R. O. Aller/MO
G. R. Blitch/MO
J. K. Holcomb/MO
T. A. Keegan/MA

MSC

Messrs. M. P. Frank/FM5
M. V. Jenkins/FM
P. Kramer/CF24
J. P. Mayer/FM
J. D. Payne/FM6
C. H. Perrine/PM
R. G. Rose/FA3
J. R. Sevier/PM3
R. J. Ward/PM2
C. F. Wasson/EG43

BTL

D. Swanay/4268

COMPLETE MEMORANDUM TO

BELLCOMM

Messrs. D. R. Anselmo
A. P. Boysen
J. O. Cappellari, Jr.
W. W. Ennis
D. R. Hagner
J. J. Hibbert
W. C. Hittinger
B. T. Howard
D. B. James
B. Kaskey
J. L. Marshall
J. Z. Menard
V. S. Mummert
I. D. Nehama
T. L. Powers
J. T. Raleigh
R. D. Raymond
I. M. Ross
J. A. Saxton
R. R. Schreib
R. L. Selden
R. V. Sperry
T. H. Thompson
R. L. Wagner
A. G. Weygand
All Members, Department 2013
Department 1023

SUBJECT: LM-Earth S-Band Communications for Powered Descent and Ascent Phases of the Lunar Mission Case 310

DATE: May 15, 1967

FROM: A. C. Merritt

TM-67-2013-3

TECHNICAL MEMORANDUM

1.0 INTRODUCTION

Experience and various planning considerations dictate the desirability of maintaining as strong a communications link as possible with Earth during LM powered descent to the lunar surface, as well as during powered ascent to a stable, pre-rendezvous orbit. For these phases of the lunar mission, the principal LM-Earth data link will be via the Unified S-Band System. The majority of the data to be transmitted to Earth will require use of the LM steerable antenna in the high-bit-rate mode. However, for some of the lunar landing sites and dates now contemplated, the LM steerable antenna cannot be directed to attain a clear line of sight to Earth without beam interference. The forward and aft RCS clusters and mounts on the right-hand-side of the LM are primarily responsible for this beam interference, for LM powered descent and ascent, respectively.

A qualitative understanding of the beam interference problem may be obtained from Figures (1) and (2). The S-Band steerable antenna elevation and azimuth angles are defined in Figure (2a). Note that antenna elevation is always measured in the LM X_B, Z_B plane; i.e., the convention for the order of rotations is elevation, then azimuth. As can be seen from Figure (1), if the antenna is oriented at a negative elevation below -30°, then looking inboard of 2° outboard will cause beam interference with the RCS clusters and possibly the ascent and descent stages. The same holds for a positive elevation beyond +210°. Figure (2b) shows the impact of both structural interference and antenna gimbal stop constraints on the available antenna angle coverage. A more detailed discussion of antenna coverage is given in Appendix C. The roll, pitch, and yaw conventions which will be used in this memorandum are also indicated on Figure (1). These definitions are pilot oriented rather than thrust axis oriented.

TELEMETRY REQUIREMENTS

In support of the assumption that LM high-bit-rate communications with Earth are considered highly desirable during descent and ascent, the following list of telemetry functions which

are available only in the high-bit-rate mode is presented: All LM guidance downlink data, all abort guidance computer downlink data, RCS command and response data, and all dynamic data from the landing radar and the rendezvous radar. (Reference 1) Lacking the above data, the ability to compare data from the MSFN, the LM guidance computer, and the abort guidance system would be lost. The total powered descent time, from initiation of Braking at 50,000 ft. lunar altitude, to the moment of touchdown, will nominally be a few seconds greater than ten minutes. This will be sufficient time to provide a limited number of real-time ground decisions concerning the state of the trajectory, subsystems, and crew. (See Reference 2) Up-link confirmation of nominal could be provided, as well as possible abort commands.

REQUIREMENTS FOR LANDING RADAR

The same unknowns concerning system performance and lunar terrain which prompt the requirement for a strong communications link also demand that a check on the estimated selenographic vehicle altitude and velocity be performed, using the landing radar system, as early in the descent trajectory as possible. Because attitude reorientation of the LM will be considered as one possible solution to the beam interference problem, it will be necessary to consider the interface between the beam interference problem and landing radar operation. If the LM should be oriented at a non-zero yaw attitude when radar data acquisition is scheduled to begin, there may be a degradation of the radar output, or loss of track on one or more beams, depending on the extent of the yaw deviation from zero. As will be shown in the subsequent sections, most combinations of mission parameters will permit a solution which satisfies both radar and communications.

1.2 QUALITATIVE ATTITUDE AND TRAJECTORY CONSIDERATIONS

Before a discussion of the parametric analysis that was performed is presented, it will be useful to define the overall beam interference problem using a qualitative approach. For this purpose, some geometry relevant to LM maneuvers during powered descent and ascent is depicted in Figure (3). The LM is shown at the start of descent to an eastern site in (a), and at the end of ascent from a western site in (b). The hypothetical case drawn has the landing site at zero latitude and the descent and ascent trajectories lying entirely within the lunar equatorial plane (270° LM landing and launch azimuths). Therefore, the plane of the paper is both the lunar equatorial plane and the plane of the LM X_B, Z_B body axes. The LM is shown at a zero yaw attitude.

As mentioned previously, beam interference will occur when the antenna azimuth is less than 2° simultaneous with the antenna elevation less than -30° (during descent) or greater than

210° (during ascent). The angle of the Earth position vector with respect to the plane of Figure (3) is equal to the lunar libration in latitude. For this hypothetical case, latitude librations less than +2° will define the Earth position vector such that beam interference will occur when the antenna elevation is less than -30° (during descent) or greater than 210° (during ascent).

Variations on the angular configuration shown in Figure (3) are of two types. First, consider angular changes within the plane of the paper. As can be seen, angular changes in the site longitude, the lunar longitude libration, the central angle between the LM and the landing site, and the LM pitch attitude all produce equivalent effects on the antenna elevation. Now consider angular changes above and below the plane of Figure (3). If the LM landing or launch azimuths are other than 270°, the LM trajectory plane will not coincide with the lunar equatorial plane (which contains the site in this example) and the LM will be either above or below the plane of Figure (3). Therefore, variations in site latitude, lunar latitude librations, and the LM trajectory plane will produce similar but non-equivalent effects on the antenna azimuth required to transmit to Earth.

YAW SOLUTION CONSIDERATIONS

The concept of a yaw solution to the S-Band beam interference problem may be explained in a qualitative manner with the aid of Figure (4). The plane of the paper in this figure is the LM Y_B, Z_B plane, and the LM is shown during powered descent. The latitude libration is shown negative, but could be shown positive by an equal angular magnitude. A zero yaw attitude, with resulting communications blackout, is shown in (a), and a reoriented yaw attitude, with no communications loss, is shown in (b). It is assumed in this memorandum, unless otherwise stated, that the LM zero yaw attitudes for powered descent and ascent are "face-up" and "face-down", with the LM+Z_B body axis pointing away from and toward the lunar surface, respectively.

SURFACE VIEWING DURING LM DESCENT

In Figure (4c), geometry associated with a 180° yaw attitude during powered descent is presented. A 180° yaw ("face-down" attitude) would enable the crew to view the lunar surface, but would be in excess of the corrective yaw angles that are required to avoid beam interference. Since the LM attitude in the latter portion of LM descent must be held at approximately zero yaw for use of the landing point designator as well as the landing radar, surface viewing during the initial portion of the descent would necessitate a 180° yaw maneuver back to zero somewhere before

High Gate. If the geometry of Figure (4) were to be changed to correspond to a southern landing site and positive latitude libration, the figure would show that yawing the LM to a 180° yaw attitude in order to view the surface could create a beam interference situation. Therefore, the effect of a 180° yaw maneuver on S-Band beam interference cannot be determined until the LM trajectory and attitude, the lunar librations, and the LM landing azimuth have been specified.

COMMUNICATIONS DURING LM COAST

Before leaving the discussion of Figures (3) and (4), it will be well to mention antenna pointing problems for the unpowered portions of the LM descent and ascent trajectories. When thrusting, the LM pitch and roll attitudes are controlled by the onboard guidance, and any constraints applied to the pitch or roll attitude would be unacceptable. Yawing about the thrust of course does not redirect the thrust vector; the only effect is a transform of the vehicle's inertia tensor. In contrast, when on a coasting trajectory, the LM pitch attitude is arbitrary except for constraints such as those associated with star sightings for platform alignment, rendezvous radar tracking, and optical tracking.

Therefore, there should be no S-Band beam interference problem for the unpowered portions of the LM trajectory, if the proper pitch attitude is established while on an inertial coast. While behind the moon, the LM will transmit low-bit-rate information via the VHF system to the CSM. This will then be recorded for subsequent transmission to Earth.

1.3 ISOLATION OF THE PROBLEM PARAMETER SPACE

The functional dependence of the S-Band communications time that may be lost and the maximum of the absolute value of the yaw time function required to recover communications is indicated by Equation (1) below:

Equation (1)

$$T_{LOST},\ \phi_{MAX} = f\left(\mu_S,\ \lambda_S,\ \mu_L,\ \lambda_L,\ \alpha,\ T_S,\ \{\theta,\ \beta,\ \psi\}\right)$$

The pairs (μ_S, λ_S) and (μ_L, λ_L) are the selenographic landing site coordinates and the lunar librations, in latitude and longitude, respectively. The plane of the LM descent trajectory, for a given landing site, is determined by the landing azimuth, α. The plane of the LM ascent trajectory for a given site is determined by

both the landing azimuth and the surface stay time, T_S. The LM attitude is determined by $\theta(t)$ and $\beta(t)$, which are the LM pitch and roll angles, respectively, and are the result of the thrusting control exercised by the LM onboard guidance. The lost time is evaluated at the yaw angle $\phi = 0°$. The angle $\psi(t)$ in Equation (1) is the lunar central angle between the local vertical at the landing site and the local vertical at the LM position.

In the sections which follow, the selection of mission parameters is discussed first, followed by a presentation of the results of a computer simulation which used selected parameters as inputs. Yaw time histories and antenna angle loci are included. This is followed by a discussion of the landing radar interface and some mention of lunar surface accessibility. The final section then summarizes the results and offers several options for solution of the problem.

2.0 SELECTION OF SPECIFIC MISSION PARAMETERS

The S-Band communications interference time cannot be determined until all parameters in Equation (1) have been determined. While the selection of these parameters is integral to overall mission design, some discussion of their variations will aid in bounding the problem and establishing a solution.

2.1 LANDING AZIMUTH AND STAY TIME SELECTION

A performance-optimum lunar orbit for a Lunar Orbital Rendezvous mission is one which minimizes SPS (Service Propulsion System) fuel usage for the entire mission. For a given lunar landing site, one may establish an infinity of orbits which pass over the site, each having a different "LM landing azimuth". The LM landing azimuth, α, may be defined as the angle between the direction vector from the landing site to lunar north, and the direction vector of the LM trajectory at the landing site. For an entirely planar LM trajectory, specification of the landing azimuth uniquely specifies the descent trajectory plane for a given site. The performance-optimum lunar parking orbit will possess a unique landing azimuth.

For any particular Earth launch date (or lunar landing date) the total SPS fuel consumed will vary with changes in the LM landing azimuth. Examples of this variation are presented in Figures (5), (a) and (b), where end-of-mission SPS fuel reserve is plotted vs. LM landing azimuth, α. These curves were calculated using the weights of Reference 4. Midcourse correction allowances were included, as were reserves for LM rescue. The line indicating

the SPS minimum operational reserve defines the maximum tolerable range of landing azimuths, for the given mission parameter conditions. Note also that these curves show the optimum azimuth varying by as much as 15° between launch dates. Superimposing lunar lighting constraints on curves such as those of Figure (5) will generally eliminate all but one launch opportunity per month, therefore reducing the overall range of azimuths shown. However, in order to obtain best and worst case conditions as concerns the S-Band beam interference problem, a comprehensive range of azimuths between 250° and 290° was scanned in this analysis.

LUNAR SURFACE STAY TIME

The lunar surface stay time will influence LM-Earth communications for two reasons. First, lunar rotation will require the LM ascent trajectory plane to be different from the descent trajectory plane, and second, the earth-moon line will change slightly between descent and ascent because of lunar librations. For this study, lunar rotation was taken into account, and the stay time was fixed at 44 hours (nominal stay plus maximum contingency). The manner in which lunar librations change during stay time will be a function of the particular landing date; in some cases there may be virtually no change, while at other times there may be a difference of up to 2° in 44 hours. Because of this landing date dependence, the change in librations during stay time was not included.

2.3 LUNAR LIBRATIONS & LANDING SITES

As discussed in Appendix D, the lunar librations for any given month follow a locus which varies about the (0°,0°) selenographic coordinate point on the face of the moon. The locus plots presented in Appendix D may be bounded by the area shown in Figure (6a), for the years 1968 and 1969. Subsequent sections will affirm that, as concerns S-Band beam interference, the corner points of this region are the approximate best and worst libration conditions, as labelled. These corner points represent extreme cases which are never actually reached in 1968-1969. The bounds used in obtaining the results presented in this report were for 1968, but do not differ greatly from the 1968-1969 bounds, as indicated in Figure (6b).

The libration conditions for a given lunar mission are determined quite strongly by the constraint on lunar lighting conditions at the time of LM descent. Current planning indicates that a rising sun at 7° to 20° above the lunar horizon would provide acceptable visual perception during LM descent manual control. This 13° range serves to select approximately one day per month during which the lighting conditions are acceptable at any given

landing site. Figure (7) indicates how the choice of sun angle selects latitude libration conditions for lunar landing sites at +45° (East) and -45° (West) longitude. These periodic curves represent a sampling from the monthly variations in latitude librations, which are themselves periodic. Corresponding curves could be drawn for longitude librations. The figure illustrates that for a given landing site, the best and worst libration conditions, as regards beam interference, will be separated by approximately six months.

LANDING SITES

Equation (1) indicated the dependence of beam interference on the lunar landing site latitude and longitude. Although a continuum of landing site longitudes was scanned in this analysis, only certain landing sites are under consideration for the first lunar mission. Nominally, landing sites will be restricted to the selenographic region bounded by the coordinates $(|\mu s|, |\lambda s|) = (5°, 45°)$. These bounds were used when selecting a worst-case site latitude and longitude for simulation purposes.

2.4 LM TRAJECTORY DATA

The communications simulation procedure that is described in detail in the Appendixes utilized LM trajectory data taken from Reference (3). The trajectory information used is plotted in Figure (8). The range angle, ψ, is the lunar central angle between the LM and the landing site, and was not included explicitly in Reference (3). An equation for this angle is given in Appendix B.

3.0 LOST TIME AND MAXIMUM YAW DEPENDENCE ON MISSION PARAMETERS

The factors discussed in a qualitative manner in Section (1.0) will now be treated quantitatively. All results which follow were generated using the simulation procedure described in the Appendixes. Since the parameter matrix of the problem would yield an inordinate amount of data if scanned completely, only particular parameter sets were selected for scanning. The values chosen yield a set of results which have general applicability and tend to bound the problem.

3.1 LANDING SITE VARIATIONS

The variation of S-Band communications interference time with changes in both the latitude and longitude of the lunar landing site is expected from the qualitative discussion accompanying Figure (3). This variation was examined by scanning the partials $\left(\frac{\partial T_{LOST}}{\partial \lambda_S}\right)$ and $\left(\frac{\partial \phi_{MAX}}{\partial \lambda_S}\right)$ for the following sets of parameters:

Equation (2)

$$\begin{cases} \text{SITE LONGITUDE: } -45° \leq \lambda_S \leq 45° \\ \text{SITE LATITUDE: } \mu_S = 0°, \pm 5° \\ \text{LIBRATIONS: } (\mu_L, \lambda_L) = (-6.85°, -7.70°), \\ \qquad\qquad (6.80°, 7.91°) \\ \text{LANDING AZIMUTH: } \alpha = 250°, 270°, 290° \end{cases}$$

The results of this scan are given in Figures (9) through (14). (The point density of these curves is 1° in site longitude; T_{LOST} is determined to 10 sec., ϕ_{MAX} to 0.1°.) The T_{LOST} and ϕ_{MAX} values for negative and positive landing site longitudes correspond to LM powered ascent and descent, respectively. In no case (given set of parameters) will communications be lost on both LM powered descent and ascent due to beam interference.

The general trend in Figures (9) through (14), as expected, is for both T_{LOST} and ϕ_{MAX} to increase with increasing magnitude of the landing site longitude. For a better visualization of these variations, isometric summary plots of T_{LOST} are included in Figures (15) and (16). Because of the sun angle selection of librations that was mentioned previously, Figures (15) and (16)should be viewed as being separated by six months in lunar landing date, for any given site longitude. Figures (9) through (14) indicate that the worst-case T_{LOST} values for descent and ascent are 370 and 270 seconds, respectively; the worst-case ϕ_{MAX} values indicated here are 47° and 33°, for descent and ascent, respectively. However, one should recall that the libration conditions shown are best/worst for LM descent. The worst-case for LM ascent will be shown subsequently in Section (3.3).

The overall trends that are shown in Figures (9) through (16) may be explained with the aid of Figure (17). The LM descent trajectory ground tracks shown on this figure are for site latitudes of 0°, ±5° and a landing azimuth, α, of 250°. The landing site longitudes in (a) and (b) are approximately 15° and 30°, respectively. The earth-moon line pierces the selenographic sphere at points lying along the representative lunar libration locus shown in Figure (17a). For discussion purposes, the antenna angle coverage has been approximated by a straight-line boundary in Figures (17 a & b); it should actually be a curved intersection of the selenographic sphere with the surface formed by the antenna azimuth coverage boundaries. The antenna elevation boundary shown in Figure (17c) is exactly a line in the LM X_B, Z_B plane, and this

boundary exists only when the antenna azimuth is less than +2°. As regards beam interference, when the moon-earth line lies below the azimuth coverage surface that is indicated as a line in (a) and (b), then antenna tracking and transmission will be interrupted.

A number of parameter effects are evident from Figure (17). Rotation of the ground track as the landing azimuth varies will change the plane of the excluded azimuth boundary shown, and as the earth-moon line passes through this plane, an abrupt change in the beam interference situation will result. However, when beam interference exists, its duration will be quite independent of changes in the landing azimuth, and will largely depend on the motion of the LM in the plane of Figure (17c). In Figure (15), certain conditions (e.g., $\alpha = 250°$, minimum librations) were shown to cause a non-monotonic variation of T_{LOST} with increasing site longitude, and this may be explained by comparing Figures (17 a & b). The site longitudes in (a) and (b) are approximately 15° and 30°, respectively, and all ground tracks are for landing azimuths less than 270°. Note that for a landing site on the equator ($\mu_S = 0°$), beam interference is indicated for "worst" librations in (a), but not in (b). As the site is moved eastward, while holding μ_S and α fixed, it is possible that a certain longitude can be reached at which the earth-moon line lies above the excluded azimuth boundary, in which case beam interference will not exist on LM powered descent. Corresponding diagrams and discussions will apply to LM powered ascent.

The major effects that have been shown in this section may be summarized as follows:

1) On lunar landing dates when the latitude librations are strongly negative, the beam interference problem will be the most severe.

2) For a fixed LM landing azimuth, the best and worst beam interference situations for a given landing site will be separated by approximately six months.

3) When the LM landing azimuth is not far from 270°, an increase in the magnitude of the site longitude will cause a monotonic increase in both T_{LOST} and ϕ_{MAX}.

4) For a fixed trajectory profile, the duration of T_{LOST} is largely a smooth function of the site longitude and the longitude libration, whereas changes in the landing azimuth, the site latitude, and the latitude libration will generally produce a discontinuous change in the time lost.

3.2 LM LANDING AZIMUTH VARIATION

Although the curves presented in the previous section indicated that variations in the LM landing azimuth will markedly affect S-Band beam interference, these curves were only for certain discrete azimuths. This variation with landing azimuth was examined further by scanning the partials $\left(\frac{\partial T_{LOST}}{\partial \alpha}\right)$ and $\left(\frac{\partial \phi_{MAX}}{\partial \alpha}\right)$ over a continuum of azimuths, for the extreme range of all parameters.

A representative example of this scan is given in Figure (18). (The point density for this plot is 0.5° in α.) The T_{LOST} and ϕ_{MAX} values for negative and positive landing site longitudes correspond to LM powered ascent and descent respectively. Note immediately that T_{LOST} is an almost discontinuous function of α: changing the landing azimuth but 1° will in some cases remove beam interference entirely.

These curves move outward (toward 250° or 290°) as the site latitude is decreased, with T_{LOST} remaining approximately unchanged, and the region of "clear" azimuths increasing. As the latitude librations are decreased toward negative values, the curves move up slightly, and toward each other until the case is reached where beam interference occurs for all landing azimuths between 250° and 290°.

The explanation of these effects is aided by Figure (19), which shows the same qualitative geometry that was presented in Figure (17), and is redrawn here for clarity. Again, the excluded azimuth boundary line is an approximation to the actual projection. As the landing azimuth is varied, the excluded antenna azimuth boundary will vary as shown, with a discontinuous change in the beam interference situation occurring as the earth-moon line passes through the boundary of azimuth coverage. One may also visualize that rotating the LM positively about its $+X_B$ axis (yawing) will reorient the excluded coverage boundary until the moon-earth line lies above this boundary, and beam interference is removed. A corresponding discussion may be developed for LM ascent.

3.3 LUNAR LIBRATIONS VARIATIONS

The plots presented in the previous sections indicated a large variation in the S-Band communications interference time when going from the worst to the best lunar libration conditions. This variation was examined further by scanning the partials

$\left(\frac{\partial T_{LOST}}{\partial \mu_L}\right)$ and $\left(\frac{\partial \phi_{MAX}}{\partial \mu_L}\right)$ over a continuum of latitude librations, for extreme cases of the remaining parameters (viz., landing site, landing azimuth, and longitude librations). If one returns to Figure (6), this scan of latitude librations is seen to be along the left and right boundaries of the libration region shown.

A representative plot showing the change in T_{LOST} and ϕ_{MAX} with changes in librations is given in Figure (20). Parameter conditions are as noted on the figure. The librations here cover the worst case for powered ascent, as was indicated in Figure (6). (The point density is 1° in μ_L.) One may note immediately that in some cases, an increase in latitude librations from negative to positive values will cause a sharp decrease in T_{LOST}, while in other cases, beam interference will occur for all latitude librations. This is a general trend seen for the various cases that were scanned. Note that the worst-case ϕ_{MAX} value of perhaps 50° exceeds the maximum value (of 33°) for powered ascent that was indicated in Section (3.1), when discussing landing site variations. The overall worst-case values of ϕ_{MAX} for LM powered descent and ascent may now be given as 47° and 50°, respectively. The ascent value is slightly greater because the CSM plane change decreases the azimuth of the LM ascent trajectory slightly, for a landing azimuth of 250°, and a site latitude of -5°.

In summary, examination of a complete set of curves such as those given in Figure (20) would indicate the following:

1) For a fixed landing site and LM landing azimuth, latitude librations will determine the landing opportunities for which beam interference will occur, whereas longitude librations will determine the duration of such interference.

2) For certain landing azimuths, interference can occur for all latitude librations in the range $-6.86° \leq \mu_L \leq +6.86°$, for landing sites far East or far West.

3) The sensitivity of beam interference to changes in the latitude librations is such that interference conditions could disappear as the latitude librations changed by 1° (a change which can occur in as little as 16 hours).

4.0 CORRECTIVE YAW VARIATIONS

Re-orientation of the LM yaw attitude during powered descent or ascent was mentioned in the Introduction as a possible solution to S-Band beam interference problems. The plots presented in Sections (3.1) through (3.3) gave only the maximum of the absolute value of the corrective yaw, designated ϕ_{MAX}, where:

$$\text{Equation (3)} \qquad \phi_{MAX} = \underset{t}{MAX} \left\{ |\phi(t)| \right\}$$

The following section presents yaw time functions which will remove beam interference for particular parameter conditions, as well as a discussion of the utilization of these functions.

4.1 YAW TIME HISTORIES

The function $\phi(t)$, (the minimum yaw required to recover communications), was generated for the following sets of mission parameters:

$$\text{Equation (4)} \quad \begin{cases} \text{LANDING SITE: } (\mu_S, \lambda_S) = (\pm 5°, \pm 45°) \\ \text{LIBRATIONS: } (\mu_L, \lambda_L) = (-6.85°, -7.70°), \\ \qquad\qquad\qquad\qquad (6.80°, 7.91°) \\ \text{LANDING AZIMUTH: } \alpha = 250°, 260°, 270°, \\ \qquad\qquad\qquad\qquad 280°, 290° \end{cases}$$

The results are plotted in Figures (21) through (24). (The point density of these plots is 10 sec. in time; $\phi(t)$ was determined to 0.1°). The small jump seen at 238.2 seconds for LM descent is due to a guidance re-targeting in roll that was included in the trajectory data used. The required yaw decreases slowly during powered descent until the sharp drop which corresponds to crossing the -30° antenna elevation constraint. Correspondingly, the yaw required on powered ascent begins sharply as the +210° antenna elevation constraint is crossed, and continues to increase slowly until APS cutoff, at which time a pitch re-orientation will be

permissible for maintaining communications. A further explanation of the shape of these curves is included in the discussion of antenna angle time histories in Section (5.3).

4.2 PROBLEMS ASSOCIATED WITH YAWING THE LM

Since re-orientation of the LM yaw attitude is to be considered as a possible solution to S-Band beam interference, it will be well to mention some of the problems and constraints associated with re-orienting the LM about its thrust axis (yawing). These may be listed as follows:

1) Landing radar interference during LM descent

2) Manual control during automatic thrusting

3) RCS fuel conservation

4) Re-orientation of inertia properties

5) Descent engine gimballing

6) Ascent engine thrust line orientation

Problems associated with the landing radar interface are discussed in a subsequent section; the remaining constraints are discussed below.

MANUAL CONTROL DURING AUTOMATIC THRUSTING

The LM attitude is controlled manually by either the LM commander or the LM pilot through the ACA (Attitude Controller Assembly) and is monitored by viewing the FDAI (Flight Director Attitude Indicator - "8-Ball"). It is expected that during Hohmann coast, the LM will have been put in the proper attitude to maintain continuous S-Band communications with Earth via the steerable antenna, (manual earth acquisition). Upon initiation of DPS automatic thrusting, therefore, the LM will be oriented in yaw at some angle equal to or greater than ϕ_{MAX}. Attitude hold would be maintained during DPS ignition. A manual attitude maneuver back to zero yaw could be performed either in steps at various altitudes or entirely at the altitude at which no yaw is required. The DPS throttle setting would of course be maintained in the automatic mode. A minimum of disturbance to automatic thrusting and attitude control would result if the attitude rate due to manual control were small, e.g., less than 1°/sec.

With the mode of manual attitude control being rate command with attitude hold, a minimum of pilot attention would be diverted to this task. Similiar procedures could be implemented for powered ascent.

RCS FUEL CONSERVATION

The $\phi(t)$ curves presented in Section (4.1) indicated that, in many cases, the yaw required does not vary greatly over the required time interval. In the interest of minimizing attitude changes and the resulting RCS fuel usage, these functions could be replaced by step functions of magnitude ϕ_{MAX}, thereby requiring only one attitude change. Only in the case of possible landing radar signal degradation at ϕ_{MAX} would one consider utilizing the exact $\phi(t)$ function.

RE-ORIENTATION OF INERTIA PROPERTIES

Yawing the LM about its thrust axis will cause the response to pitching in the trajectory plane to vary according to the extent of such yaw. Since automatic thrusting control will be mostly through pitch re-orientation, it is well to consider this variation. The moment of inertia in pitch will transform as follows, where ϕ is the yaw excursion from zero.

Equation (5)

$$I_P = I_{YY} \cos^2 \phi + I_{ZZ} \sin^2 \phi + 2I_{YZ} \cos \phi \sin \phi$$

This moment of inertia is plotted as a function of yaw in Figure (25), for various inertia conditions during a lunar mission. (Data from Reference 5). From this figure, one may note that in the time between the Braking and Hover phases of LM descent, deviation from zero yaw will not greatly affect the LM pitching moment of inertia. For LM descent, the inertia changes due to fuel consumption will cause a much greater variation in pitch response than any yaw maneuver would cause.

However, during LM ascent, the reverse is true: for LM ascent inertia conditions, yawing will change the LM pitch response more than the nominal inertia changes at zero yaw. Since the LM inertias are markedly different during powered descent and ascent, the constant RCS torques will cause the attitude control response rates on ascent to be higher than on descent. Compared to this effect, the change in pitch response due to yawing is a secondary consideration.

DESCENT ENGINE GIMBALLING

Reorienting the LM about its thrust axis is not strictly the same as yawing about the $+X_B$ axis, because of descent engine gimballing. The DPS (Descent Propulsion System) gimbal and gimbal-rate limits are $\pm 6°$ and 0.2°/sec., respectively. (Reference 4). However, the actual gimbal angles experienced by the engine during automatic thrusting control from Braking to High Gate (the period during which such a yaw would be performed) should be quite small, since the c.g. deviation from the LM $+X_B$ axis will be 0.3 in or less during this time interval. (Reference 5). Therefore, yawing at a low rate should have only a small effect on LM control and fuel consumption during powered descent.

ASCENT ENGINE THRUST LINE ORIENTATION

In order to compensate for moments produced by c.g. changes during ascent, the ungimbaled LM Ascent Propulsion System will be mounted so that its thrust line goes through an average c.g. position. From the data of Reference 5, it may be shown that the maximum angle between the thrust vector and the LM $+X_B$ axis would be 3°40', because of engine mounting. The resultant precessing of the thrust vector about the $+X_B$ axis when yawing the LM should have only a small transient effect on attitude and thrusting control.

For the reasons given, none of the above mentioned factors appears to be so restrictive as to preclude a yaw solution to S-Band beam interference.

5.0 ANTENNA ANGLE LOCI

Discussions included in the previous sections have indicated that S-Band beam interference during LM powered descent and ascent is caused by the steerable antenna having to look through certain excluded areas of antenna coverage in order to track the Earth. This is shown explicitly by the antenna angle time histories which are presented in the section which follows. Definitions of the antenna elevation and azimuth angles indicated in these plots were given in Figure (2); excluded coverage is discussed in Appendix C.

5.1 UNCORRECTED ANTENNA LOCI

Figures (26) through (29) present plots of uncorrected (zero yaw, "face-out" during descent, "face-down" during ascent)

antenna angle loci for the following parameter cases:

Equation (6)

$$\begin{cases} \text{Landing Site:} & (\mu_S, \lambda_S) = (\pm 5°, \pm 45°) \\ \text{Librations:} & (\mu_L, \lambda_L) = (-6.85°, -7.70°), (6.80°, 7.91°) \\ \text{Landing Azimuth:} & \alpha = 250°, 270°, 290° \end{cases}$$

The locus plots for powered descent (eastern sites) begin at initiation of Braking, and those for powered ascent begin at 32 seconds after LM liftoff. Time is indicated at approximately every 100 seconds along each locus. Those parts of the LM which cause beam interference for any particular locus may be identified by comparing these plots with the overall excluded coverage plot given in Appendix C.

The antenna angle loci shown in Figures (26) through (29) are nearly straight lines, and would be exactly so if the pilot-roll angle, β, was constant at 180° for LM descent and ascent. This may be explained as follows: Disregarding parallax, the earth position vector forms an essentially constant angle with respect to the CSM parking orbit plane and therefore, the plane of the LM trajectory. The plane of the LM trajectory, however, is the same as the LM X_B, Z_B plane, when $\beta = 180°$. Referring to Figure (2a), one may recall that the antenna azimuth is always measured from the LM X_B, Z_B plane. Therefore, as the LM pitches over during either descent or ascent, the earth position vector makes a constant angle with the LM X_B, Z_B plane, effecting no change in the antenna azimuth.

5.2 CORRECTED ANTENNA LOCI

If the LM is reoriented in yaw through the minimum angle required to correct for beam interference, the antenna angle locus will be modified as in Figure (30a), for example. The yaw time function, $\phi(t)$, which effects such a locus for the indicated parameter conditions was given in Figure (21). The yaw angle is determined at 0.1°, causing the antenna to track along the excluded azimuth boundary.

Also included, in Figure (30b), is an antenna angle locus for holding constant maximum yaw rather than the actual $\phi(t)$ function. The yaw angle is $\phi_{MAX} = 23.2°$ for the parameter conditions indicated, as may be verified by referring to Figure (21).

5.3 ANTENNA ANGLE YAW LOCI

In order to indicate the effect of yawing from a "face-down" (180° yaw) to a "face-out" (0° yaw) attitude following a period of surface viewing during descent, the curves of Figure (31) are included. Three separate yaw locus plots are shown. The closed curve in the center of the figure establishes regions of gimbal stop encounter: For all initial antenna orientations which correspond to points lying outside this region, a 180° yaw will always cause gimbal stop encounter. The remaining loci show the effect of yawing through 180° when there is either a clear or obscured line-of-sight to Earth when at zero yaw. For each of the three locus plots, the LM is held at a fixed point on the descent trajectory with no motion in either pitch or roll (static LM). Yaw angles are indicated every 20° from 0° to 360°.

The dotted lines in Figure (31) which connect points at 0° and 180° yaw emphasize the "reflection" of the antenna coordinates about the $+X_B$ axis. As regards beam interference, this figure should indicate to the reader that, for every case where the antenna elevation at zero yaw is less than -30° and no beam interference is encountered, a 180° yaw will cause beam interference. Conversely, whenever beam interference occurs at zero yaw with the antenna azimuth less than -2°, a 180° yaw will remove beam interference, although there will be losses due to gimbal stop encounter and earth re-acquisition time. Finally, if the initial antenna azimuth at zero yaw is between -2° and +2° when the initial elevation is less than -30° or greater than +210°, then beam interference will occur at both 0° and 180° yaw.

The plots of Figure (31) also afford an explanation for the particular shape of the yaw time function, $\phi(t)$, which was shown in the figures presented in Section (4.0). The two curves on the left of Figure (31) show that the change in antenna azimuth when yawing through a given angle (e.g., 20°) will increase as the antenna elevation increases between -75° and 0°. Therefore, during powered descent to eastern landing sites when the antenna is tracking through negative antenna elevations toward 0° elevation, the yaw deviation required to effect the same change in antenna azimuth will decrease with time. A corresponding discussion would explain why the required yaw will increase during powered ascent from western sites when antenna elevations are increasing from 180° toward 255°.

In summary, the following may be stated concerning S-Band antenna tracking during LM descent and ascent:

1) If the lunar surface is viewed between Braking and landing radar display-data acquisition at 30,000 ft., then the required 180° yaw maneuver will in many cases result in S-Band antenna gimbal stop encounter. The beam interference situation at either 0° or 180° yaw during powered descent cannot be determined until the landing site, the landing date, the trajectory plane, and the trajectory and attitude profiles have been specified.

2) Direct surface viewing (vertical line-of-sight to ground track) will not be possible for all cases if continuous communications are to be maintained. A deviation of up to -47°, i.e., a yaw attitude of 133°, will be required in the worst case while surface viewing is being performed. In addition, the LM may not always be returned to a zero yaw attitude following surface viewing, but may have to be returned to a non-zero yaw attitude if communications are to be maintained.

3) For a worst-case landing azimuth, site latitude, and libration conditions, it may be shown, using Figure (31), that if the landing site is located between -4° and -45° (West longitude), then yawing through 180° at 300 seconds from Braking (i.e., starting at an altitude of 32,500 ft.) may be done without gimbal stop encounter.

4) In cases of gimbal stop encounter, it will be highly desirable for the crew to carry onboard a chart (like Figure 31) which will enable quick manual Earth reacquisition following a 180° yaw. Yawing at 2°/sec. at an altitude of 30,000 ft., for example, would cause about 20 seconds of communications loss due to gimbal stop encounter if the antenna were properly repositioned using charts while outside the gimbal limits.

6.0 LANDING RADAR INTERFACE

As mentioned in the Introduction, it will be desirable to obtain a landing radar measurement of the LM altitude above the lunar surface as early in the descent trajectory as possible. Because reorientation of the LM yaw attitude might interfere with such a measurement, or even with radar state-vector updates, it is important to consider landing radar operations when discussing solutions to the S-Band interference problem. Some salient details of the landing radar system will be given first, followed by a discussion of yawing effects.

6.1 RADAR CHECKOUT & OUTPUT WEIGHTING

Figure (32) indicates the landing radar beam designation and depicts the two antenna tilt positions which are available. (As per current design considerations, Reference 6) In position no. 1, the group centerline of the beam pattern is inclined approximately 24° to the LM + X_B axis. This position proves to provide for a minimum of beam dropouts when the range of pitch angles experienced by the LM from Braking to High Gate is considered. (Reference 6) Position no. 2 will be utilized from High Gate to touchdown, and is not of concern here.

The beams labelled 1, 2, and 3 in Figure (32) are velocity beams; beam "A" is the radar altimeter beam. In order to avoid spurious reflections from the aft landing pad, the beam pattern has been inclined-6° to the LM X_B, Z_B plane (Reference 8). That is, the angle between beam "A" and the X_B, Z_B plane is approximately 6°, in the sense of negative rotation about the $+X_B$ axis. Beams 1 and 2 are separated from the altimeter beam by approximately 13.5°, so that beam 1 is inclined to the X_B, Z_B plane by about 7.5°. The LM is shown at a zero yaw attitude in Figure (32). Note that reorienting the LM about the X_B axis through a positive yaw will degrade the return on beam no. 1 but will first improve and then degrade the return on beam no. 2 and the altimeter beam, depending on the extent of such reorientation. (Assuming a flat lunar surface.) Note that beam no. 3 will be giving a low return signal for the initial portion of powered descent, when the LM pitch angles are small.

LANDING RADAR CHECKOUT

The landing radar circuitry may be checked out by means of a self-test arrangement, without any return signals received by its antenna. (Reference 9) This is done by feeding signals of known frequency into the same pre-amplifiers and subsequent circuits which process actual return signals. A certain altitude, altitude rate, and forward and lateral velocity should then appear on the LM control panels. This check is best done when no signals are being received by the antenna, and is scheduled to be performed before or during Hohmann descent on the lunar mission.

When return signal strength is sufficient, the LM command pilot may then check the radar output against the PGNCS (Primary Guidance, Navigation, and Control System) and the AGS (Abort Guidance System), by displaying altitude or altitude rate as well as forward and lateral velocities. (Reference 9) When

the LM is at other than 90° pitch angle, the radar display information will not compare exactly with the PGNCS or AGS information. A cosine 15° correction has been included to provide an average compensation for this difference in displayed data. (Reference 6)

As regards attitude reorientation for S-Band communications, the inclusion of the self-check system should remove any strict requirement for a long checkout period of observing actual landing radar return signals prior to updating. However, it will be highly desirable to have observed some display data prior to the initiation of state vector updating at 25,000 ft. The period of time from 30,000 ft. to 25,000 ft., for example, would leave approximately 25 seconds for display data observations.

UPDATE WEIGHTING AND DATA ACQUISITION

Landing radar measurements of LM altitude and velocity will be weighted into navigation estimates of the LM state vector in order to improve the estimates and to correct for unknowns in lunar terrain. It is currently planned that the altitude and velocity weighting functions will be stored in the LM onboard computer as uncoupled linearized functions of LM altitude and total velocity, respectively. According to Reference 10, altitude updating will begin when the total velocity has decreased to 1500 fps. The latest antenna position design (24°) will not permit altitude data acquisition above 26,000 ft., or velocity data acquisition above 15,000 ft., for a zero yaw attitude. (Reference 6) From Reference 3, the LM will be at altitudes of 25,000 and 15,000 ft. at 340 and 410 seconds from the initiation of Braking, respectively. Since it has been shown that, in the worst case, beam interference at zero yaw could exist during the first 370 seconds of powered descent, there could be an interface between yaw correction for communications purposes and altitude updating at 340 seconds. With velocity data acquisition at 410 seconds, there will be no interface with velocity updating.

Because the data acquisition altitudes given above are based on a lunar reflectivity model which is considered to be 5 to 10 db conservative, it is expected that altitude display data will be available at 30,000 ft., or about 312 seconds into powered descent. (Reference 6) As concerns the S-Band communications problem, it appears reasonable to require that any corrective LM attitude reorientation should not interfere with the earliest possible reception of good radar altimeter display data between 30,000 ft. and 25,000 ft., or with either the initiation of LGC updating or with its continuity once it begins. These requirements will in some cases impose constraints on the yawing maneuver solution to S-Band beam interference.

6.2 BEAM LOSSES DUE TO YAWING

Of prime concern in assessing the interface between LM landing radar operation and S-Band communications during powered descent is the effect of LM attitude reorientation on landing radar return signal strength. If the return power for any given beam is sufficiently low, the frequency trackers in the landing radar electronics subsystem will not lock on to the signal and the doppler velocity will not be determined for that beam. The landing radar circuits are arranged such that no velocity information is used by the LGC for updating if either beam 1, 2, or 3 gives a no-track condition. Correspondingly, no range information is used by the LGC for updating if either beam 1, 2, or the altimeter beam gives a no-track condition. (Reference 9)

UPDATE ERRORS

Figures (33), (a) through (d), present some modified results from a simulation which defined the velocity and range errors in landing radar updates which would be caused by yawing the LM about zero yaw. (Reference 7) The referenced simulation was done before the radar antenna mounting was redesigned to effect a -6° canting to the LM X_B, Z_B plane. Therefore, the scan of $\pm$10° in yaw which was performed in Reference 7 is now approximately equivalent to +16°, -4°. In addition, Reference 7 used an antenna angle of 40° (group center line, X_B axis) for antenna position no. 1, as well as Design Reference Mission I trajectory data. Despite these shortcomings, these plots of update errors vs. vehicle yaw appear to be the best data presently available. The four plots included here are for LM altitudes from 40,000 ft. to 10,800 ft. Beam 3 is in a no-track condition until about 15,000 ft. This is primarily a function of the LM pitch attitude and is a weaker function of vehicle yaw.

Examination of Figure (33) indicates that the update errors associated with yawing the LM within the range of -4° to +16° are of the order of 2% or less. However, one should really speak of the increment in error as the LM is yawed from zero yaw; this increment is very small over the range shown. Based on the data of Figure (33), it will be assumed that below 30,000 ft., the LM may be yawed up to +16° during powered descent without experiencing loss of track on beams 1,2, or the altimeter beam.

7.0 LUNAR SURFACE ACCESSIBILITY

The classification of lunar landing areas according to LM-Earth S-Band communications time for particular landing dates has been treated by others. (Ref. 11 and 12)* Data was presented in Sections (3.1) through (3.3) which defined the extent of the communications problem over all landing dates. Rather than present accessibility maps which would be essentially cross plots of Figures (15) and (16), this section will define certain landing areas which take into account the constraints associated with the LM landing radar, as discussed in the previous section.

The functional dependence of the yaw required to recover communications was given in Section (1.3) as follows:

$$\text{Equation (7)} \quad \phi(t) = f\left(\mu_S, \lambda_S, \mu_L, \lambda_L, \alpha, T_S, \left[\theta(t), \beta(t), \psi(t)\right]\right)$$

All symbols are as previously defined. The landing radar operational considerations discussed in Sections (6.1) and (6.2) will apply constraints to the yaw function, $\phi(t)$. If a particular constrained yaw function is given by $\hat{\phi}(t)$, then the lunar landing sites which will satisfy Equation (7) may be given as follows:

$$\text{Equation (8)} \quad (\mu_S, \lambda_S) = \bar{f}\left(\mu_L, \lambda_L, \alpha, T_S, \left[\theta(t), \beta(t), \hat{\phi}(t), \psi(t)\right]\right)$$

Assuming the trajectory profile of Ref. 3, one may give the constraint on $\phi(t)$ as follows:

$$\text{Equation (9)} \quad \hat{\phi}(t) < 16^\circ \text{ for } t > 310 \text{ sec. (or altitude } < 30{,}000 \text{ ft.)}$$

Equation (8) may then be used to determine two classes of landing areas, viz., those which satisfy the given radar constraint and those which do not. These two classes will of course be functions of the librations and the landing azimuth. The extent of these classes was evaluated for the following parameter conditions.

$$\text{Equation (10)} \begin{cases} \text{LIBRATIONS:} & (\mu_L, \lambda_L) = (-6.85^\circ, -7.70^\circ), \\ & \qquad\qquad\quad (6.80^\circ, 7.91^\circ) \\ \text{LANDING SITE:} & -45^\circ \leq \lambda_S \leq 45^\circ \\ & \mu_S = 0^\circ, \pm 5^\circ \\ \text{LANDING AZIMUTH:} & \alpha = 250^\circ, 270^\circ, 290^\circ \end{cases}$$

---

*Both references use a fixed LM landing azimuth of 270°, and treat the case of zero longitude librations. See Sections (3.1) through (3.3) for landing azimuth and longitude libration effects.

Curves of corrective yaw at 30,000 ft. vs. landing site longitude are given in Figure (34), for $(\mu_L, \lambda_L) = (-6.85°, -7.70°)$, which are the worst-case librations for communications during LM descent. Landing azimuths of 270° and 290° are shown on the plots; no interference will occur at 250° aximuth for the parameter conditions indicated. For the maximum positive libration conditions, no yaw is required at 30,000 ft. during LM descent, for any of the remaining parameter conditions given by Equation (10). Note that if the landing radar yaw tolerance at 30,000 ft. is assumed to be 16°, then there will be a 3.5° impingement on the landing area bounded by $(|\mu_S|, |\lambda_S|) = (5°, 45°)$.

8.0 HARDWARE REDESIGN; LOW-BIT-RATE COMMUNICATIONS

The only apparent alternative to an attitude and/or trajectory re-orientation solution for maintaining high-bit-rate communications is hardware redesign. Adding an extension to the LM S-Band steerable antenna mount has been considered previously. (Ref. 13) This was rejected because of the following:

1. Antenna vibration is aggravated during DPS/APS thrusting.
2. A fold-up mechanism is required to remain within the SLA space limitations.
3. An additional cable loss (0.6 db) is encountered.
4. The LM weight is increased by about 20 lbs.
5. Certain test platforms under the SLA must be moved.

Re-orienting the gimbal axes of the present system would only re-define the antenna angles for which structural interference would exist; the RCS clusters would still cause beam interference for certain Earth position vectors relative to the LM body axes. Also, re-orientation of the antenna gimbal mounting would eliminate gimbal stop encounter during a 180° yaw only in special cases.

This entire memorandum has implicitly assumed the requirement for real-time, high-bit-rate communications during LM descent and ascent; a list of telemetry signals which are available only in the high-bit-rate mode of USB (Unified S-Band) communications was presented in Section (1.1). In the event that information from test mission data is considered sufficient to remove the requirement for the high-bit-rate signals, then one might consider using the LM VHF

system during powered descent and ascent. As when behind the moon, data would be transmitted to the CSM and recorded for subsequent playback to Earth. Direct voice contact at a low signal level could be maintained using the S-Band omni antennas.

9.0 SUMMARY AND SOLUTIONS

This memorandum has analyzed the problem of maintaining continuous high-bit-rate communications between the LM and Earth during LM descent and ascent, and has discussed the major interfaces involved. The most salient results from the information that was previously presented are given in the following conclusions.

I. In the worst cases, beam interference will occur on LM descent to sites east of +8° longitude or on LM ascent from sites west of -6° longitude. A requirement for continuous LM-Earth communications during LM descent and ascent for all launch opportunities will then eliminate all but one of the candidate Apollo lunar landing sites (the Sinus Medii site) if the LM is held strictly to either a zero or 180° yaw attitude during initial powered descent and terminal powered ascent. Landing sites in the southern lunar hemisphere (negative latitudes) will offer a greater number of launch opportunities (lunar landing dates) for which beam interference will not occur at zero yaw attitude.

II. The extent (and existence) of beam interference for a given lunar landing site will vary from one launch opportunity to another; the LM-Earth vector during descent and ascent is a function of the earth-moon geometry and the optimum lunar parking orbit of date.

III. Beam interference on LM descent or ascent can be avoided by re-orienting the LM in yaw attitude. In the worst cases, the required yaw will be +47° on powered descent or -50° on powered ascent.

IV. Landing radar requirements will impose a constraint on the yaw time function that might be required to avoid beam interference during powered descent. The use of landing radar data for state vector updates is planned to begin when the LM altitude has decreased to 25,000 ft. It will be advantageous to observe display data as soon as it is available prior to the initiation of updating.

V. The best available data indicates that the landing radar could tolerate up to +16° yaw at 30,000 ft. or below without significant errors. Constraining the corrective yaw to +16° at 30,000 ft. or below will still allow a yaw solution for all of the lunar landing sites now being considered for the first lunar landing.

VI. Beam interference during LM descent and ascent could be avoided by properly choosing the plane of the lunar parking orbit and therefore the LM trajectory plane. Deviation from the optimum parking orbit plane would require additional expenditure of SPS (Service Propulsion System) fuel. However, the amount of SPS fuel available for this will depend on a variety of mission constraints, including the landing site and landing date. In some cases, it would be possible to avoid beam interference by changing the LM landing azimuth by only 1°.

VII. Flying in a "face-down" (180° yaw) attitude during the initial portion of LM descent is not a systematic solution. Although beam interference encountered during a "face-out" flight will generally be eliminated when flying "face-down," there are many landing sites and dates for which beam interference will occur during descent when the LM is at a 180° yaw ("face-down") attitude, but will not occur at a 0° yaw ("face-out") attitude.

VIII. Yawing the LM through 180° while the steerable antenna is tracking the earth will in many cases result in loss of track because of gimbal stop encounter. Manual earth re-acquisition would then be required, and the crew would need to be aware of the correct antenna coordinates within a 10° capture angle. A 180° yaw beginning at 32,500 ft. may always be done for descent to landing sites west of -4°, <u>without</u> gimbal stop encounter.

IX. Hardware redesign, as limited to extension of the antenna tripod, has been considered and was not recommended. Transmitting low-bit-rate information to the CSM with subsequent relay to Earth would not only result in the loss of various data, but would also deny the possibility of real time monitoring at the mission control center.

X. CONCLUSIONS

This memorandum has assumed a requirement for real time, high-bit-rate communications during LM descent and ascent, and has shown that, as per the nominal trajectory and attitude profile, this requirement cannot be met for some of the lunar landing sites and dates now contemplated. On the basis of the foregoing analysis, the following procedures are offered as solutions to the problem:

1. Re-orient the LM in yaw attitude until a clear line-of-sight to Earth is obtained and beam interference is removed.

2. If the landing radar system cannot operate at the required yaw, or if the required deviation from a 180°, "face down" attitude is unacceptable, consider changing the lunar parking orbit plane with the resulting additional expenditure of SPS fuel.

3. Change the launch date and/or landing site if SPS fuel, LR, and possible surface viewing constraints cannot be satisfied while maintaining continuous communications.

A. C. Merritt

2013-ACM-wcs

A. C. Merritt

Attachments
References
Appendixes
A, B, C, & D
Figures 1-34, A1-A7, B1-B6, C1, D1-D2

REFERENCES

1. Hodge, J. D., "Telemetry Requirements for Mission AS-504," Encl. 10 of 7th AS-504 Flight Operations Plan Minutes, August 5, 1966.

2. Maynard, O. E., "LM Communications Capability During Lunar Landing Descent and Ascent",MSC Internal Note No. PM5/M-1126, August, 1966.

3. "AS-504 Preliminary Spacecraft Reference Trajectory" (U), MSC Internal Note No. 66-FM-70, July 1, 1966. (Confidential)

4. "Apollo Mission Data Specification B,AS-504 and Subsequent" (U), TRW Rep. No. 2131-H002-T8-000, March 1, 1966. (Confidential)

5. Arder, R., "LM Monthly Mass Property Status Report," Memo No. LSR-490-41, Grumman, February 1, 1967.

6. "Landing Radar Antenna Angle Study Results," Handout for joint MSC/GAEC CCB, January 9, 1967.

7. "LEM Landing Radar Eighth Quarterly Design Report, Volume I," Rep. No. 53967-8-1, Ryan Aeronautical Company, March 11, 1966.

8. "LM (Landing Radar) Monthly Technical Meeting Minutes," Ryan Aeronautical Company, January 20, 1967.

9. "Lunar Module Systems Handbook, Vehicle LM-1, AS-206, Rev. A," prepared by Flight Control Division, MSC, October 27, 1966.

10. Kriegsman, B., and Sears, N., "LEM PGNCS and Landing Radar Operations During the Powered Lunar Landing Maneuver," Rep. No. E-1982, MIT. Inst. Lab., August, 1966.

11. Dobson, W. F., "Final Report - Investigation of LEM Trajectory and Attitude Constraints due to S-Band Steerable Antenna Limitations," TRW Note No. 66-FMT-407, March 30, 1966.

12. Payne, J. D., "Limitations of LM S-Band Communications for Powered Descent and Ascent for a Typical year," MSC Internal Note No. 66-FM-152, December 23, 1966.

REFERENCES

13. Gallegro, G., Nathan, A., and Collins, P., "S-Band Steerable Antenna - Continuous LEM/Earth Communications Problem," Grumman Memo. No. LM0-380-301, February 16, 1965.

14. "LM-2 Mission Modular Data Book," Grumman, Rep. No. LED-540-47, January 1, 1967.

APPENDIX A

TRANSFORMATION EQUATIONS FOR SIMULATION

The sequence of transformations required to determine the state of LM-Earth S-Band communications via the LM high-gain steerable antenna is diagrammed in Figure (A-1). The overall indicated operation transforms the Earth's position vector from selenographic spherical coordinates to the elevation-azimuth coordinate system of the steerable S-Band antenna.

The transformations that have been grouped within the dashed block are given by the following equation:

Equation (A-1)

$$\underline{X}^{(B)} = \Lambda_2 \, \Lambda_1 \, \underline{X}^{(SG)}$$

The vectors $\underline{X}^{(SG)}$ and $\underline{X}^{(B)}$ give the Earth's position in the selenographic and LM body coordinate systems, respectively. The transformation of Equation (A-1) has been separated into two matrix operators, Λ_1, and Λ_2, with the local horizontal system as an intermediate coordinate reference.

Although it could have been included as an integral part of the simulation sequence, the problem of lunar libration generation was treated separately. The latitude and longitude librations, μ_L and λ_L, respectively, are therefore treated as inputs. Obtaining the $\underline{X}^{(SG)}$ vector is then the result of a scalar transformation on the librations as given by the following equation, derived from Figure (A-2a).

Equation (A-2)

$$\underline{X}^{(SG)} = \begin{bmatrix} \cos(\mu_L)\cos(\lambda_L) \\ \cos(\mu_L)\sin(\lambda_L) \\ \sin(\mu_L) \end{bmatrix}$$

Before describing the explicit subdivisions of matrices Λ_1 and Λ_2, it should be noted that two coordinate translations have been ignored in the sequence of Figure (A-1). These consist of a translation of the local horizontal system from the origin of the selenographic system to the altitude of the LM above the

lunar surface, and a translation of the antenna system from the origin of the LM body axes to the antenna position onboard the vehicle. Such translations would have a negligible effect on the Earth position vector. Translation to the vehicle altitude would contribute 1/4 degree at most, while the contribution due to translation to the onboard antenna position would be several orders of magnitude less.

The antenna is assumed to track the center of the Earth, while it will actually be tracking a signal from an Earth ground station. Such stations are located at other than zero latitude, and will not necessarily be located at the center of the 2° disk that the Earth presents at lunar distances. The parabolic S-Band steerable antenna radiates a beam of 13° full-cone angle, however, so ignoring ground station locations seems justifiable.

Once the above discussed translations have been omitted, the Moon-Earth vector, $\underline{R}_{ME}$ of Figure (A-2a), may be assigned any magnitude. In order that the Earth's coordinates in any of the several reference systems will be direction cosines, one may set the norm of the Moon-Earth vector equal to unity, or $||\underline{R}_{ME}|| = 1$.

SELENOGRAPHIC TO LOCAL HORIZONTAL TRANSFORMATION; Λ_1

Because the LM descent and ascent guidance controls the orientation of the thrust vector in a local horizontal coordinate system along the vehicle trajectory, one must transform to this system before inputting any particular LM attitude time history. The local horizontal system is defined by Figure (A-2b). The ξ-η plane is the local horizontal plane and the $+\zeta$ axis is the local outward vertical. The $+\xi$ axis is in the direction of the projection of the local vehicle velocity vector, $\underline{V}$, on the local horizontal plane. This (ξ, η, ζ) system then moves along the descent or ascent trajectory as the LM progresses toward or away from the landing site, respectively.

The selenographic to local horizontal transformation, Λ_1, is different for LM descent and ascent, and may be separated into individual rotations as follows in Equation (A-3).

Equation (A-3)

$$\Lambda_1 = \begin{cases} D\ C(\nu_D)\ B(i_D)\ A(\Omega_D), & \text{for descent} \\ D\ C3(\psi_A)\ C2(\Delta i)\ C1(\Delta\nu_D)\ B(i_D)\ A(\Omega_D), & \text{for ascent} \end{cases}$$

The triad of orbital elements (Ω_D, i_D, ν_D) is defined by Figure (A-2c). The transformation Λ_1 is essentially an Euler transformation, for LM descent. In standard nomenclature, Ω, i, and ν are the longitude of the ascending node, the orbital inclination, and the argument of perigee plus the true anomaly, respectively.

The descent and ascent transformations will now be treated separately.

DESCENT ORBIT TRANSFORMATIONS

Figure (A-3) gives a diagrammatic description of the rotation sequence necessary to define the LM descent trajectory plane and the vehicle position within this plane. The Earth's position vector undergoes the following transformations as the rotation sequence is performed.

Equation (A-4) $$\underline{X}^{(1)} = A(\Omega_D)\ \underline{X}^{(SG)}$$

Equation (A-5) $$\underline{X}^{(2)} = B(i_D)\ \underline{X}^{(1)}$$

Equation (A-6) $$\underline{X}^{(3)} = C(\nu_D)\ \underline{X}\ (2)$$

The rotation matrices can be derived from Figure (A-3) and are given as follows:

Equation (A-7)

$$A(\Omega_D) = \begin{bmatrix} \cos(\Omega_D) & \sin(\Omega_D) & 0 \\ -\sin(\Omega_D) & \cos(\Omega_D) & 0 \\ 0 & 0 & 1 \end{bmatrix}$$

Equation (A-8)

$$B(i_D) = \begin{bmatrix} 1 & 0 & 0 \\ 0 & \cos(i_D) & \sin(i_D) \\ 0 & -\sin(i_D) & \cos(i_D) \end{bmatrix}$$

Equation (A-10) $$\underline{X}^{(21)} = C1(\Delta\nu_D)\underline{X}^{(2)}$$

Equation (A-11) $$\underline{X}^{(22)} = C2(\Delta i)\underline{X}^{(21)}$$

The matrices $C1(\Delta\nu_D)$ and $C2(\Delta i)$ may be obtained from Figure (A-4) and are given as follows:

Equation (A-12)
$$C1(\Delta\nu_D) = \begin{bmatrix} \cos(\Delta\nu_D) & \sin(\Delta\nu_D) & 0 \\ -\sin(\Delta\nu_D) & \cos(\Delta\nu_D) & 0 \\ 0 & 0 & 1 \end{bmatrix}$$

Equation (A-13)
$$C2(\Delta i) = \begin{bmatrix} \cos(\Delta i) & 0 & -\sin(\Delta i) \\ 0 & 1 & 0 \\ \sin(\Delta i) & 0 & \cos(\Delta i) \end{bmatrix}$$

The CSM maneuver which corresponds to the transformation of Equation (A-11) is a burn at the common node line, which is the $+X_2^{(21)}$ axis. This burn will be 90° from the landing site as measured in the ascent orbit. The $+X_1^{(22)}$ axis will be the local vertical at the landing site at liftoff.

The instantaneous LM position within the ascent trajectory plane is now obtained by a rotation through the angle ψ_A, which is positive in the direction of motion in the ascent trajectory, and is the lunar central angle from the local vertical at the landing site to the local vertical at the LM position. The following equation properly transforms the Earth position vector as the LM progresses away from the landing site by the angle ψ_A.

Equation (A-14) $$\underline{X}^{(3)} = C3(\psi_A)\underline{X}^{(22)}$$

The matrix $C3(\psi_A)$ is given as follows:

Equation (A-15)

$$C3(\psi_A) = \begin{bmatrix} \cos(\psi_A) & \sin(\psi_A) & 0 \\ -\sin(\psi_A) & \cos(\psi_A) & 0 \\ 0 & 0 & 1 \end{bmatrix}$$

GUIDANCE LOCAL HORIZONTAL SYSTEM

Although the $\underline{X}^{(3)}$ system, as obtained for either descent or ascent, could be validly called a local horizontal system, it is not the same as the aforementioned system of Figure (A-2b), in which the LM thrust yaw and pitch are defined. Figure (A-5a) serves to compare the $\underline{X}^{(3)}$ and $\underline{X}^{(LH)}$ systems. As can be seen, it is necessary to rotate +90° about the $+X_3^{(3)}$ axis and then rotate +90° about the reoriented $+X_1^{(3)}$ axis in order to obtain the proper local horizontal system. This reordering of the coordinate triples is accomplished by the transformation of Equation (A-16) below, where D is given in Equation (A-17).

Equation (A-16)

$$\underline{X}^{(LH)} = \begin{bmatrix} \xi \\ \eta \\ \zeta \end{bmatrix} = D\,\underline{X}^{(3)}$$

Equation (A-17)

$$D = \begin{bmatrix} 0 & 1 & 0 \\ 0 & 0 & 1 \\ 1 & 0 & 0 \end{bmatrix}$$

All component matrices of the selenographic to local horizontal transformation, Λ_1, have now been determined for both descent and ascent.

LOCAL HORIZONTAL TO LM BODY AXES TRANSFORMATION; Λ_2

Having obtained the local horizontal system, let us now place the LM in this system such that the LM body axes and the local horizontal axes are similarly ordered triples. Thus,

the zero attitude (pitch=yaw=roll=0) for the LM will be that given in Figure (A-5b). The normalized coordinates of the Earth in the LM body system for this "zero attitude" orientation are given by Equation (A-18) below, where I is a unit matrix.

Equation (A-18) $$\underline{X}^{(B1)} = I\,\underline{X}^{(LH)}$$

THRUST YAW (Pilot Roll)

In LM thrust vector redirection, the order of rotations is thrust-yaw first and then thrust-pitch, which correspond to pilot-roll first and then pilot-pitch, the latter terms being defined in Figure (1). Figure (A-6a) shows an attitude reorientation for thrusting approximately 30° off the forward horizontal velocity. For powered descent, thrusting is mostly 180° from the total vehicle velocity until High Gate. The Earth position vector is transformed by a thrust-yaw or pilot-roll according to Equation (A-19), where matrix $E(\beta)$, as given by Equation (A-20), may be derived from Figure (A-6a).

Equation (A-19) $$\underline{X}^{(B2)} = E(\beta)\underline{X}^{(B1)}$$

Equation (A-20)
$$E(\beta) = \begin{bmatrix} \cos(\beta) & \sin(\beta) & 0 \\ -\sin(\beta) & \cos(\beta) & 0 \\ 0 & 0 & 1 \end{bmatrix}$$

THRUST PITCH

With the LM at some thrust yaw, β, we now pitch the vehicle about the $+Y_B$ axis (out the right-hand-side of the LM). From a pilot-vehicle point of view, positive thrust pitch, as shown in Figure (A-6b), is a "pitch-down" maneuver; a positive pilot-vehicle pitch is in a "pitch-up" sense. The coordinates of the Earth are transformed by pitching as in Equation (A-21). Matrix $F(\theta)$ is given in Equation (A-22).

Equation (A-21) $$\underline{X}^{(B3)} = F(\theta)\underline{X}^{(B2)}$$

Equation (A-22)

$$F(\theta) = \begin{bmatrix} \cos(\theta) & 0 & \sin(\theta) \\ 0 & 1 & 0 \\ -\sin(\theta) & 0 & \cos(\theta) \end{bmatrix}$$

ROLL-ABOUT-THRUST (Pilot-Yaw)

For the purpose of communications corrections, a yaw maneuver (roll-about-thrust) is performed. A positive yaw, as given by Figure (A-6c), corresponds to a positive, right-handed rotation about the LM + X_B axis. The transformation of the Earth position vector that is associated with yawing the LM is given as follows:

Equation (A-23)

$$\underline{X}^{(B4)} = G(\phi)\underline{X}^{(B3)}$$

Equation (A-24)

$$G(\phi) = \begin{bmatrix} 1 & 0 & 0 \\ 0 & \cos(\phi) & \sin(\phi) \\ 0 & -\sin(\phi) & \cos(\phi) \end{bmatrix}$$

This completes the LM attitude orientation within the local horizontal system, which was indicated as an overall transformation, A_2, in Equation (A-1). The vector $\underline{X}^{(B4)}$ now gives the Earth direction in the LM body system for a given trajectory and attitude.

LM BODY AXES TO ANTENNA ANGLES TRANSFORMATION

The S-Band steerable antenna is positioned onboard the LM in the X_B, Y_B plane at an X_B coordinate near the roof line. As noted previously, the Earth position vector will be affected to a negligible extent if translated from the LM body system to this onboard position.

The gimballing of the S-Band steerable antenna is defined in a shaft-trunnion system as shown in Figure (A-7). This is equivalent to an ordered rotation first through elevation (positive in a right-hand-sense about the LM + Y_B axis), and then through azimuth (positive from the X_B, Z_B plane to the $+Y_B$ axis). Therefore, Figure (A-7) shows a positive elevation and negative azimuth. Since the sequence of rotations is not a universal convention, it will be well to mention that rotation through azimuth and then elevation (as in the usual radar sequence) is not an equivalent sequence.

The antenna angles are given as follows:

Equation (A-25)

$$\begin{bmatrix} EL \\ AZ \end{bmatrix} = \begin{bmatrix} TAN^{-1}\left[\dfrac{X^{(B4)}}{Z^{(B4)}}\right] \\ TAN^{-1}\left[\dfrac{Y^{(B4)}}{\sqrt{\left[X^{(B4)}\right]^2 + \left[Z^{(B4)}\right]^2}}\right] \end{bmatrix}$$

By further convention, the range of the elevation angle, EL, and the azimuth angle, AZ, may be given as follows:

Equation (A-26)

$$-90° \leq EL \leq +270°$$

$$-90° \leq AZ \leq +90°$$

The reader may now return to Figure (A-1) and note that all indicated operations on the Earth coordinates have been performed. The matter of antenna angle constraints is discussed in Appendix C and Sections (1.0) and (5.0).

APPENDIX B

DETERMINATION OF THE TRANSFORM ANGLES

Given a landing site, (μ_S, λ_S), we wish to obtain the transform sets, (Ω_D, i_D, ν_D) and $(\Omega_D, i_D, \Delta\nu_D, \Delta i, \psi_A)$, for LM descent and ascent, respectively. The descent orbit set will be considered first, and the angles will be determined in the order given.

Transform Angles for the Descent Orbit

Figure (B-1) depicts the descent orbit track on the selenocentric sphere. The point labelled (0°, 0°) corresponds to the intersection of the prime lunar meridian with the lunar equator. The LM landing azimuth, α, may be defined as the angle between the direction vector from the site to lunar north, and the direction vector of the LM trajectory track at the site. It is measured positive North-to-East, or clockwise, in the tangent plane at the landing site. Since the LM landing azimuth is generally about 270°, the corresponding negative (counter-clockwise) azimuth is shown on all figures for convenience.

The longitude of the ascending node of the descent orbit, as referenced to the (0°, 0°) point, may be found from Figure (B-1) and is given as follows:

Equation (B-1)

$$\Omega_D = \lambda_S + \psi_1$$

The arc ψ_1, also obtained from Figure (B-1), is given by the following equation:

Equation (B-2)

$$\psi_1 = \text{TAN}^{-1}\left[\frac{\text{SIN}(\mu_S)}{-\text{COT}(\alpha)}\right], \qquad -\pi \leq \psi_1 \leq \pi$$

The value of the arctangent function in Equation (B-2) is determined according to the quadrant in which the numerator and denominator of its argument lie, and is bounded as indicated. It may be shown that Equations (B-1) and (B-2) hold for $\alpha \lesssim 270°$, $\mu_S \lesssim 0°$, and $\lambda_S \lesssim 0°$.

The orbital inclination, i_D in Figure (B-1), is given by Equation (B-3) below:

Equation (B-3)

$$i_D = \pi - \text{COS}^{-1}\left[-\text{COS}(\mu_S)\,\text{SIN}(\alpha)\right]$$

The remaining angle of the descent set is the anomaly, ν_D. This angle may be found from Figures (B-1) and (B-2) and is given as follows:

Equation (B-4)

$$\nu_D = (\psi_2 - \psi_D)$$

Equation (B-5)

$$\psi_2 = \text{TAN}^{-1}\left[\frac{\text{TAN}(\mu_S)}{\text{COS}(\alpha)}\right]$$

Equation (B-6)

$$\psi_D = \text{COS}^{-1}\left[\frac{(\text{RMM} + \text{ALT})^2 + (\text{RMS})^2 - (\text{RANGE})^2}{2\ (\text{RMS})\ (\text{RMM} + \text{ALT})}\right]$$

The angle ψ_D, as given by Equation (B-6) and obtained from Figure (B-2), is the lunar central angle from the LM position to the landing site.

The variables ALT and RANGE are the altitude above the mean lunar sphere and the slant range to the landing site, respectively. Both are functions of time and belong to the set of parameters which define a descent trajectory. It was therefore necessary to assume a "standard" descent and ascent trajectory profile for use in this simulation. The AS-504 Spacecraft Preliminary Reference Trajectory (PRT) results were used for this purpose. The only slight inaccuracy in adopting these results for a generalized simulation arises when the lunar site altitude (elevation with respect to the mean lunar sphere) is not equal to that used in the PRT. All landing sites were assumed to lie on the mean lunar sphere (RMM = RMS, or zero elevation), and the altitude data of the PRT was adjusted (biased) for this; the slant range to the landing site was not adjusted.

This completes the determination of the set (Ω_D, i_D, ν_D), for LM descent.

Transform Angles for Ascent Orbit

As an aid in determining relations between the several variables, it is useful to introduce the reference orbit which passes through the inertial position of the site at both landing and liftoff. This orbit is assigned a landing azimuth, α_{REF}, as indicated in Figure (B-3).

The dotted arc is the track of the extended landing site radius on a selocentered sphere; it is not an arc of a great circle. The angle $\Delta\chi$ is the angle between meridians through the inertial site locations at landing and liftoff, and is given by Equation (B-7) below, where ω_{MOON} is the rotation rate of the moon about its polar axis. The stay time, T_S, was rounded off to the next highest CSM orbit in this simulation.

Equation (B-7)

$$\Delta\chi = T_S \, \omega_{MOON}$$

The reference azimuth, α_{REF}, may then be determined from the spherical geometry of Figure (B-3), as follows:

Equation (B-8)

$$\alpha_{REF} = TAN^{-1} \left[\frac{-COS\left(\frac{\Delta\chi}{2}\right)}{-SIN\left(\frac{\Delta\chi}{2}\right) \; SIN(\mu_S)} \right]$$

In the subsequent determination of the transform angles, it will be necessary to utilize the arcs γ_1 and γ_2 of Figure (B-4). From Figure (B-3), it may be shown that γ_1 is given as follows:

Equation (B-9)

$$\gamma_1 = 2 \, SIN^{-1} \left[COS\,(\mu_S) \; SIN\left(\frac{\Delta\chi}{2}\right) \right]$$

The arc γ_2 is then determined from Figure (B-4), and is given by the following equations:

Equation (B-10)

$$\gamma_2 = TAN^{-1} \left[TAN(\gamma_1) \; COS\,(\delta\alpha) \right]$$

Equation (B-11)

$$\delta\alpha = (\alpha - \alpha_{REF})$$

The LM descent and ascent orbit tracks on the selenocentric sphere are shown in Figure (B-5). Returning to Figure (A-4) of Appendix A, note that $(\Delta v_D + 90°)$ is the angle, measured in

the direction of motion, from the descent orbit ascending node to the node line common to the descent and ascent orbits. The increment in descent anomaly is given as follows:

Equation (B-12)

$$\Delta\nu_D = (\psi_2 - \gamma_2)$$

It may be shown that Equation (B-12) will hold for $\alpha \lesssim 270°$, $\mu_S \gtrsim 0°$, and $\lambda_S \lesssim 0°$.

The node line common to the descent and ascent orbits is determined once the arc $\Delta\nu_D$ is known; this fixes the position of the CSM plane change burn. For a particular landing azimuth, α, the required plane change is determined by Equation (B-13) below, with reference to Figure (B-4):

Equation (B-13)

$$\Delta i = \text{SIN}^{-1}\left[\text{SIN}(\gamma_1)\ \text{SIN}(\delta\alpha)\right]$$

There remains the determination of ψ_A in the ascent transform set (Ω_D, i_D, $\Delta\nu_D$, Δi, ψ_A). Reference to Figures (B-5) and (B-6) indicates that ψ_A is given by Equation (B-14) below:

Equation (B-14)

$$\psi_A = \text{COS}^{-1}\left[\frac{(\text{RMM} + \text{ALT})^2 + (\text{RMS})^2 - (\text{RANGE})^2}{2(\text{RMS})\ (\text{RMM} + \text{ALT})}\right]$$

This is the range angle between the LM and the landing site, and the variables on the right side of the equation were taken from the AS-504 PRT, as previously mentioned for powered descent.

This completes the determination of all transform angles needed in the equations for simulation that were presented in Appendix A.

APPENDIX C

ANTENNA ANGLE CONSTRAINTS

A qualitative discussion of antenna angle constraints was presented in Section (1.0), and excluded antenna coverage was indicated on the figures of Section (5.1). This appendix will serve to explain in detail the determination of antenna constraints.

Gimbal Limits

The physical gimbal limits for the S-Band steerable antenna are as follows: (Reference 14)

Equation (C-1)

$$-75° \leq \text{Antenna Azimuth} \leq 75°$$

$$-75° \leq \text{Antenna Elevation} \leq 255°$$

For the trajectories of current mission planning, these gimbal limits will not impose a constraint on LM-Earth communications during powered descent and ascent, provided yawing from a "face-down" to a "face-out" attitude is not planned. During coasting descent and ascent, these limits will be no problem if the proper pitch and roll attitudes are maintained.

Structural Interference

Figure (C-1) gives the limits on antenna coverage imposed by beam interference. (Reference 15) The steerable antenna will track an RF Signal from Earth in order to maintain transmission in the proper direction. Reflection of this RF beam off the RCS nozzles as well as the outer skin of the LM may cause the antenna to lose earth-lock. A guardband of 8-1/2° (or a 32 inch diameter cylinder) about the antenna boresight has been established to prevent RF track interference, and these limits are indicated on Figure (C-1). Note that blockage of transmission through the excluded areas on Figure (C-1) will not be nearly as severe a problem as track interference, so that with manual tracking, for example, one could possibly overcome much of the communications loss. An inertial hold system for the antenna was proposed in Reference 14, but discarded because of a variety of implementation problems.

The region on Figure (C-1) that is marked off by a heavy solid boundary represents the limits used in this analysis. These limits are the same as those appearing on the figures of Section (5.1). Note that the guardband is compromised slightly by these limits, but that in general these are conservative.

APPENDIX D

LUNAR OPTICAL LIBRATIONS

Figure (D-1) (a) depicts an "edge-on" view of the earth-moon orbit plane and the plane of the ecliptic (earth-sun orbit plane). The geometry shown is for a mean lunar motion. As can be seen, the moon appears to tip its polar axis toward or away from the Earth when it is below or above the ecliptic, respectively. To an earth-based observer, this results in an apparent oscillation in latitude, or an optical libration. Figure (D-1) (b) presents a view of the earth-moon plane from the ecliptic pole. Since the lunar orbit is not precisely circular, the Moon's angular rate of motion in orbit is not exactly equal to its angular rotation about its polar axis. This results in an apparent oscillation in longitude to an earth based observer. The sun perturbs the mean motion of the moon so as to cause a 360° regression of the line of nodes as well as a progression of the line of apsides, in 18.6 and 8.85 years, respectively. The orbital eccentricity and inclination are also perturbed by the sun. These effects cause the latitude and longitude librations to vary from month to month.

When the latitude and longitude librations are considered simultaneously, they cause the moon-earth line to describe a path or locus on the selenographic sphere. Figures (D-2), (a) through (d), indicate examples of the variation of this locus from July, 1968 through June, 1969. The data used in the generation of these curves was taken from JPL ephemeris tapes.

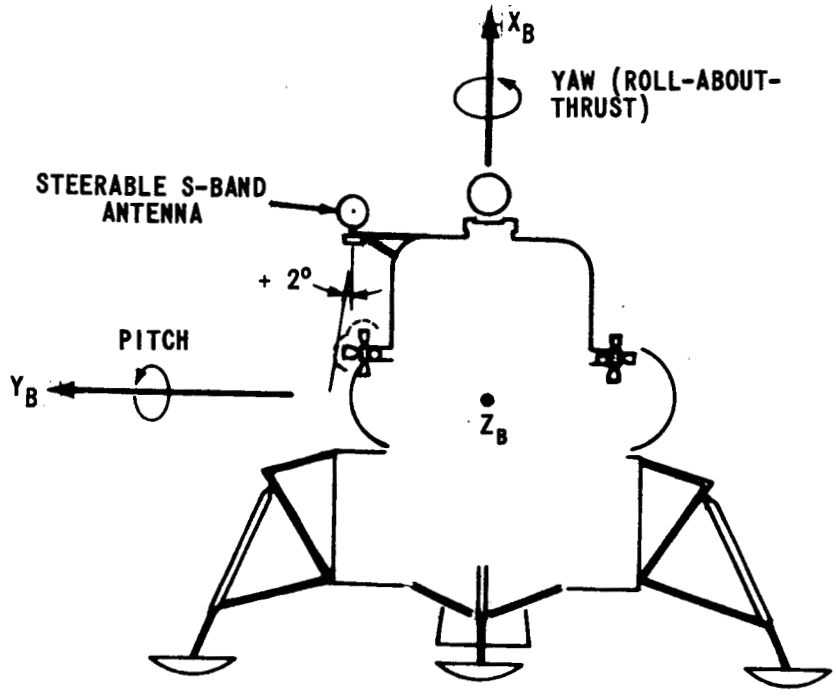

(a) LM FRONT VIEW

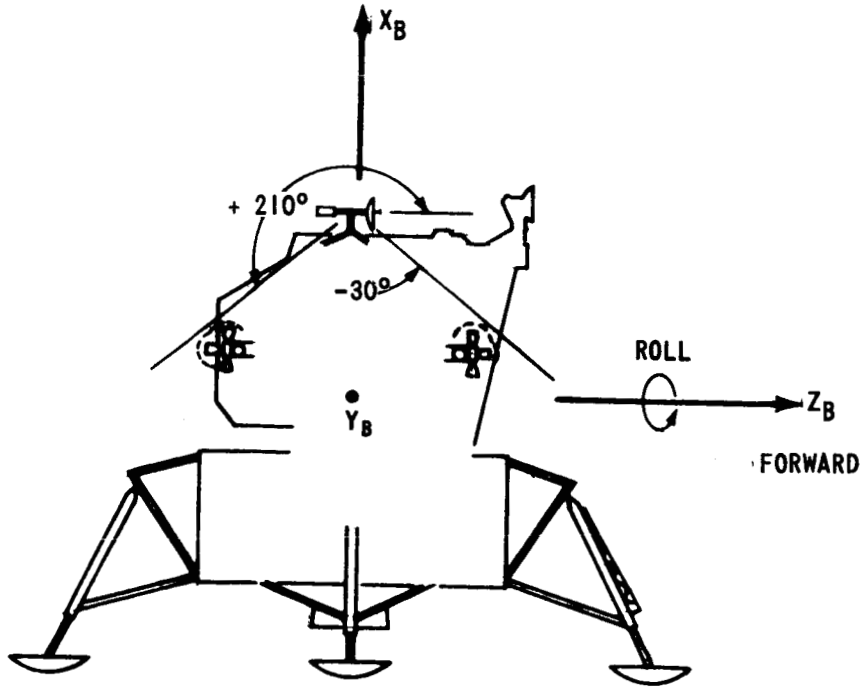

(b) LM RIGHT-HAND-SIDE

S-BAND ANTENNA BEAM INTERFERENCE

FIGURE (1)

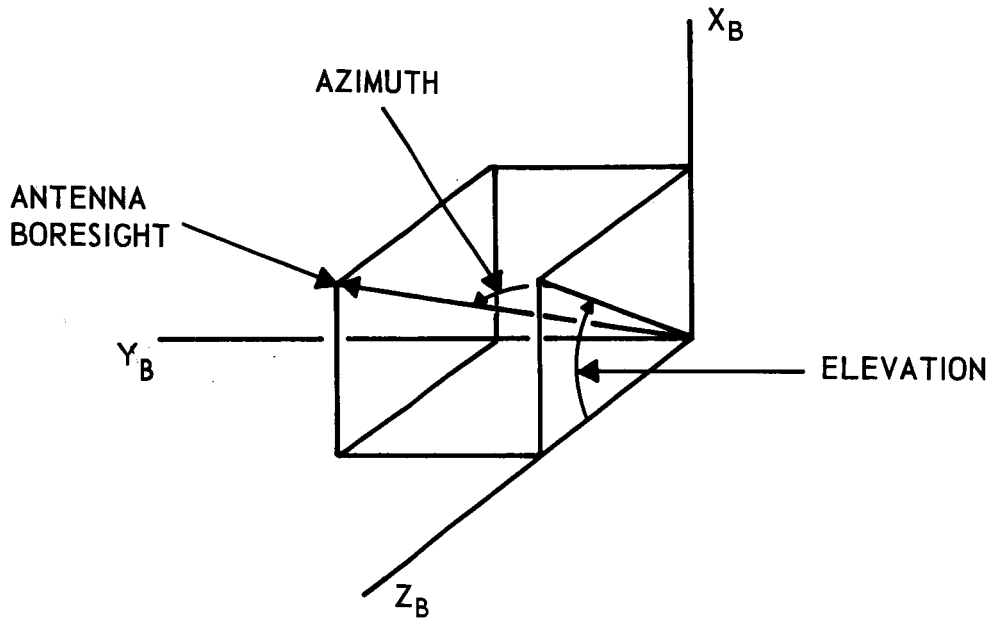

(a)

DEFINITION OF ANTENNA ANGLES

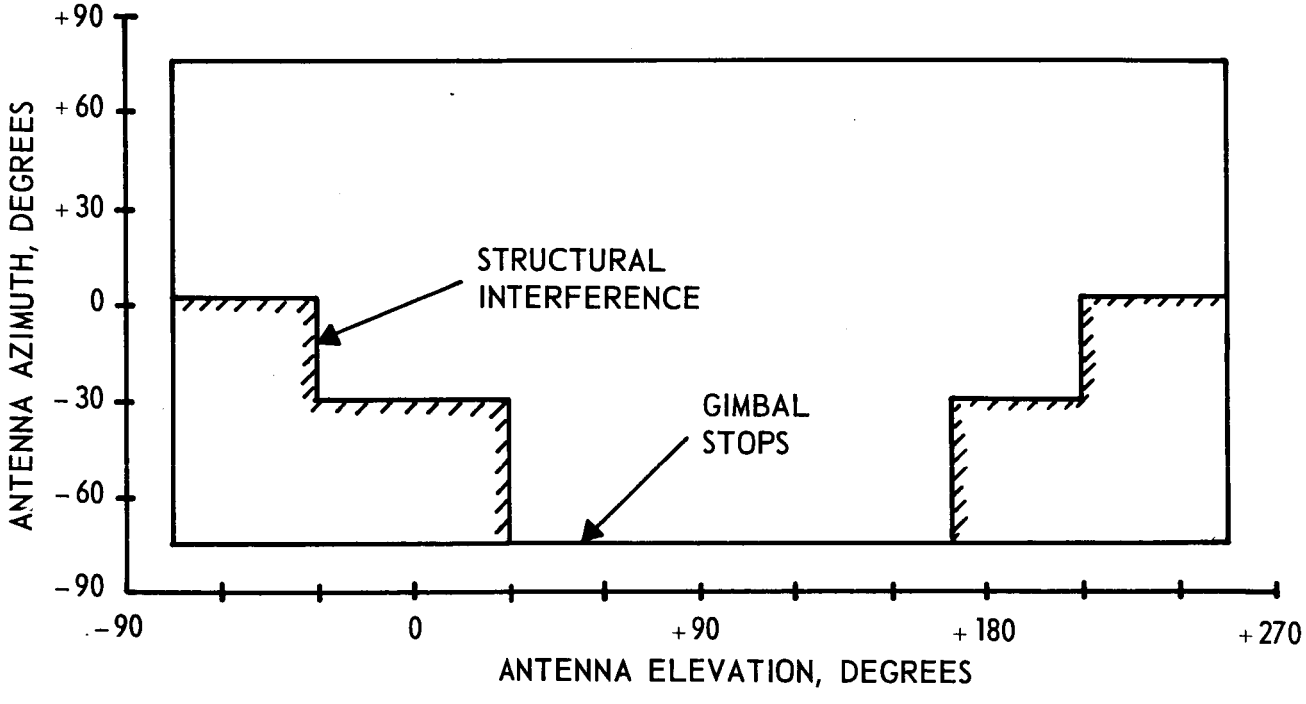

(b)

ANTENNA COVERAGE

FIGURE (2)

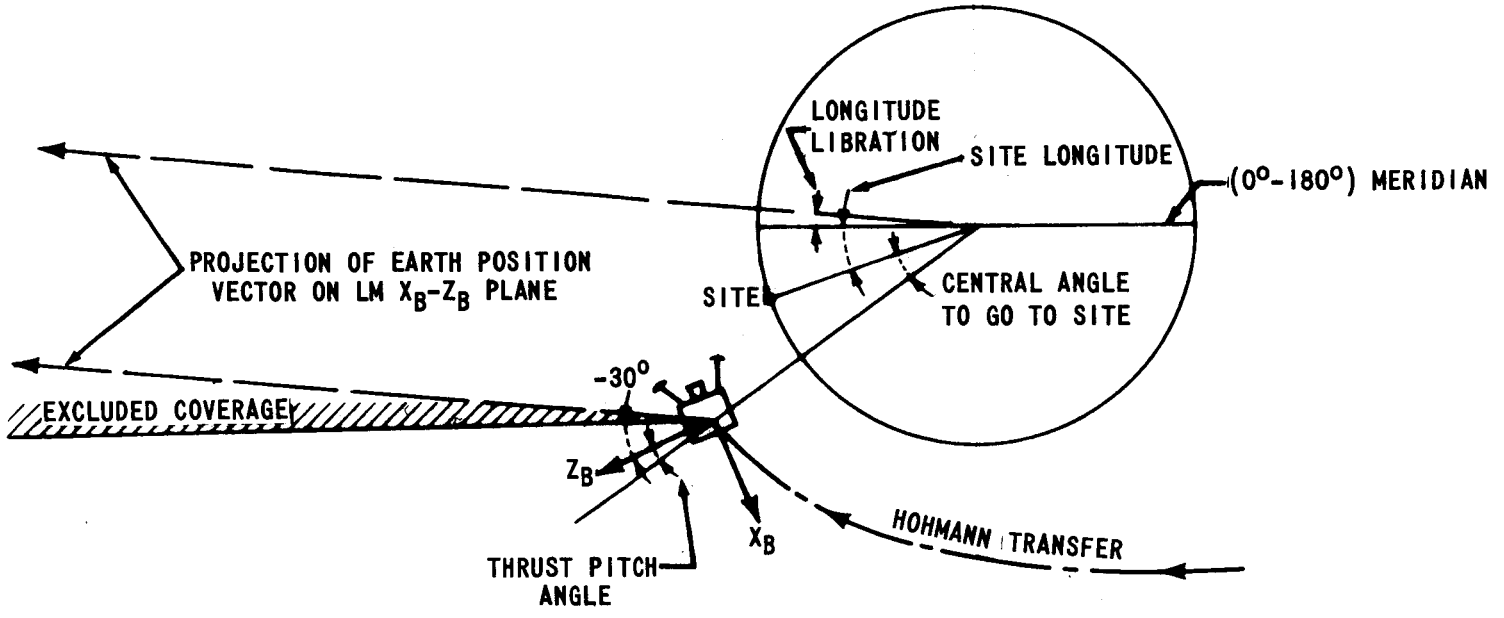

(a) POWERED DESCENT

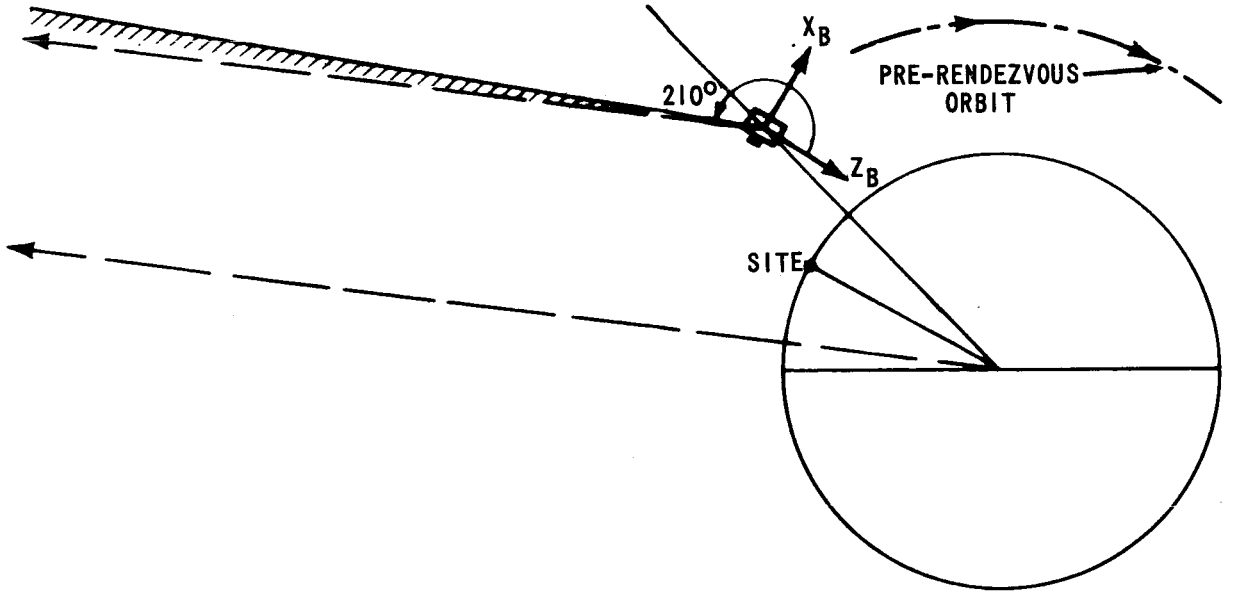

(b) POWERED ASCENT

IN-PLANE GEOMETRY FOR LM DESCENT AND ASCENT

FIGURE (3)

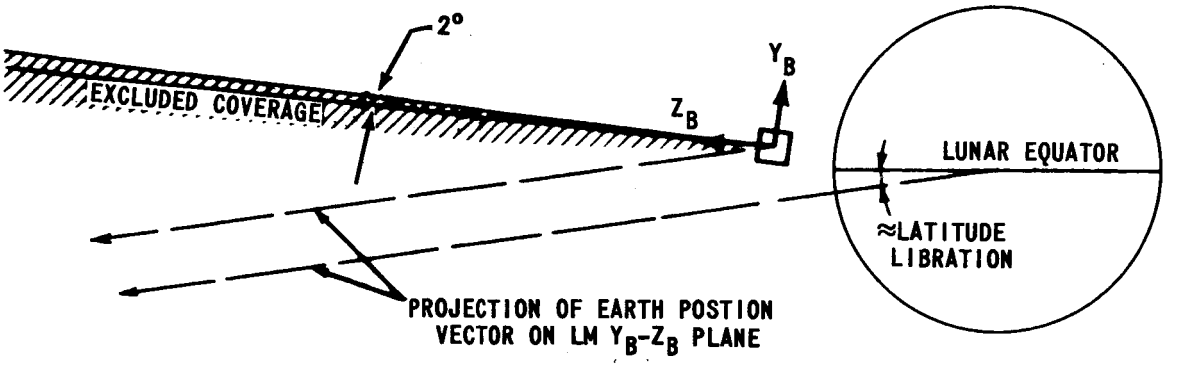

(a) BLACKOUT SITUATION

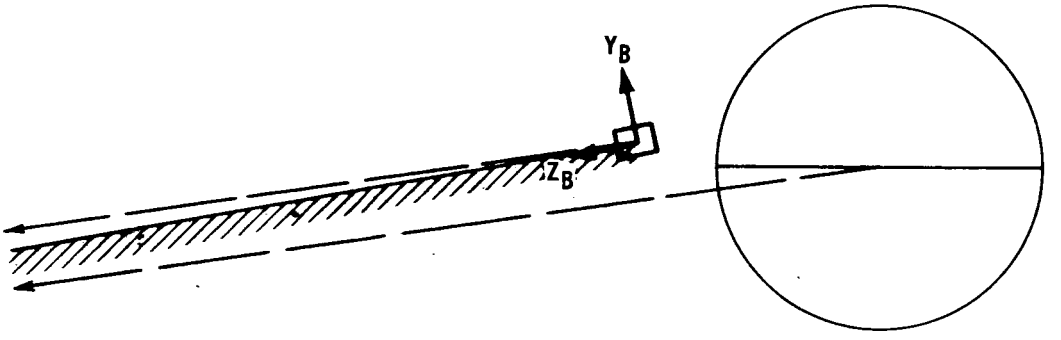

(b) CORRECTIVE YAW RE-ORIENTATION

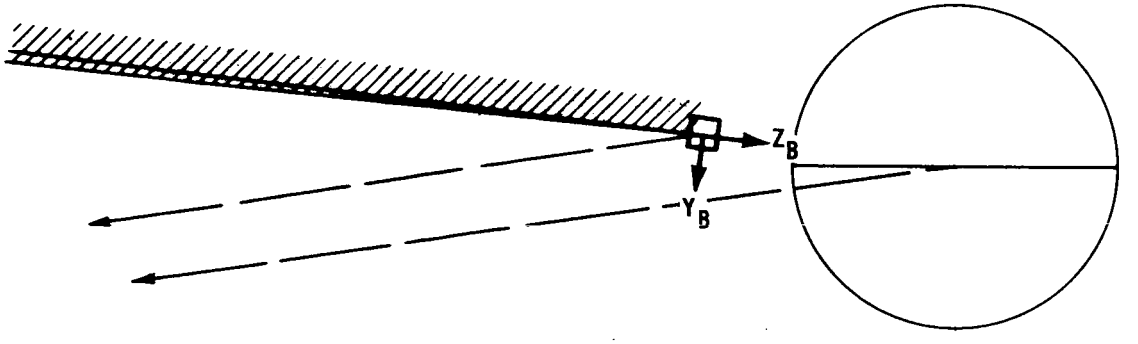

(c) 180° YAW (SURFACE VIEWING)

CROSS-PLANE GEOMETRY FOR LM DESCENT

FIGURE (4)

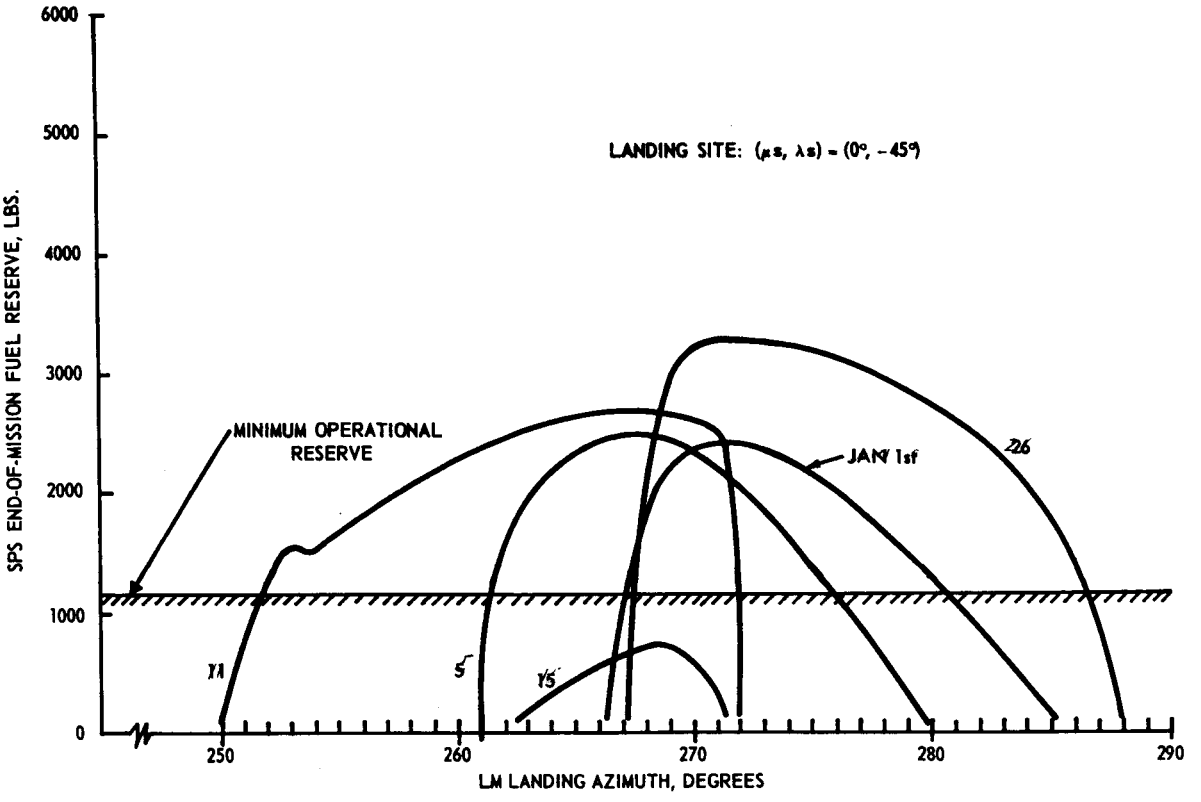

(a)

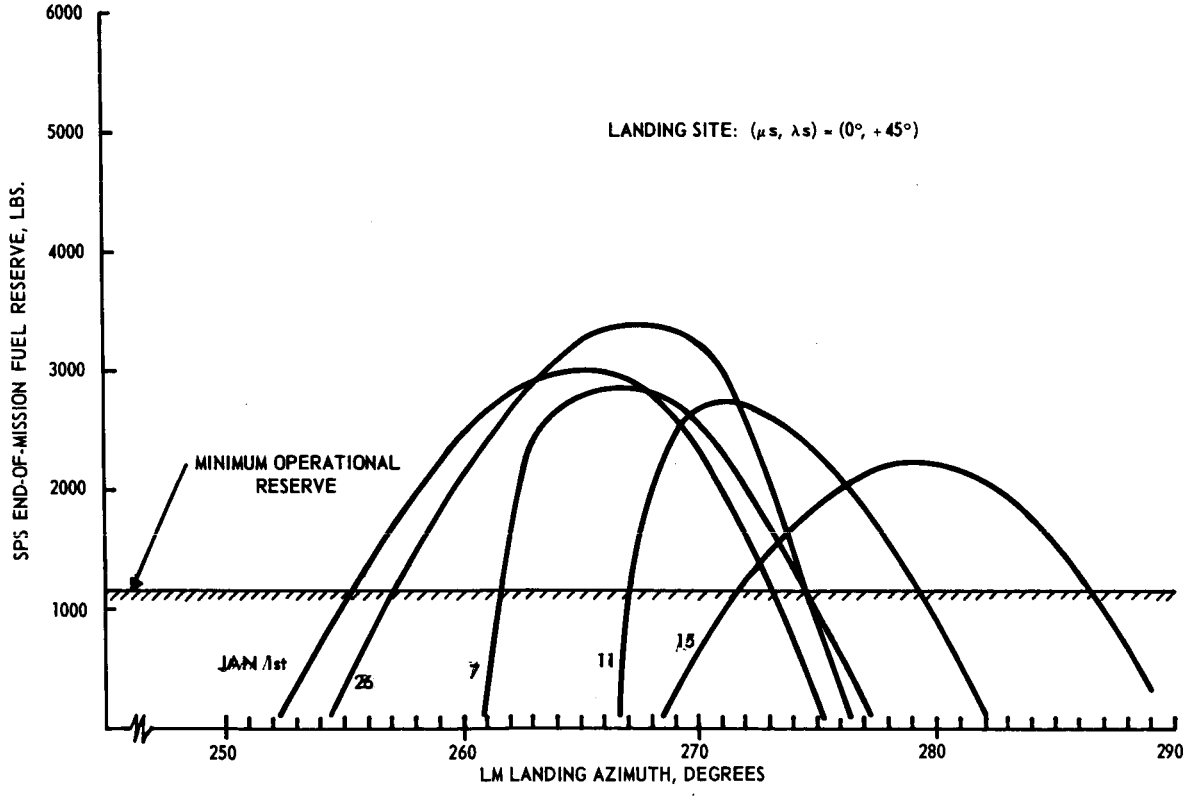

(b)

SPS FUEL RESERVE VS. LM LANDING AZIMUTH
PACIFIC INJECTION
LAUNCH DATES IN JANUARY 1969

FIGURE (5)

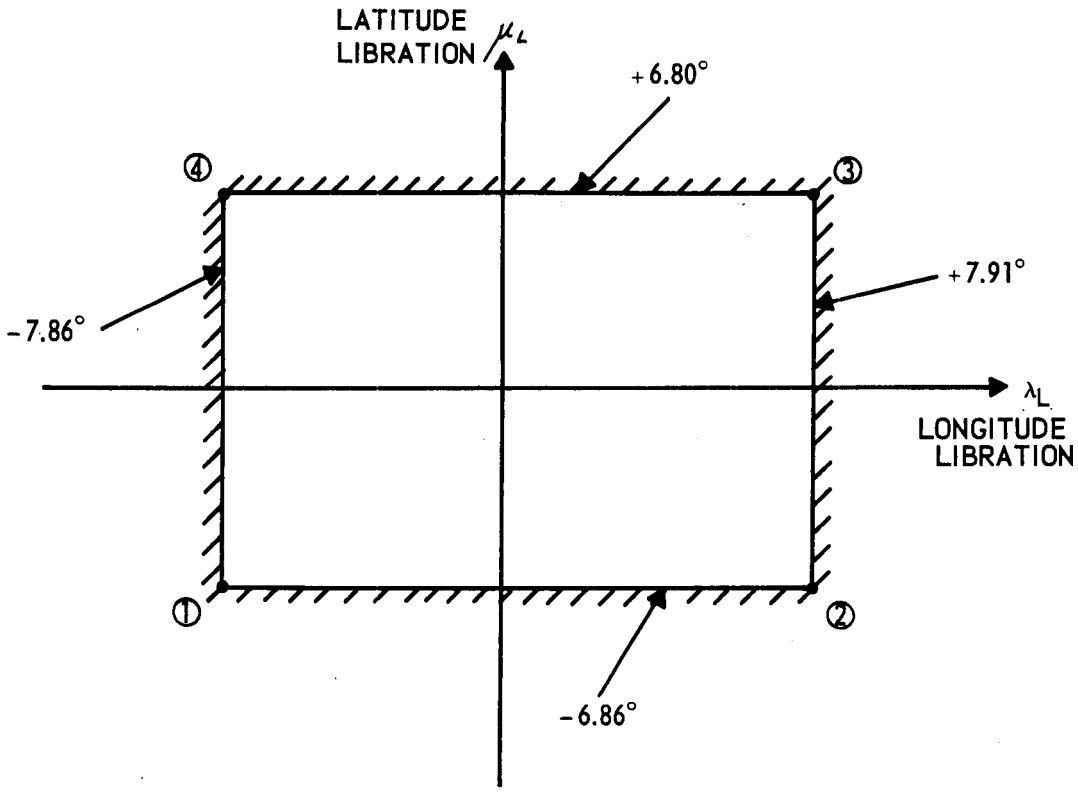

① : "WORST" CASE LIBRATIONS FOR DESCENT INTERFERENCE
② : "WORST" CASE LIBRATIONS FOR ASCENT INTERFERENCE
③ : "BEST" CASE LIBRATIONS FOR DESCENT INTERFERENCE
④ : "BEST" CASE LIBRATIONS FOR ASCENT INTERFERENCE

(a)

JAN. 1968 THRU DEC. 1969

μ_{LMAX}	= +6.80°	APR. 19, 1968, 0^h
μ_{LMIN}	= -6.86°	MAR. 25, 1969, 12^h
λ_{LMAX}	= 7.91°	DEC. 25, 1968, 12^h
λ_{LMIN}	= -7.86°	JUNE 24, 1969, 0^h

JAN. 1968 THRU DEC. 1968

μ_{LMAX}	= +6.80°	APR. 19, 1968, 0^h
μ_{LMIN}	= -6.85°	APR. 6, 1968, 12^h
λ_{LMAX}	= 7.91°	DEC. 25, 1968, 12^h
λ_{LMIN}	= -7.70°	MAY 6, 1968, 12^h

(b)

BOUNDS ON THE LUNAR LIBRATIONS

FIGURE (6)

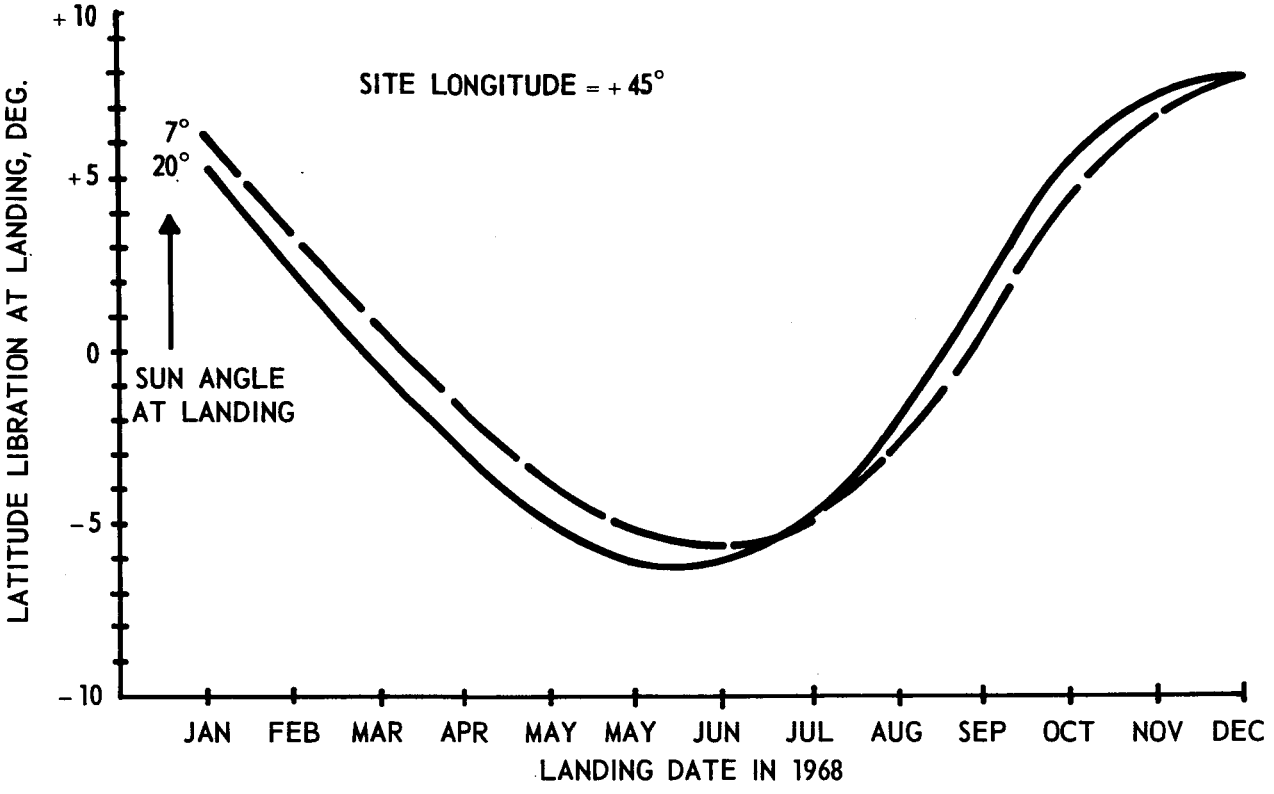

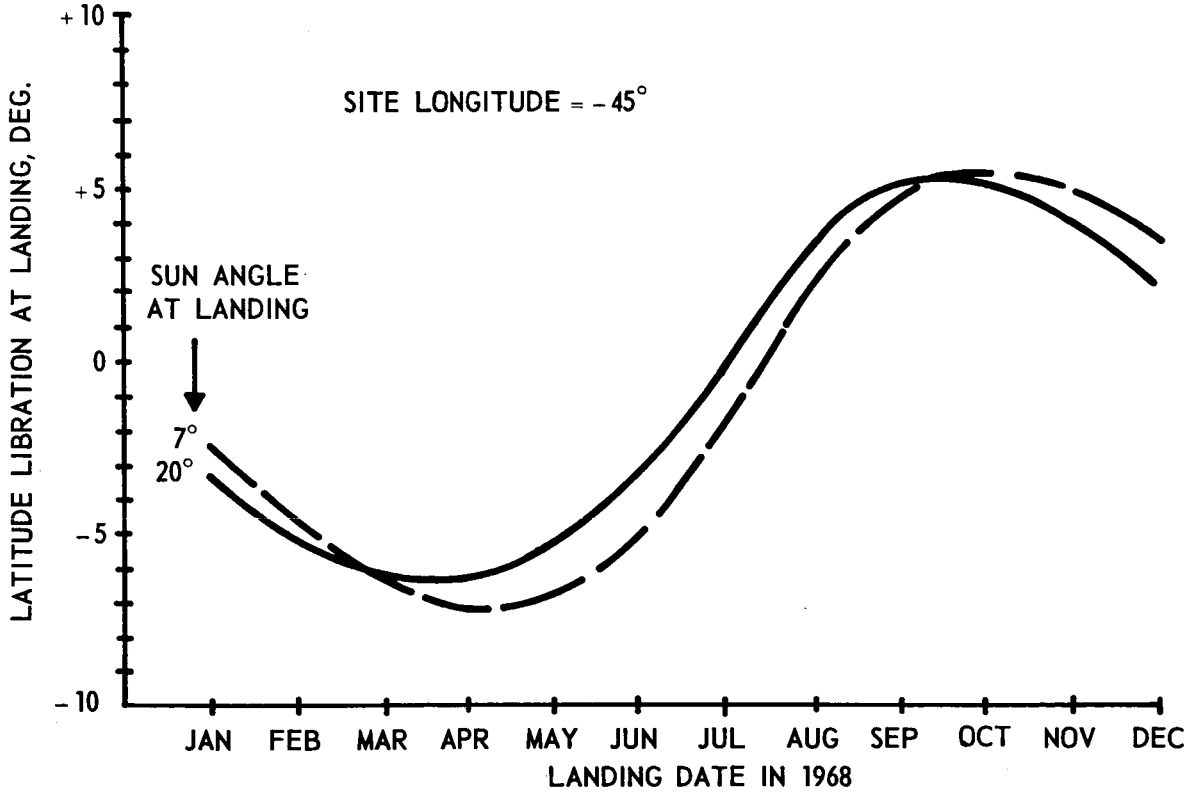

VARIATION OF LATITUDE LIBRATIONS FOR PARTICULAR LANDING OPPORTUNITIES

FIGURE (7)

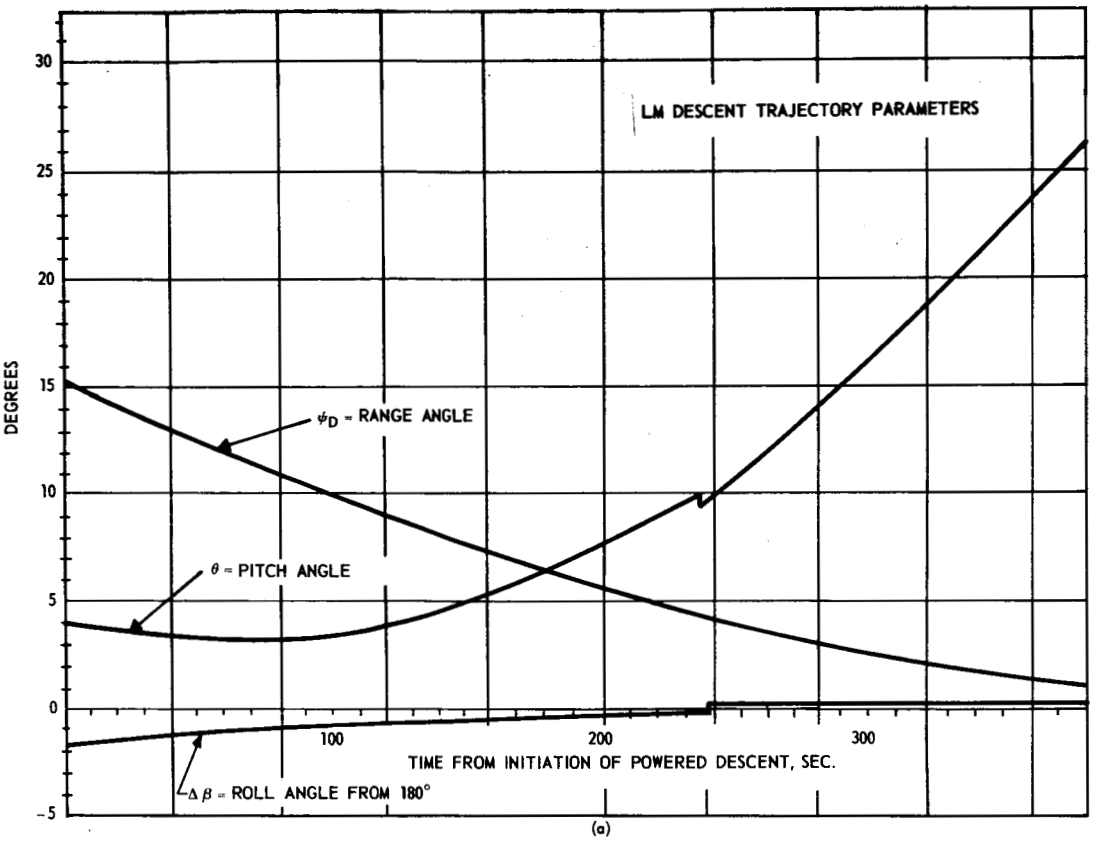

(a)

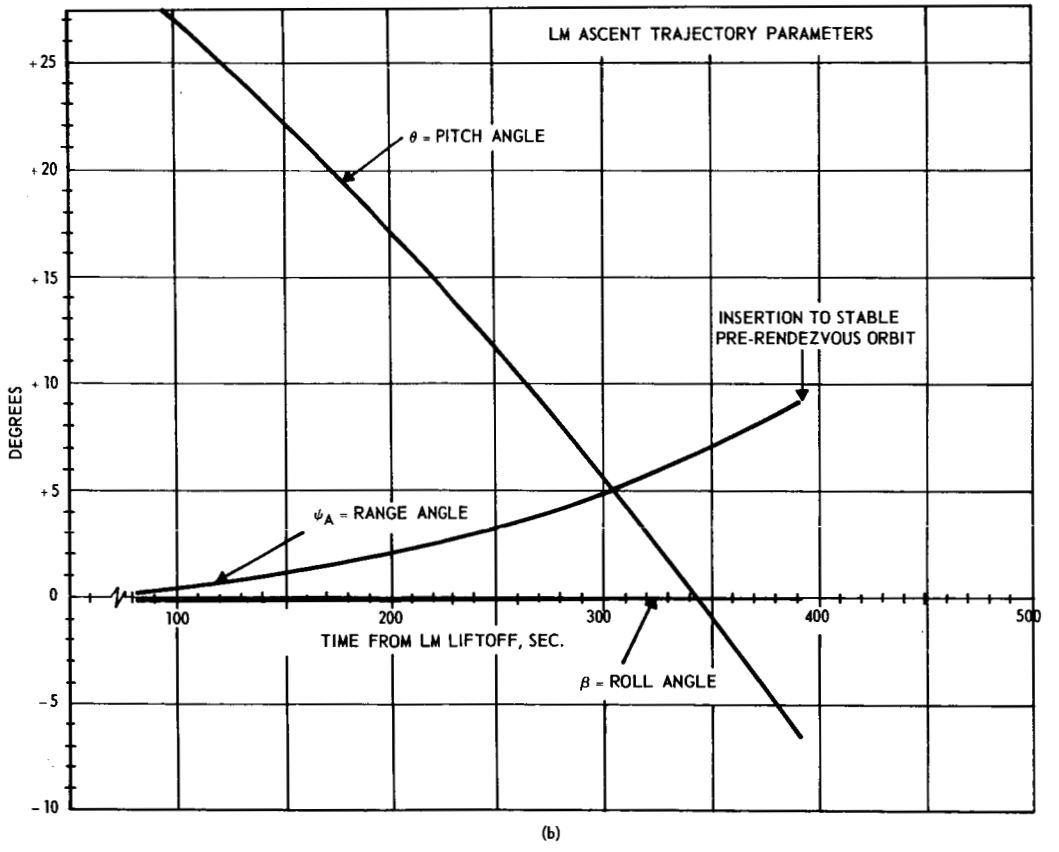

(b)

FIGURE (8)
LM TRAJECTORY AND ATTITUDE DATA (REF. 3)

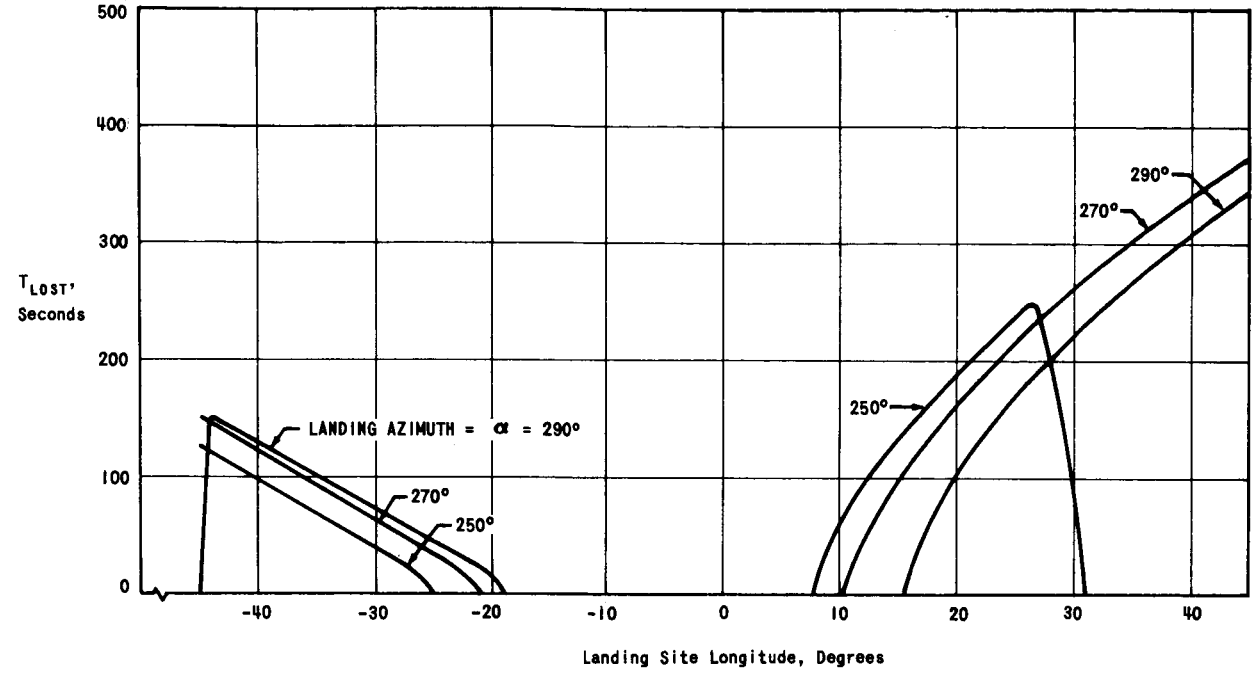

(a)

INTERFERENCE TIME VS. LANDING SITE LONGITUDE

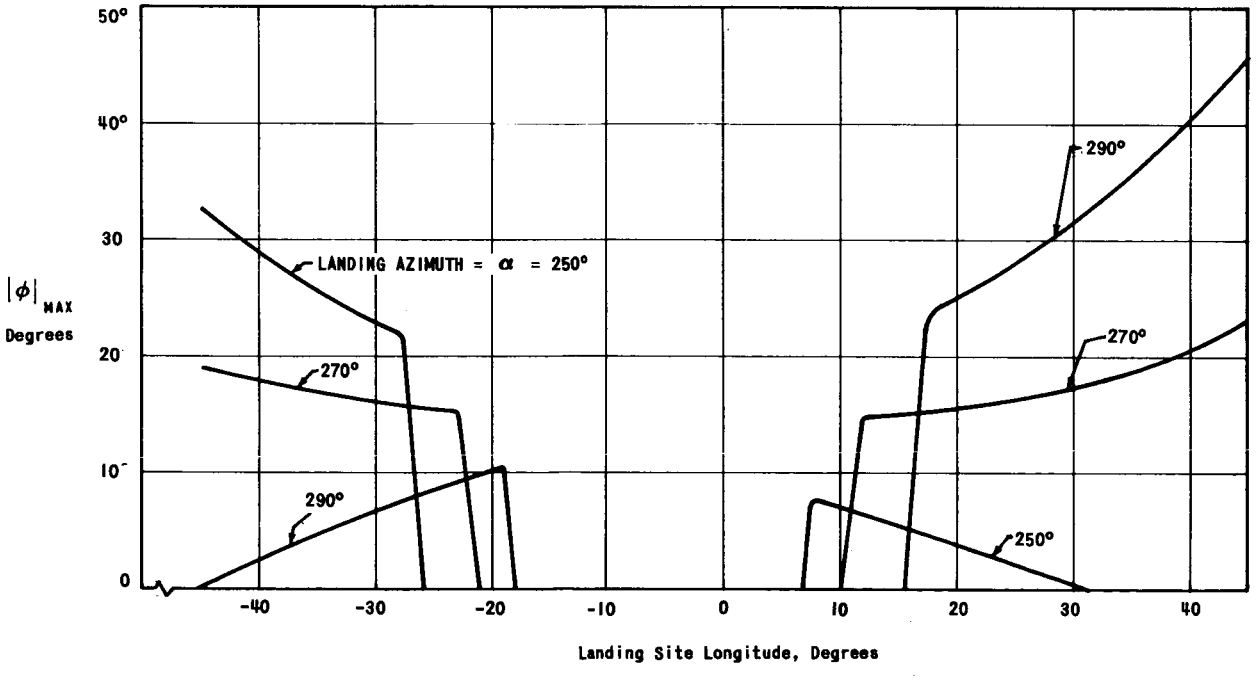

(b)

MAXIMUM YAW VS. LANDING SITE LONGITUDE

FIGURE (9)

LIBRATIONS: $(\mu_L, \lambda_L) = (-6.85°, -7.70°)$

SITE LATITUDE: $\mu_s = +5°$

STAY TIME: $T_s = 44$ HOURS

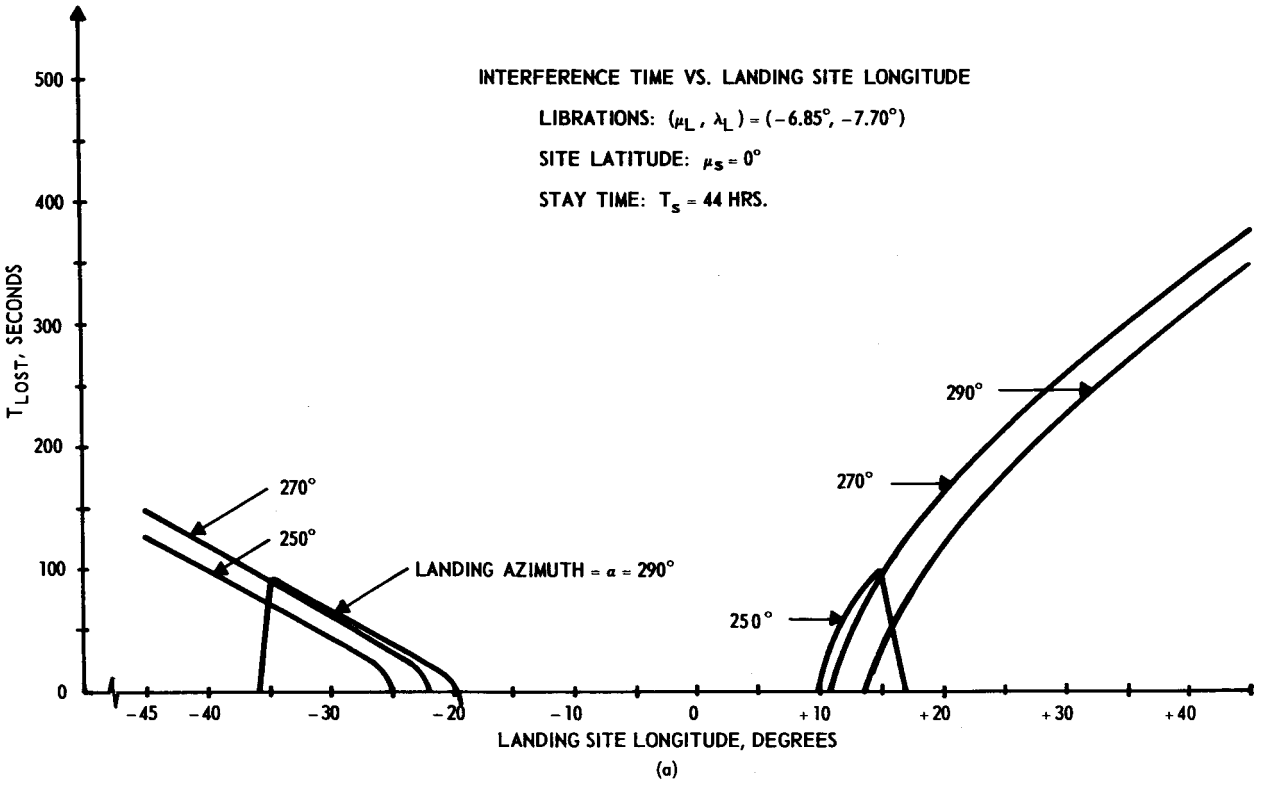
INTERFERENCE TIME VS. LANDING SITE LONGITUDE
LIBRATIONS: $(\mu_L, \lambda_L) = (-6.85°, -7.70°)$
SITE LATITUDE: $\mu_S = 0°$
STAY TIME: $T_S = 44$ HRS.
T_{LOST}, SECONDS
500
400
300
200
100
0
270°
250°
LANDING AZIMUTH = α = 290°
290°
270°
250°
-45
-40
-30
-20
-10
0
+10
+20
+30
+40
LANDING SITE LONGITUDE, DEGREES

(a)

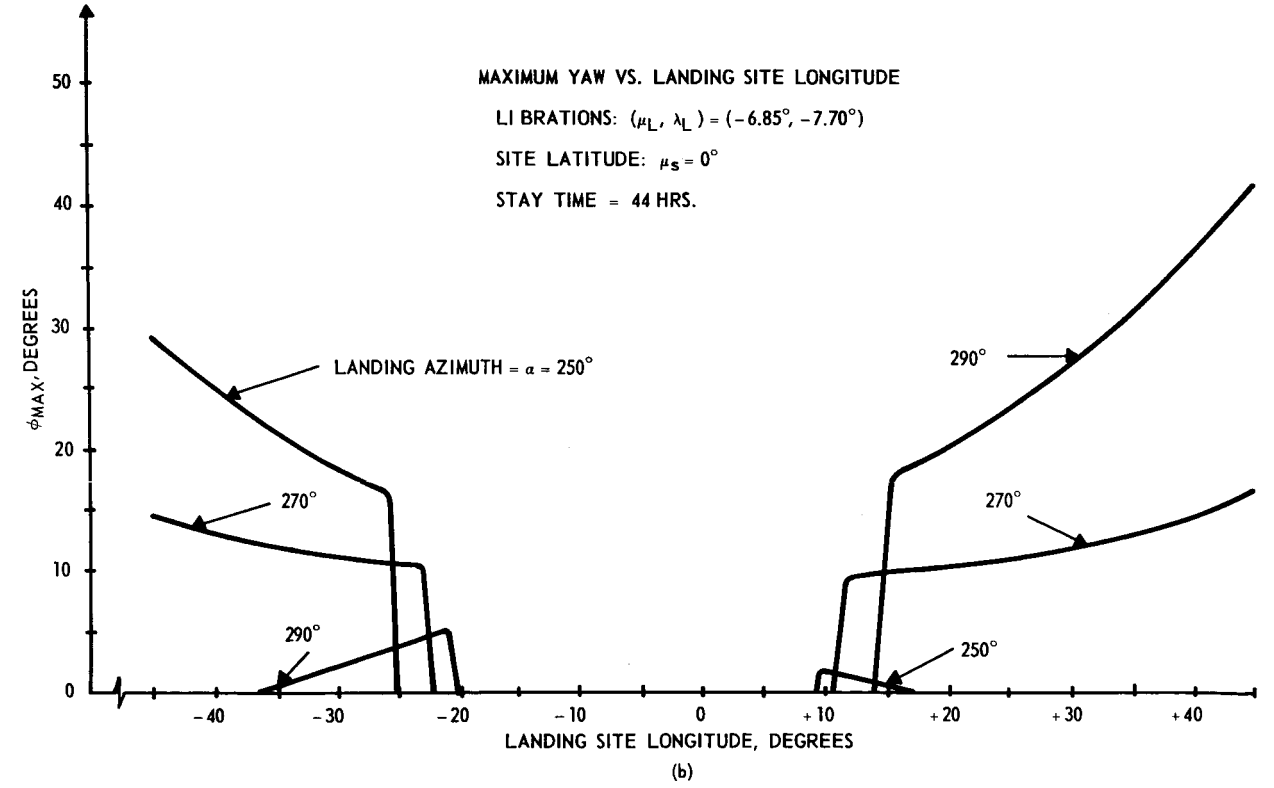
MAXIMUM YAW VS. LANDING SITE LONGITUDE
LIBRATIONS: $(\mu_L, \lambda_L) = (-6.85°, -7.70°)$
SITE LATITUDE: $\mu_S = 0°$
STAY TIME = 44 HRS.
ϕ_{MAX}, DEGREES
50
40
30
20
10
0
LANDING AZIMUTH = α = 250°
270°
290°
290°
270°
250°
-40
-30
-20
-10
0
+10
+20
+30
+40
LANDING SITE LONGITUDE, DEGREES

(b)

FIGURE (10)

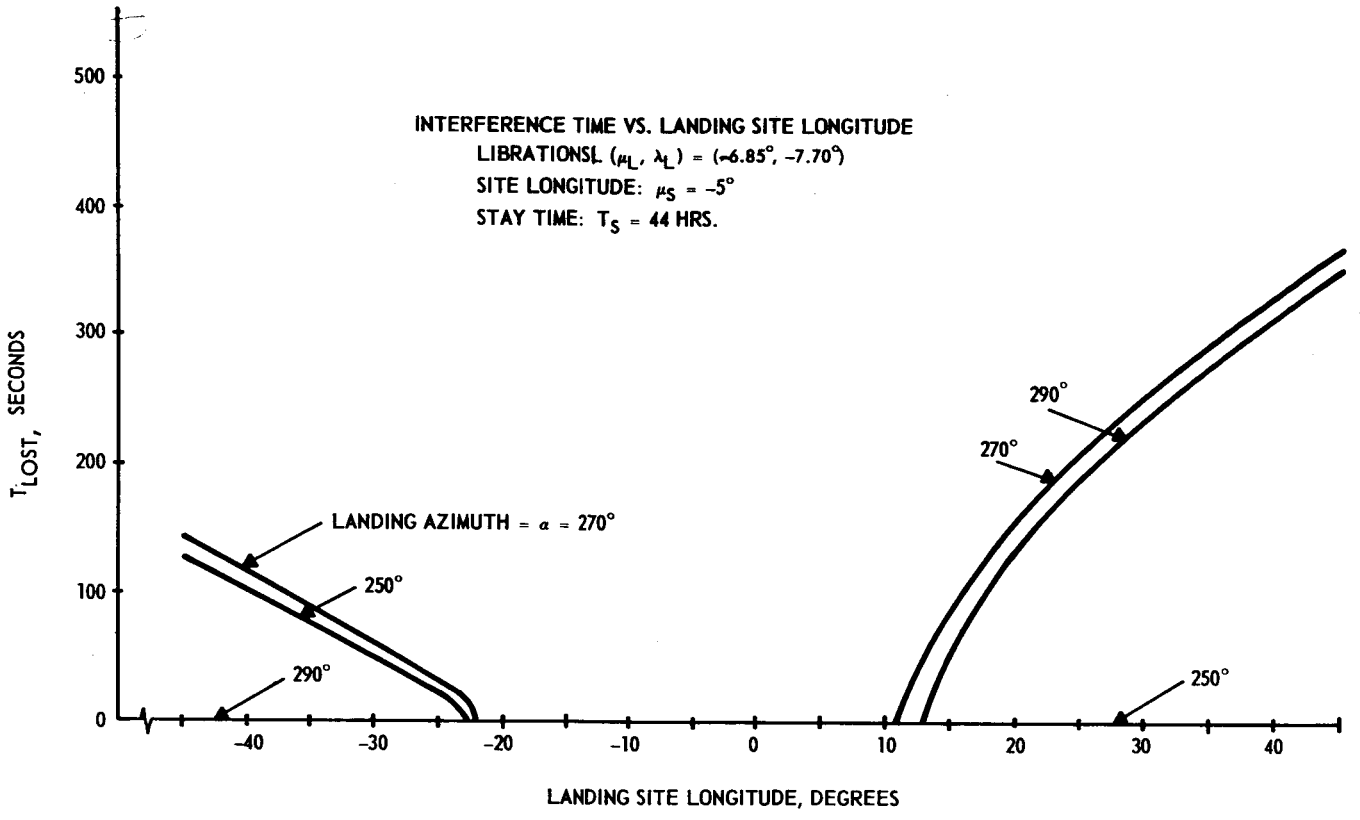
INTERFERENCE TIME VS. LANDING SITE LONGITUDE
LIBRATIONSL (μ_L, λ_L) = (-6.85°, -7.70°)
SITE LONGITUDE: μ_S = -5°
STAY TIME: T_S = 44 HRS.
T_{LOST}, SECONDS
LANDING AZIMUTH = α = 270°
250°
290°
290°
270°
250°
LANDING SITE LONGITUDE, DEGREES

(a)

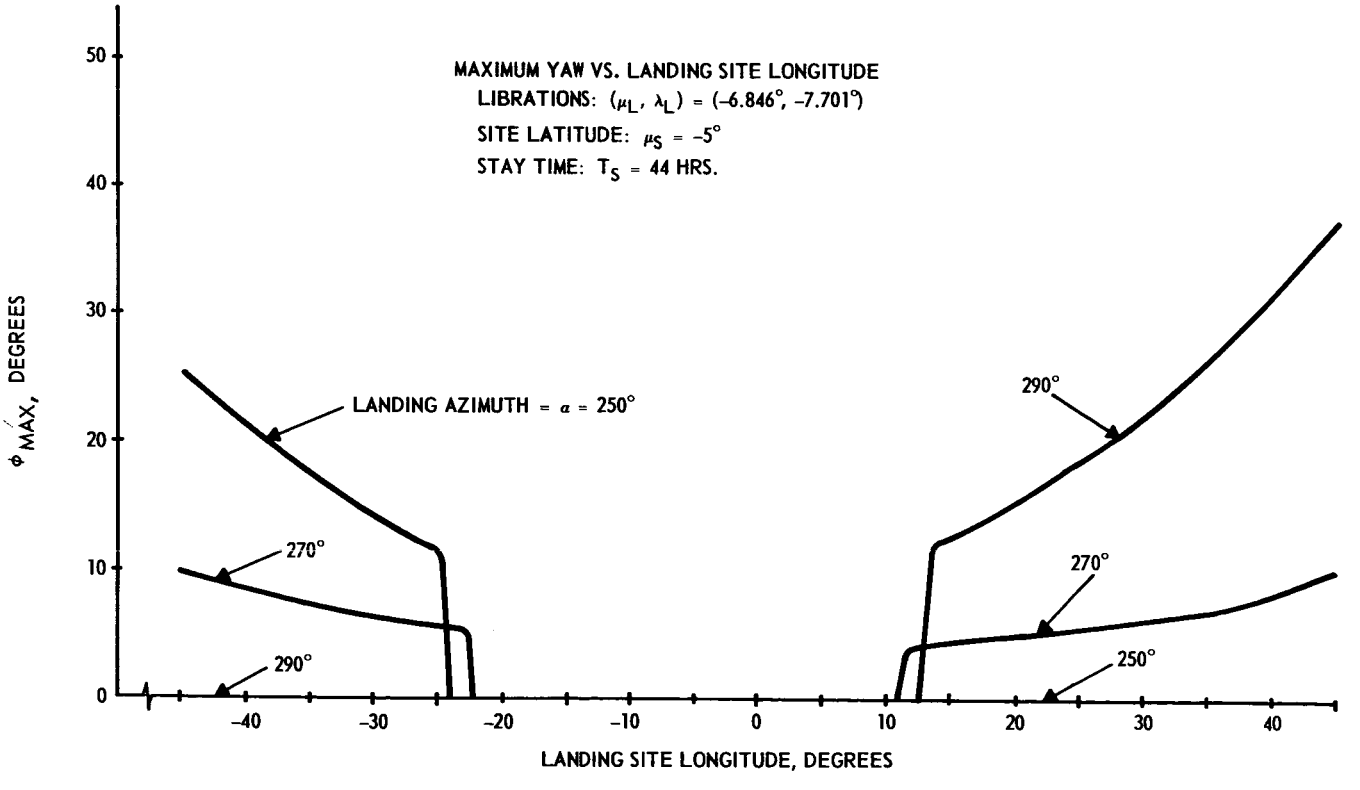
MAXIMUM YAW VS. LANDING SITE LONGITUDE
LIBRATIONS: (μ_L, λ_L) = (-6.846°, -7.701°)
SITE LATITUDE: μ_S = -5°
STAY TIME: T_S = 44 HRS.
ϕ_{MAX}, DEGREES
LANDING AZIMUTH = α = 250°
270°
290°
290°
270°
250°
LANDING SITE LONGITUDE, DEGREES

(b)

FIGURE (11)

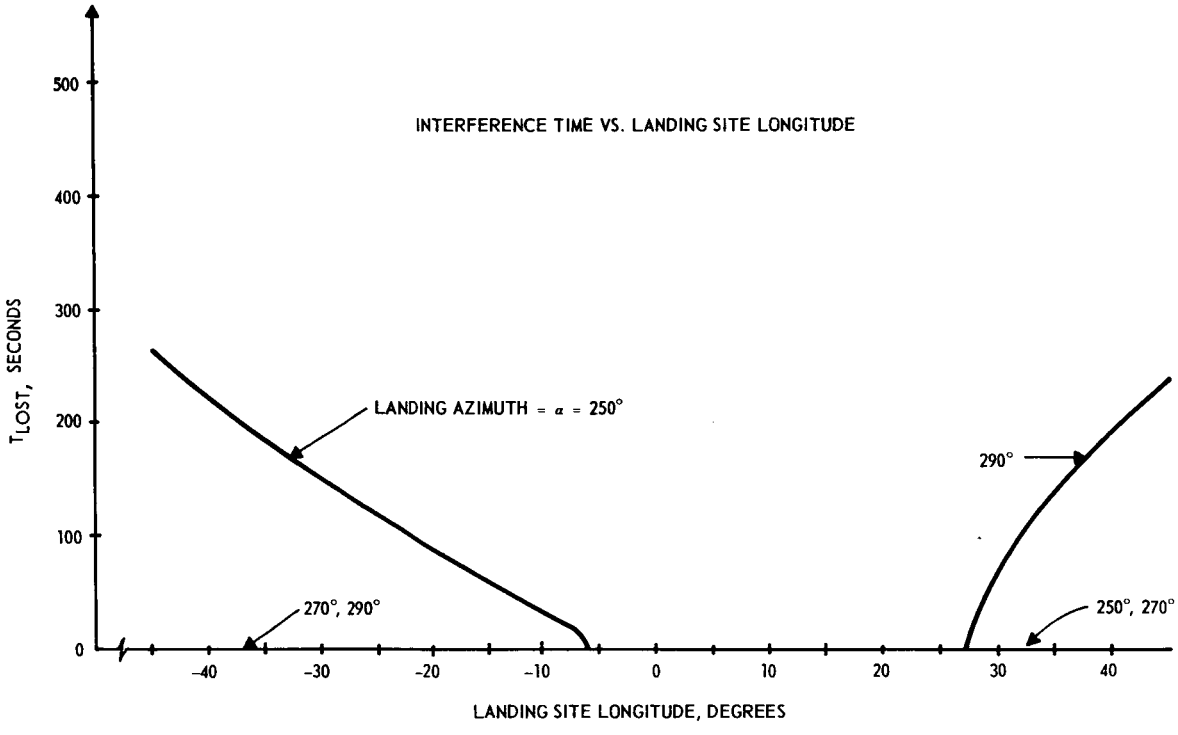

(a)

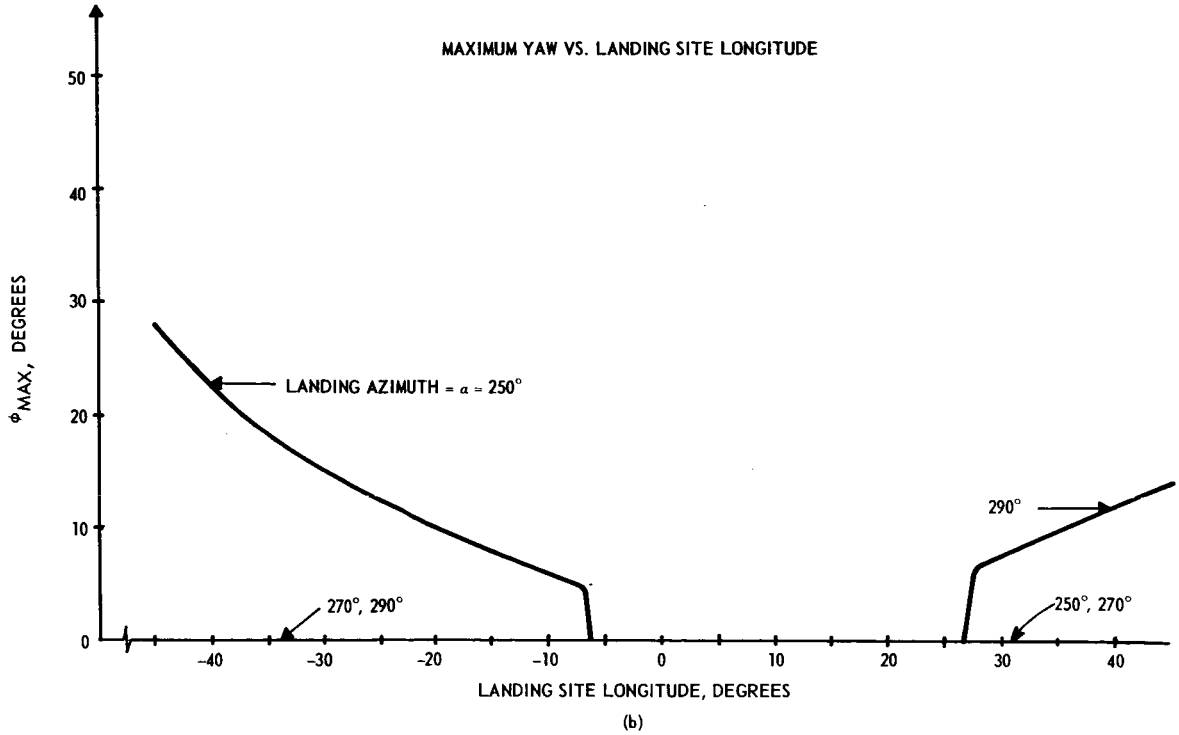

(b)

LIBRATIONS: $(\mu_L, \lambda_L) = (6.80°, 7.91°)$
SITE LATITUDE: $\mu_S = 5°$
STAY TIME: $T_S = 44$ HRS

FIGURE (12)

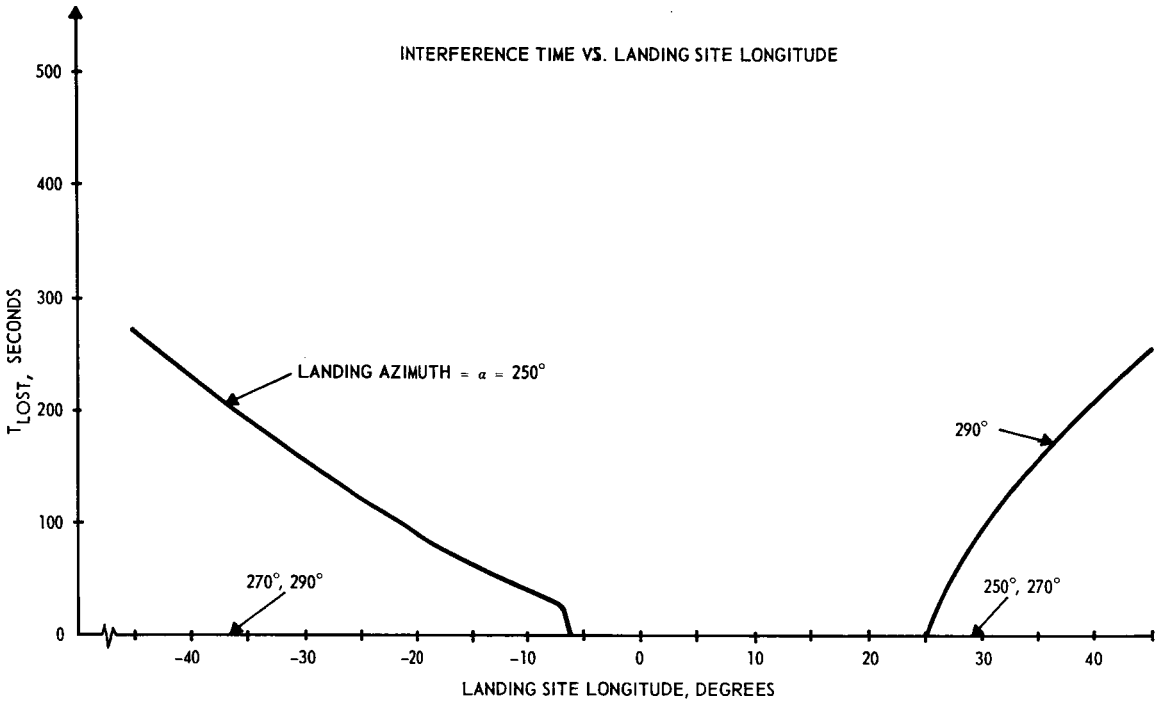

(a)

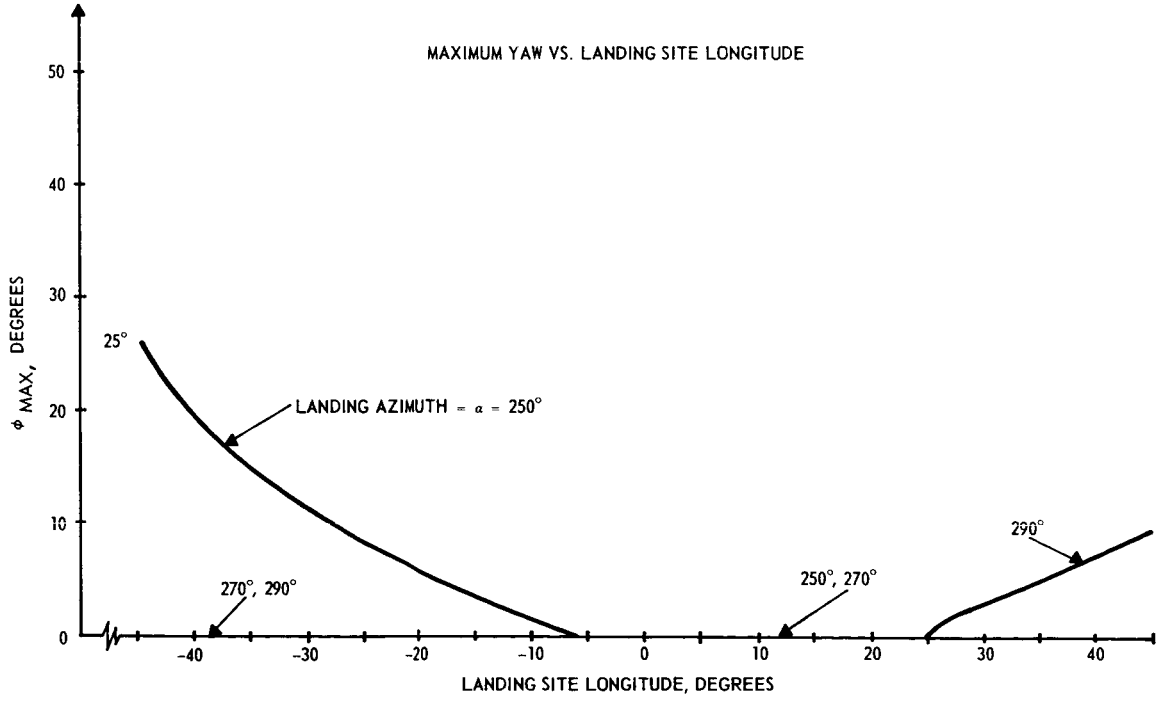

(b)

LIBRATIONS: $(\mu_L, \lambda_L) = (6.80°, 7.91°)$
SITE LATITUDE: $\mu_S = 0°$
STAY TIME: $T_S = 44$ HRS.

FIGURE (13)

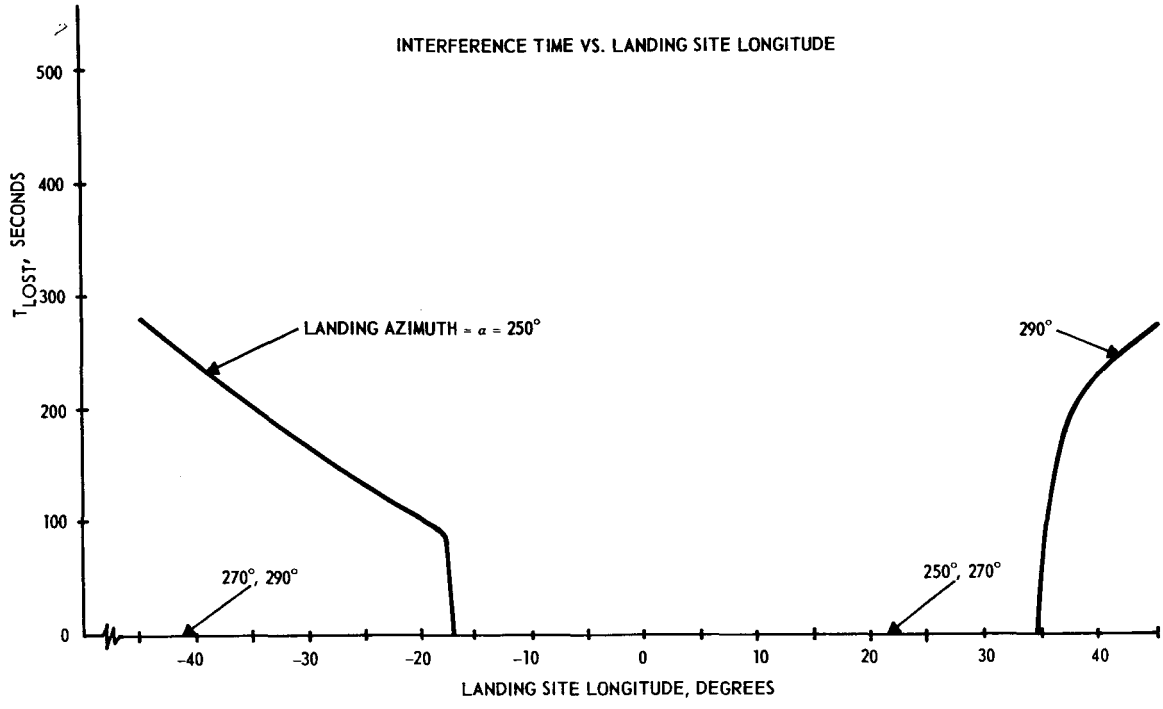

(a)

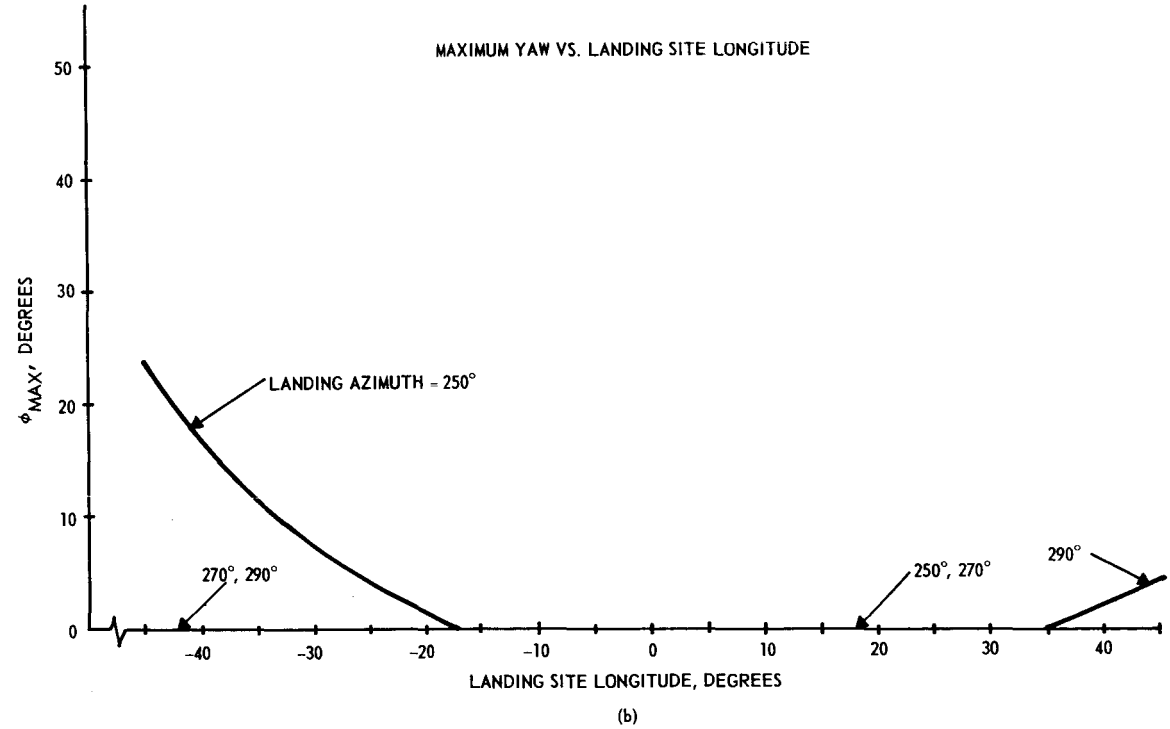

(b)

LIBRATIONS: $(\mu_L, \lambda_L) = (6.80°, 7.91°)$
SITE LATITUDE: $\mu_S = -5°$
STAY TIME: $T_S = 44$ HRS.

FIGURE (14)

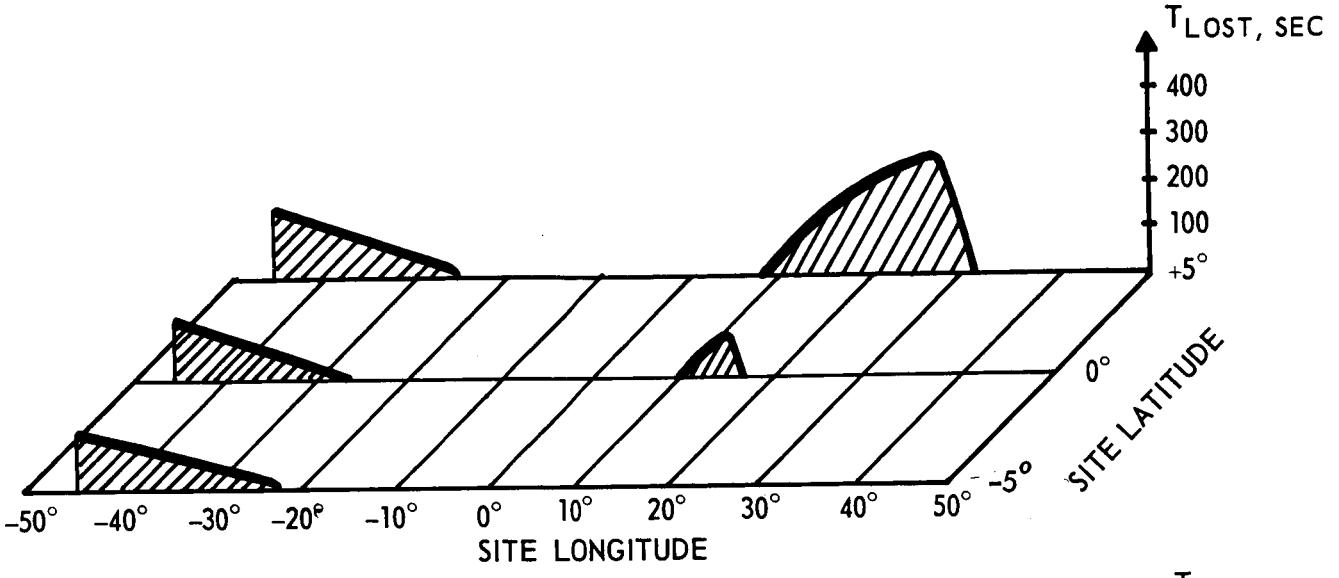

$\alpha = 250°$

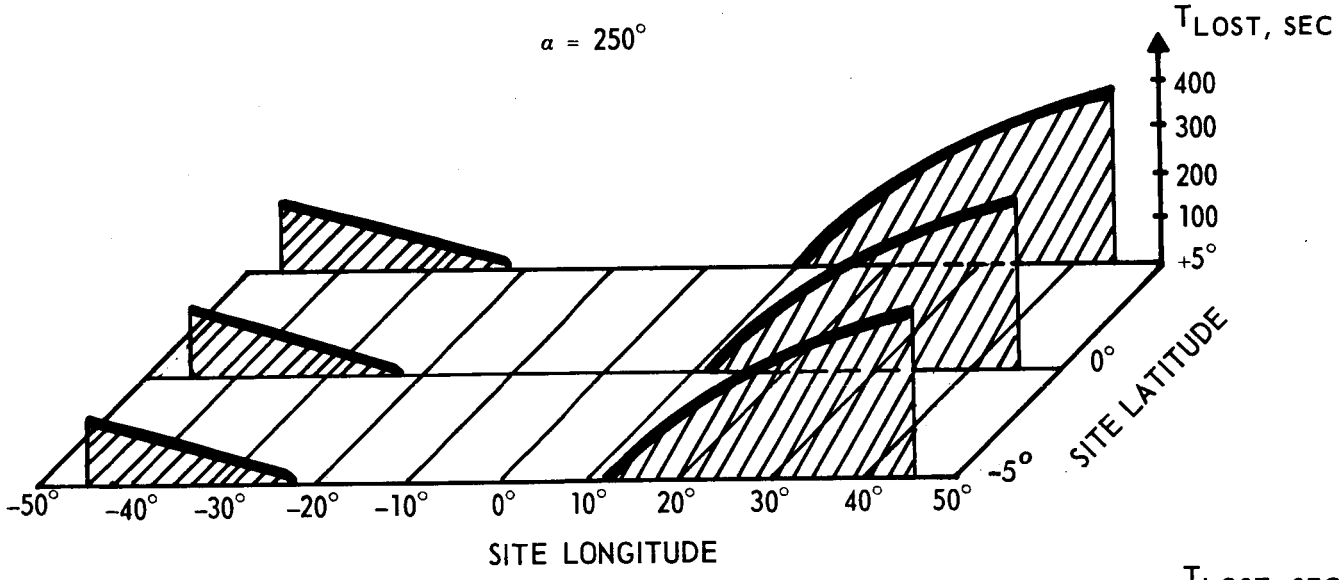

$\alpha = 270°$

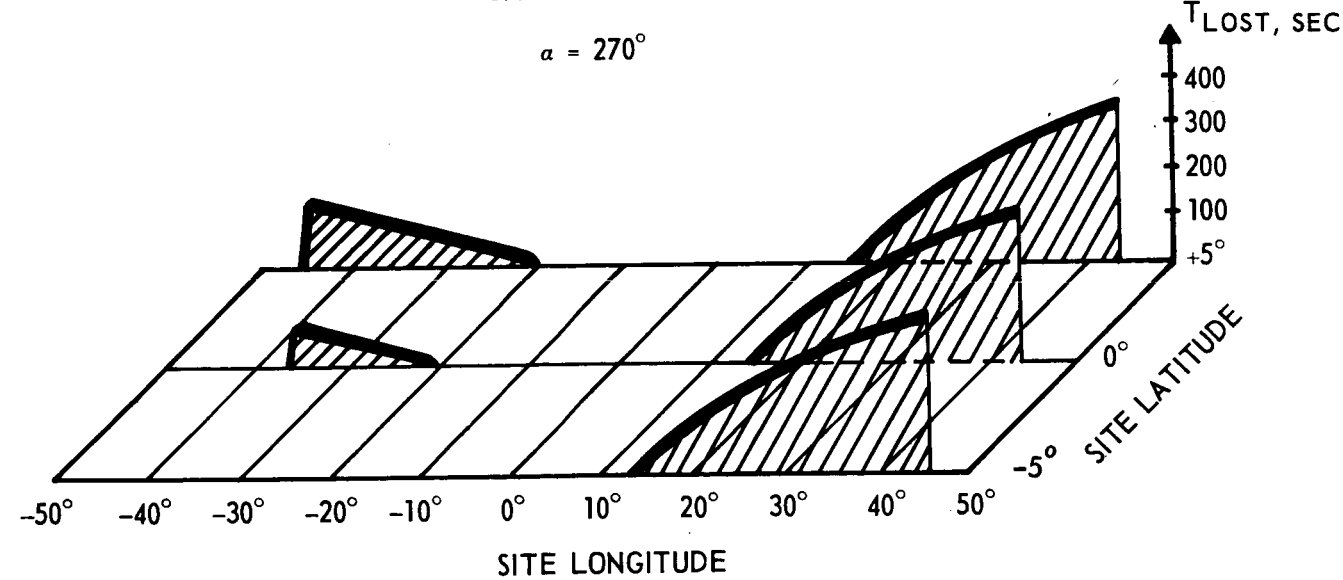

$\alpha = 290°$

LOST TIME VARIATIONS FOR $(\mu_L, \lambda_L) = (-6.85°, -7.70°)$

FIGURE (15)

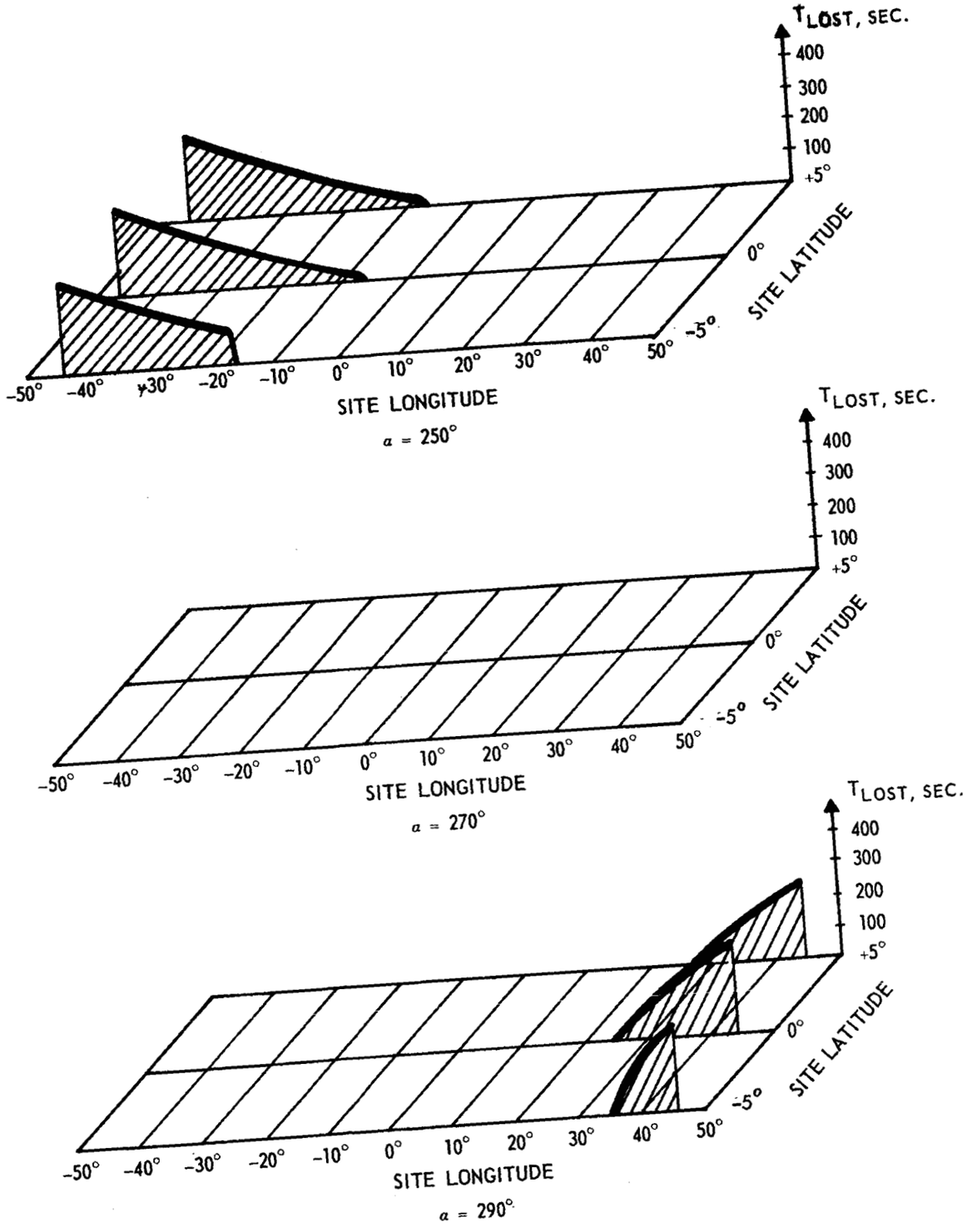

LOST TIME VARIATIONS FOR $(\mu_L, \lambda_L) = (6.80°, 7.91°)$

FIGURE (16)

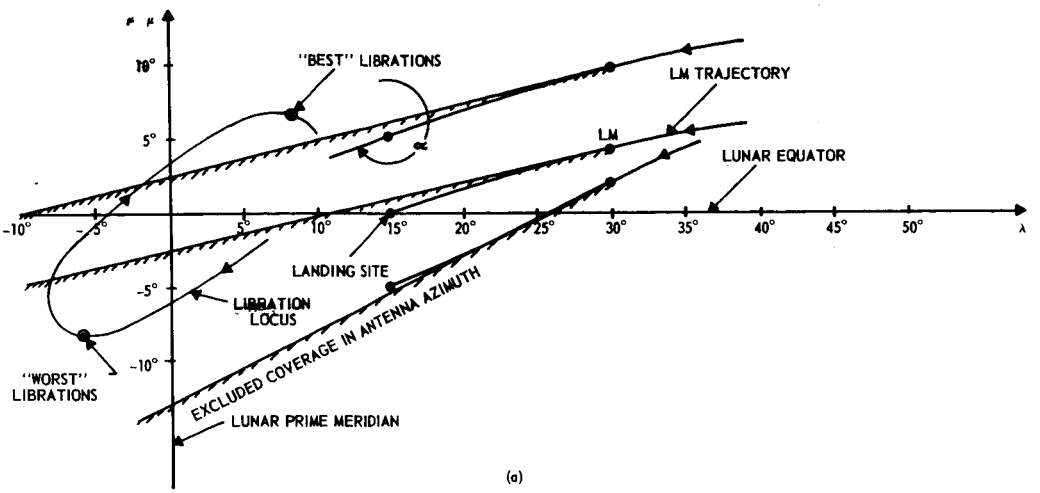

(a)

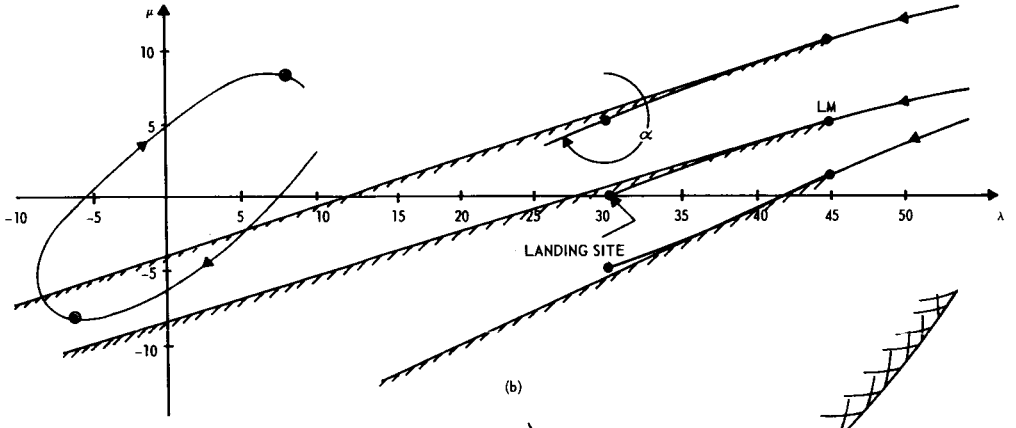

(b)

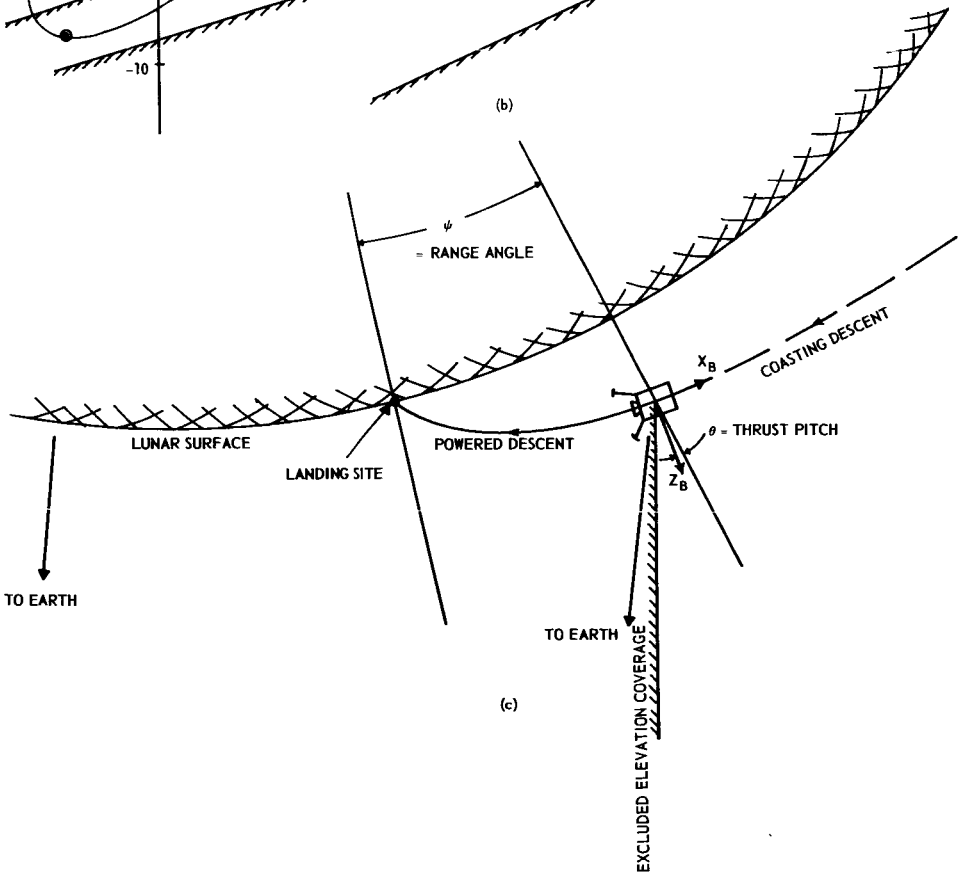

(c)

LM DESCENT GEOMETRY

FIGURE (17)

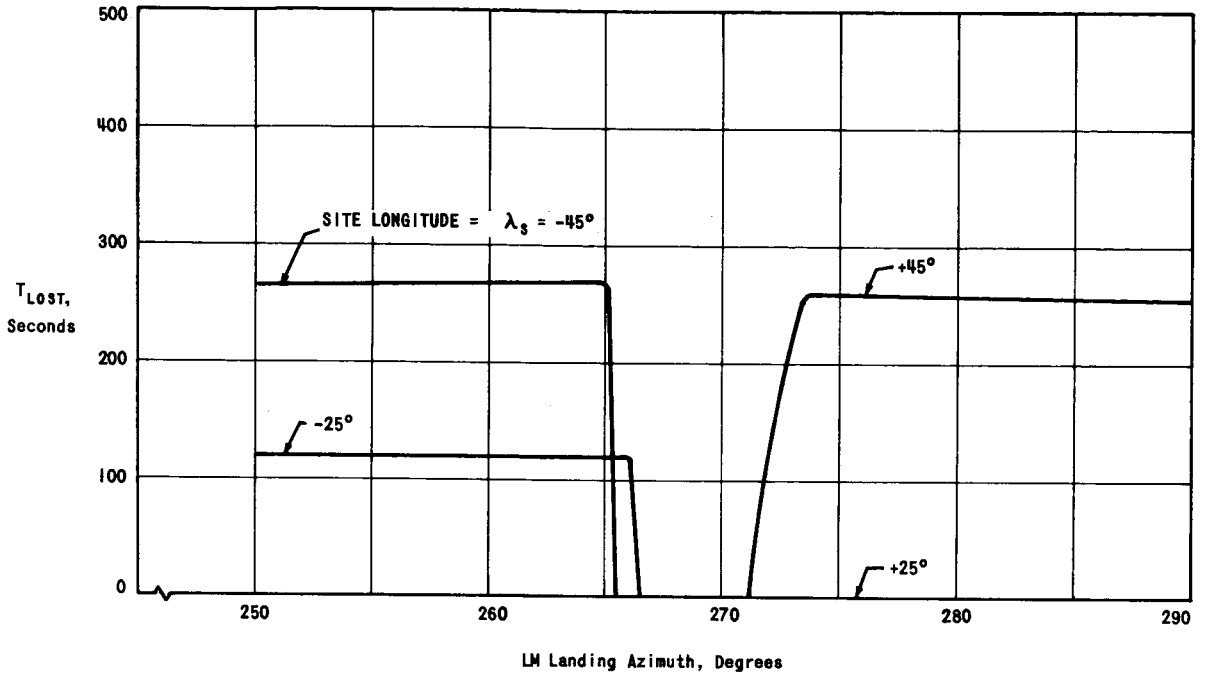

(a)

INTERFERENCE TIME VS. LM LANDING AZIMUTH

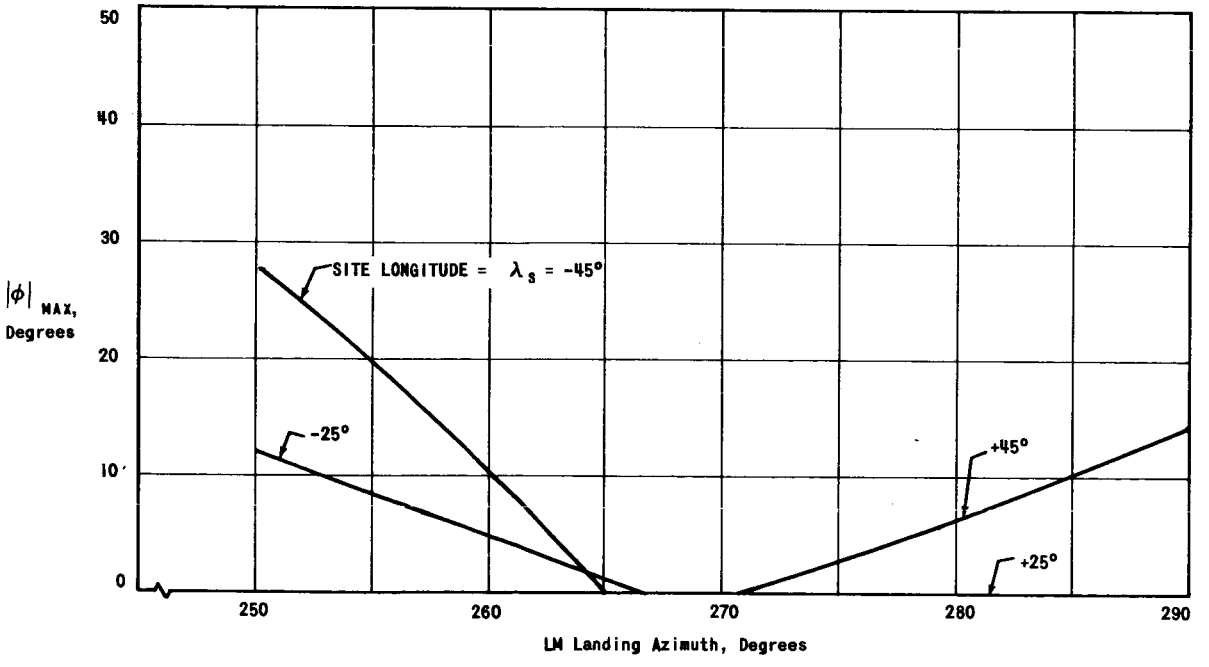

(b)

MAXIMUM YAW VS. LM LANDING AZIMUTH

FIGURE (18)

LIBRATIONS: $(\mu_L, \lambda_L) = (6.80°, 7.91°)$

STAYTIME: T_S = 44 HOURS

SITE LATITUDE: $\mu_S = 5°$

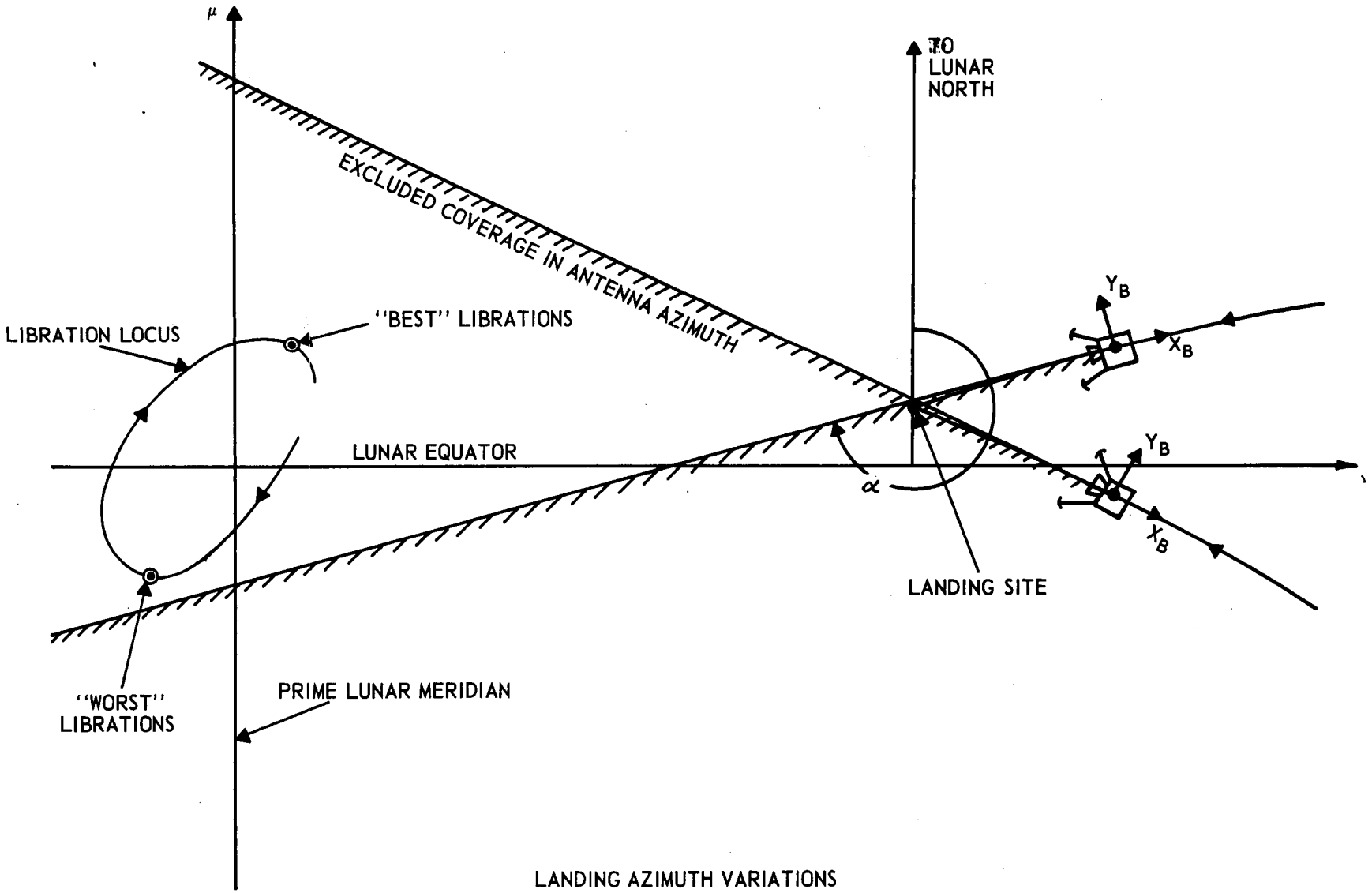

LANDING AZIMUTH VARIATIONS

FIGURE (19)

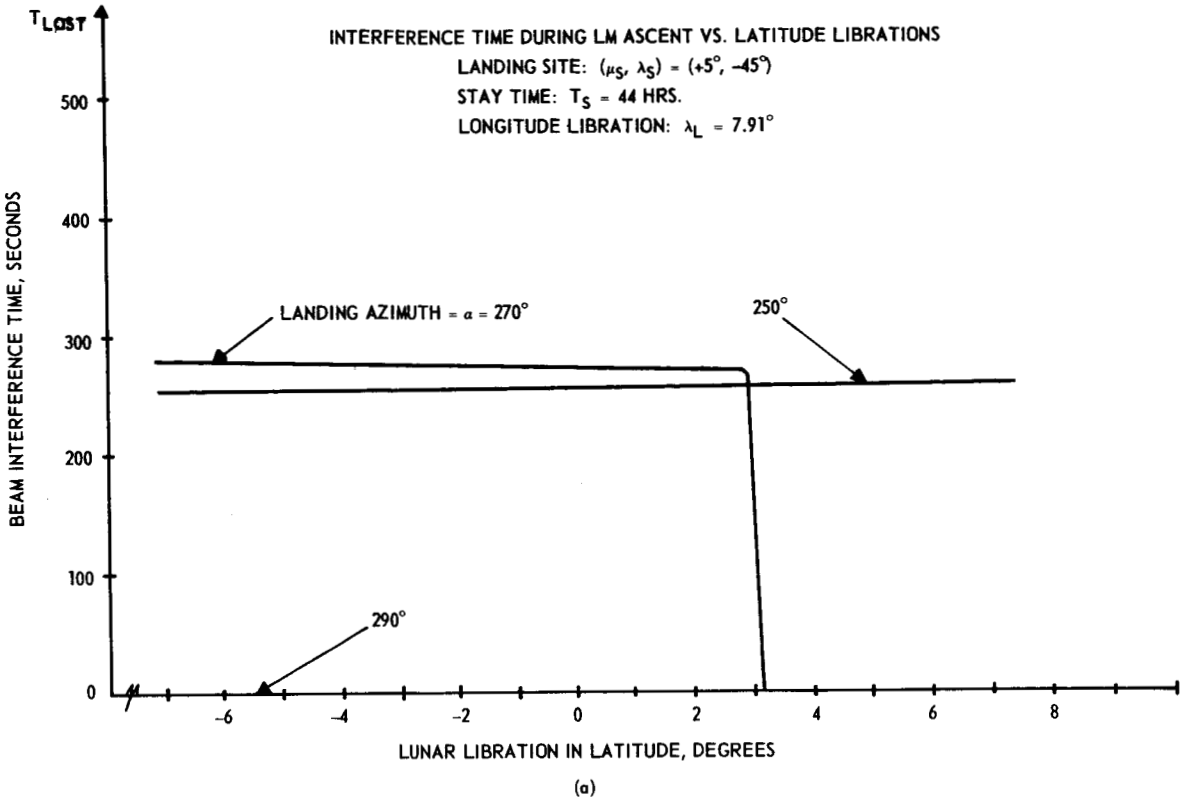

(a)

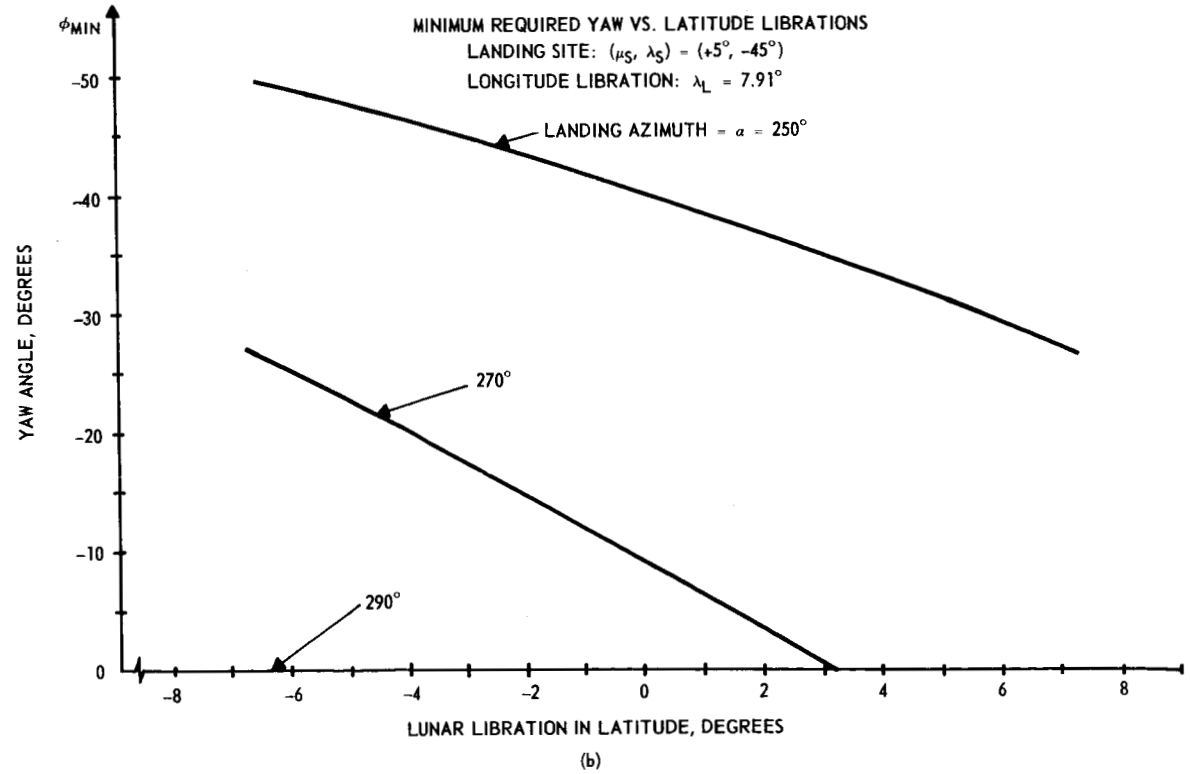

(b)

EFFECT OF LATITUDE LIBRATIONS

FIGURE (20)

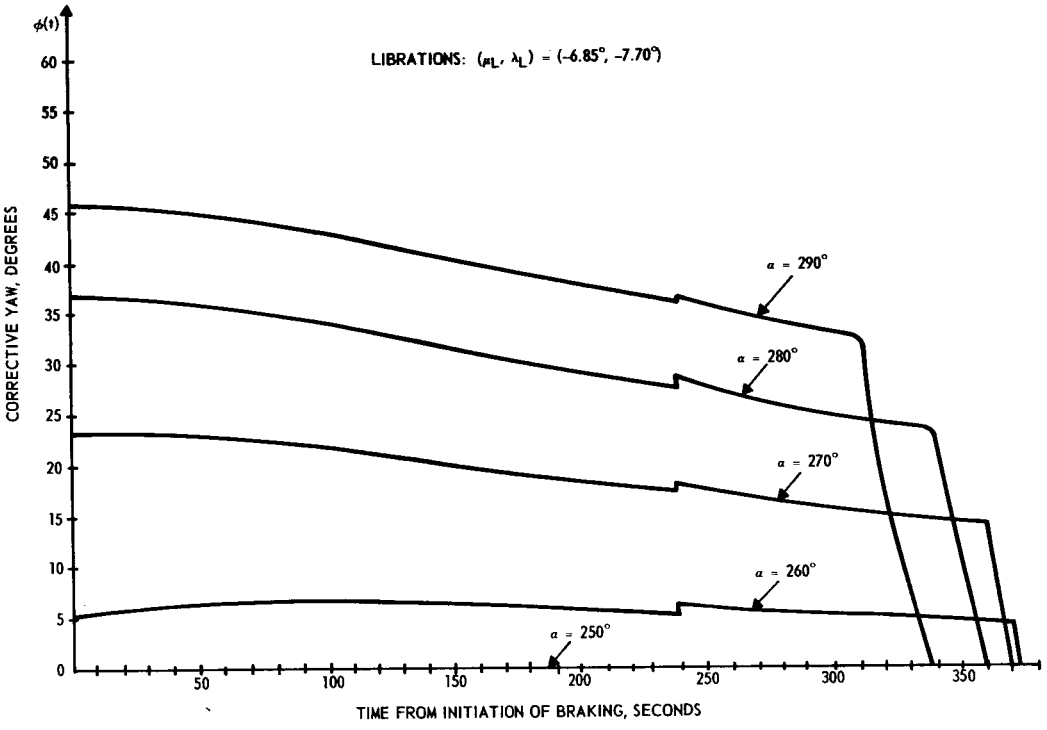

(a)

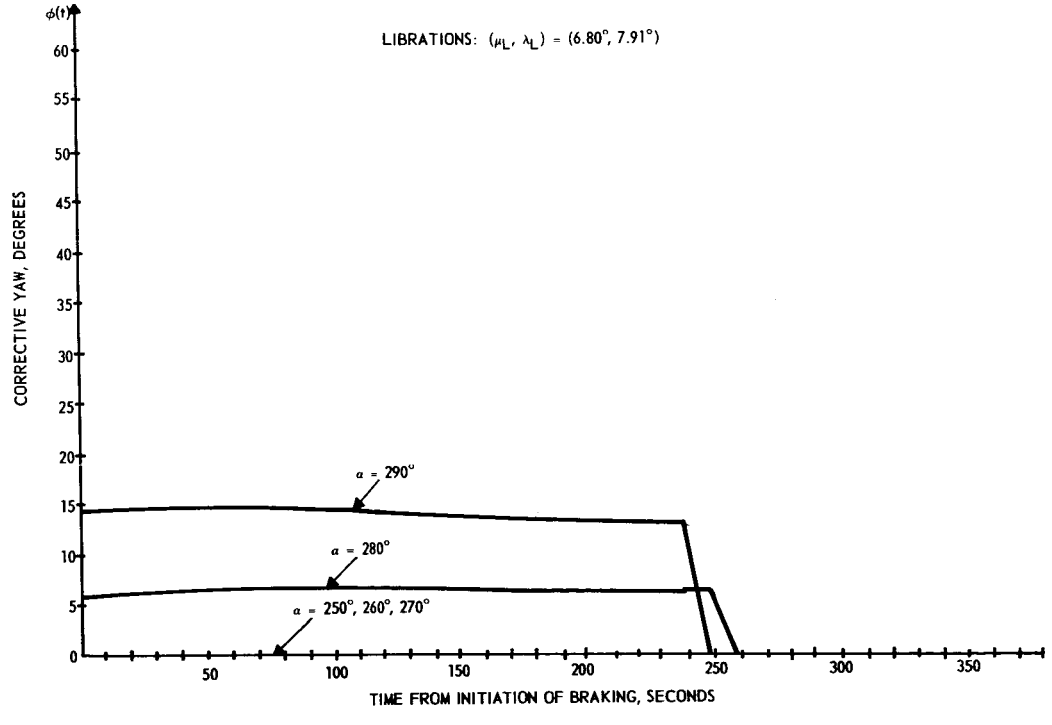

(b)

YAW REQUIRED TO RECOVER COMMUNICATIONS
LANDING SITE: $(\mu_S, \lambda_S) = (5°, 45°)$

FIGURE (21)

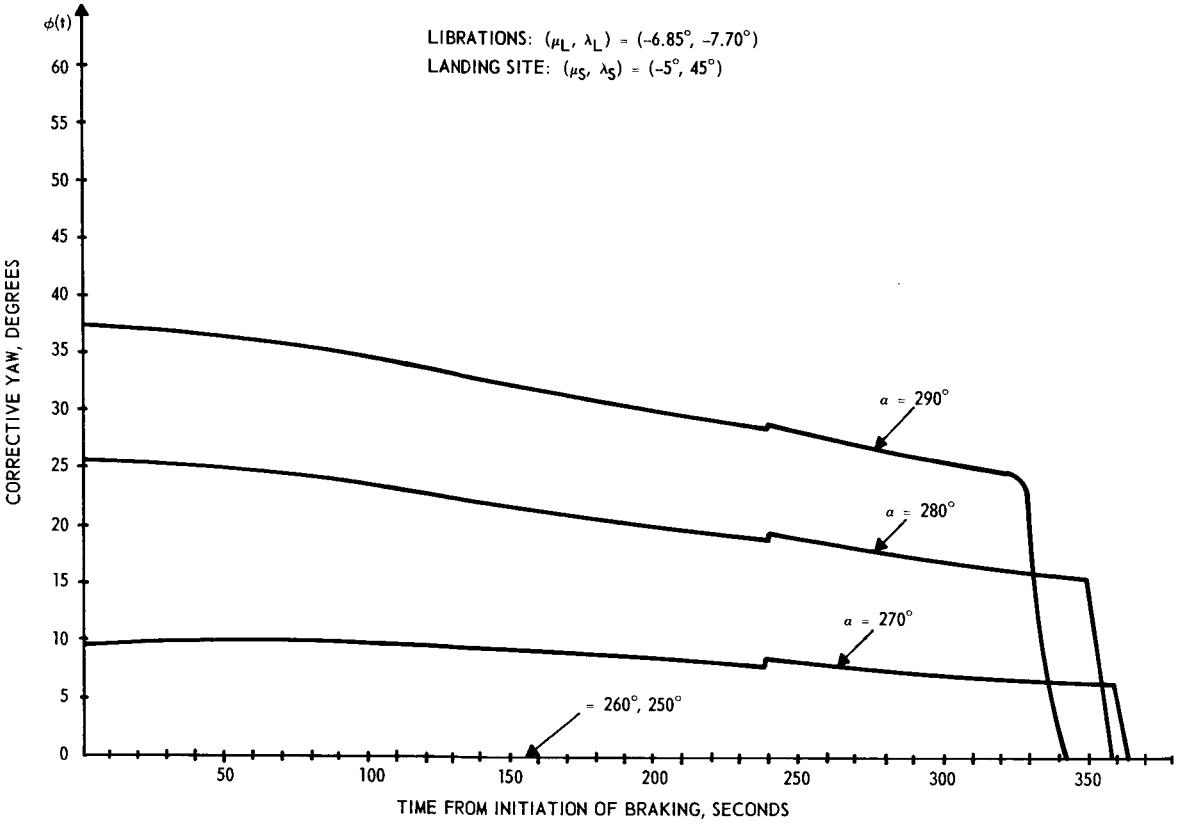

(a)

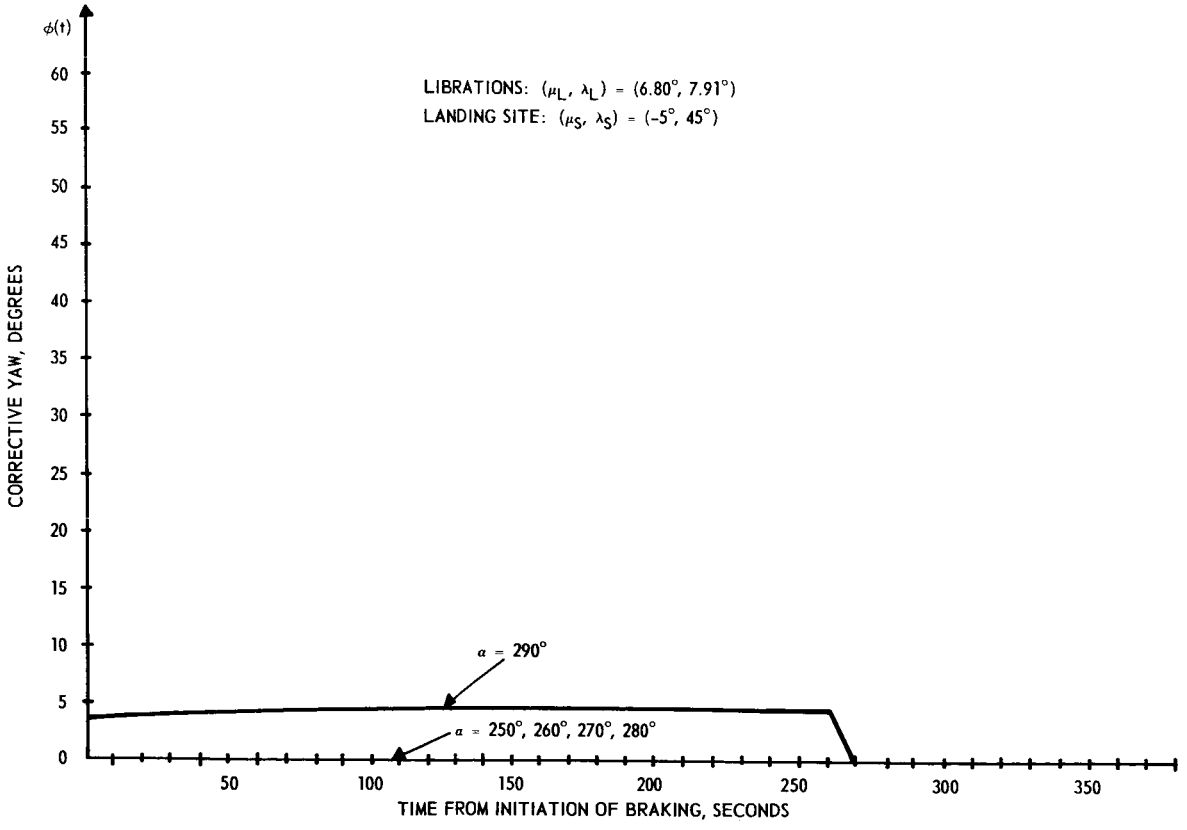

(b)

YAW REQUIRED TO RECOVER COMMUNICATIONS

FIGURE (22)

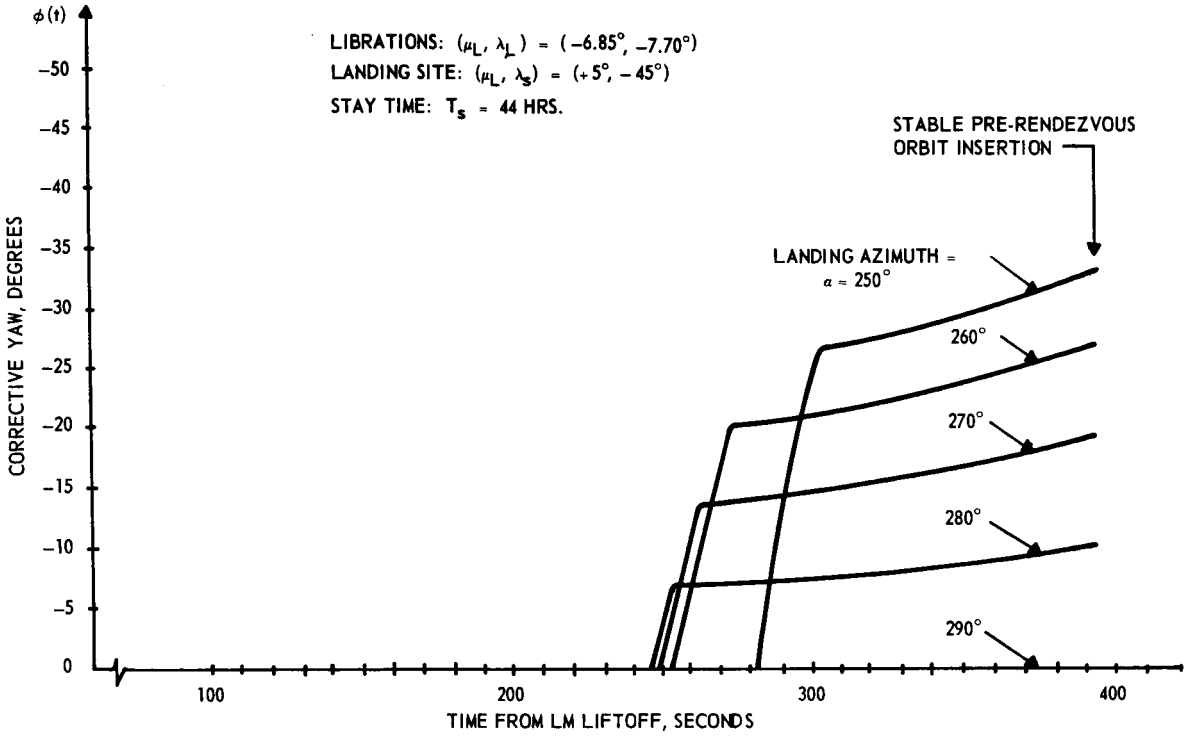

(a)

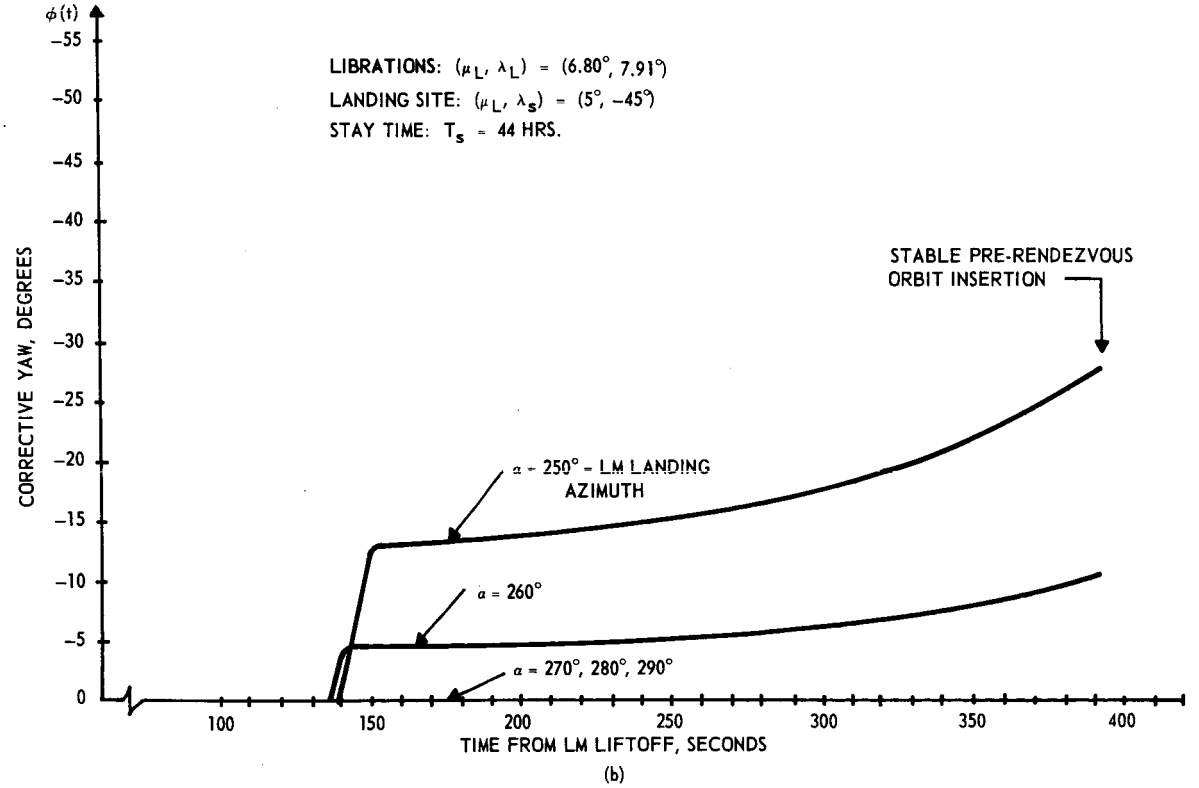

(b)

YAW REQUIRED TO RECOVER COMMUNICATIONS

FIGURE (23)

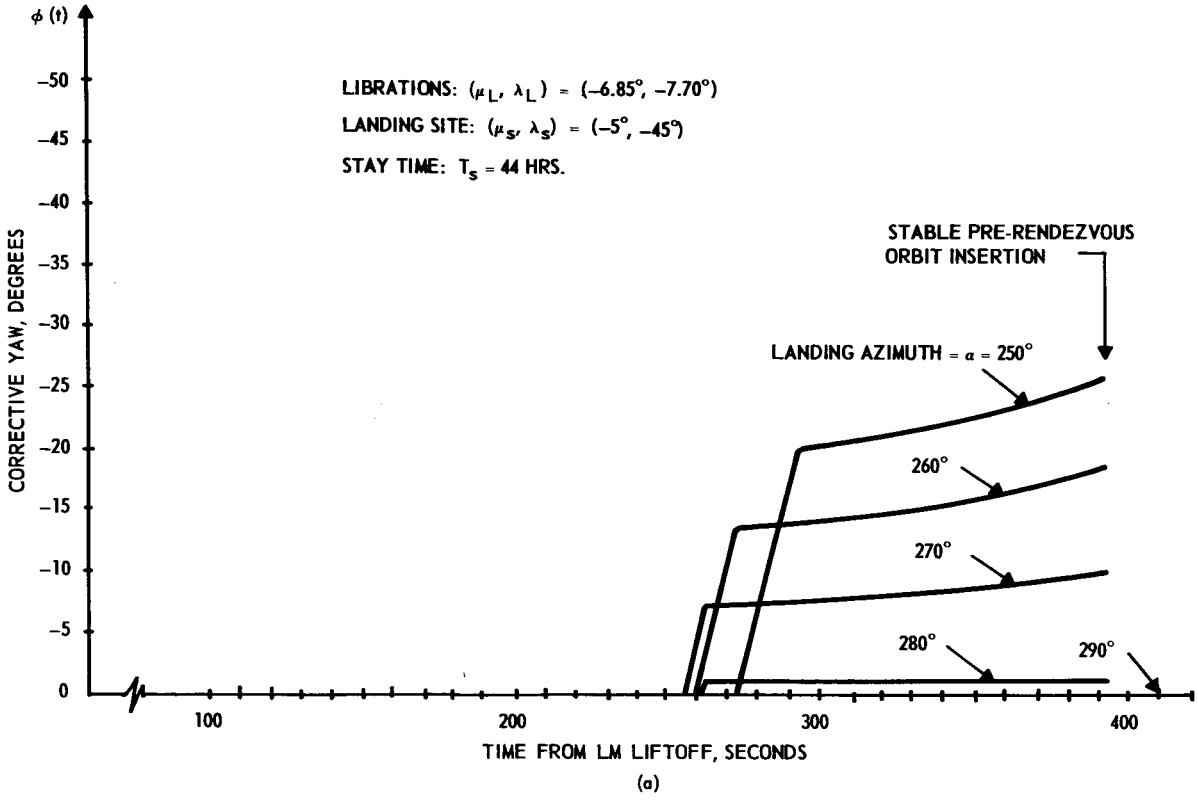

(a)

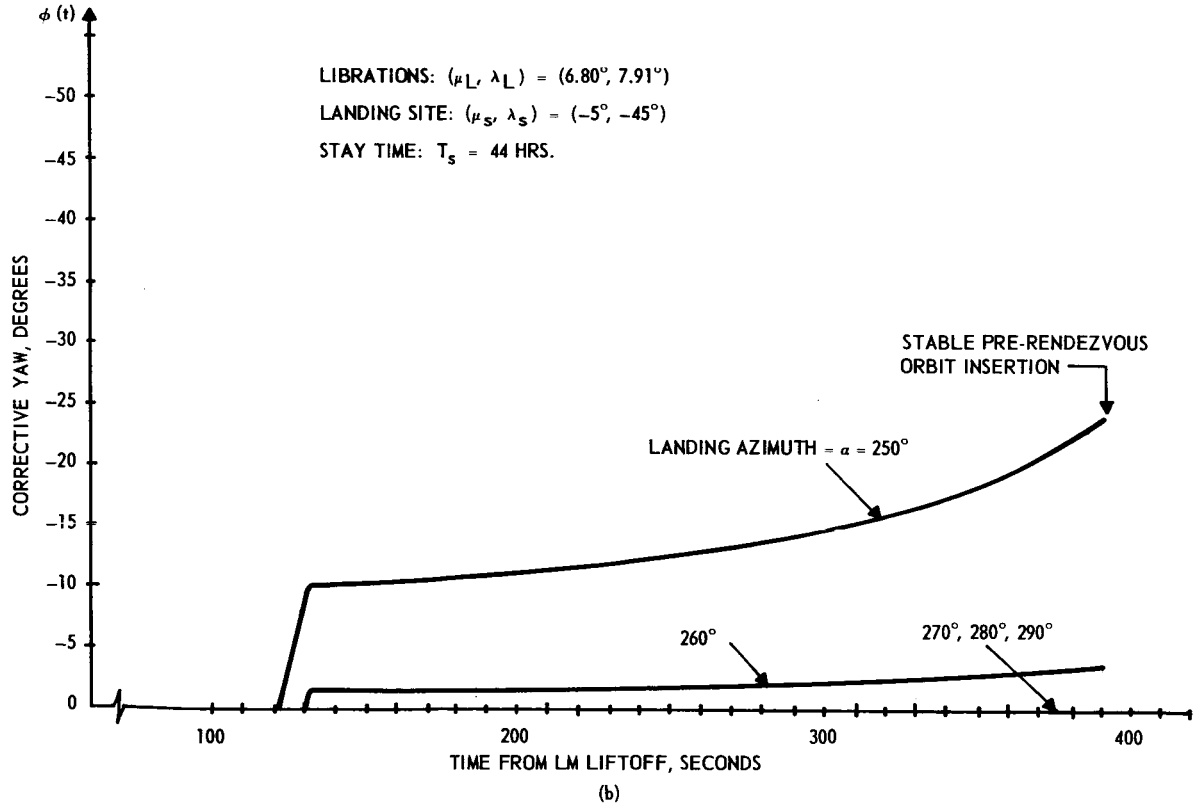

(b)

YAW REQUIRED TO RECOVER COMMUNICATIONS

FIGURE (24)

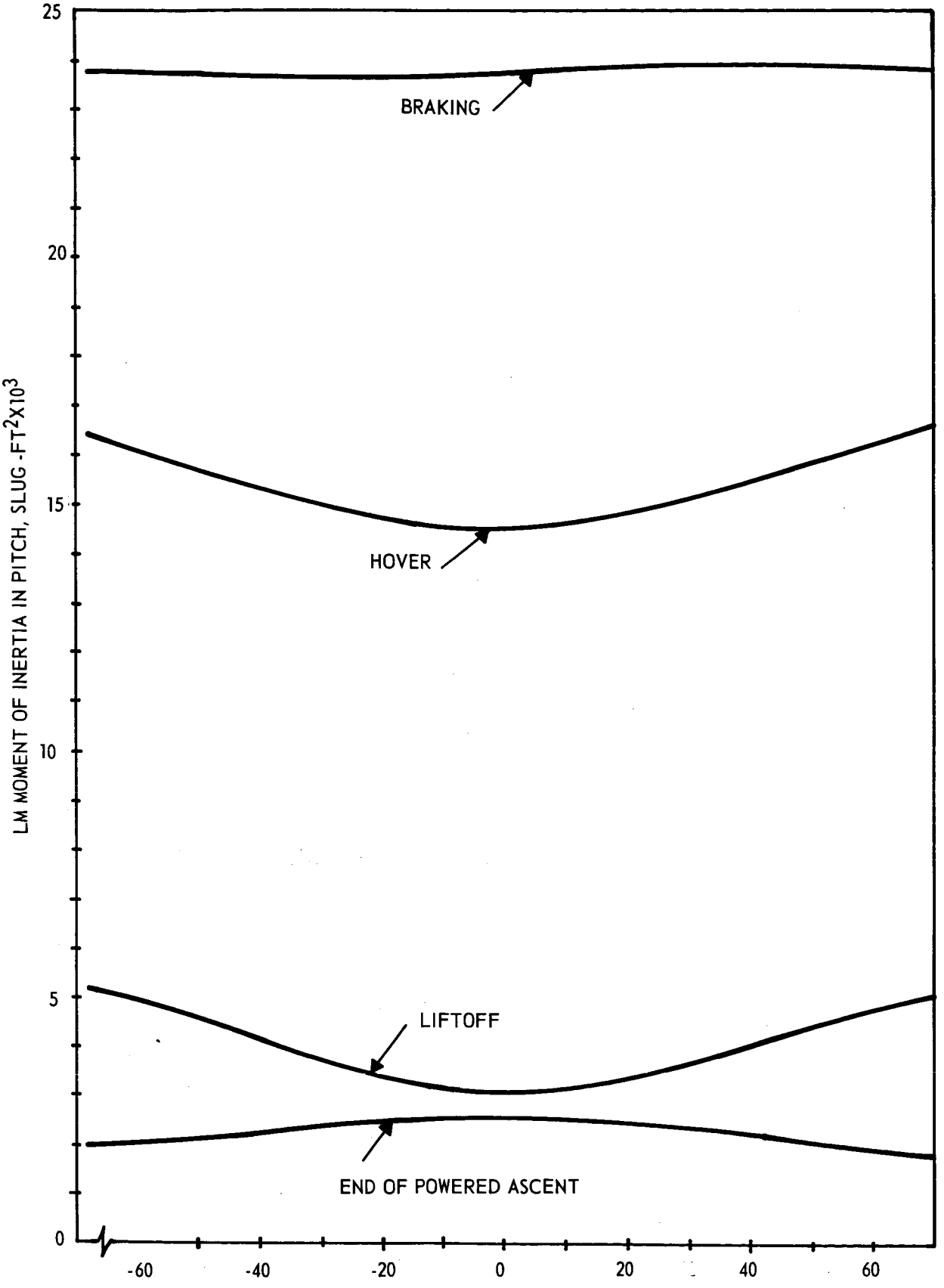

IN-PLANE PITCHING MOMENT AS A FUNCTION OF YAW

FIGURE (25)

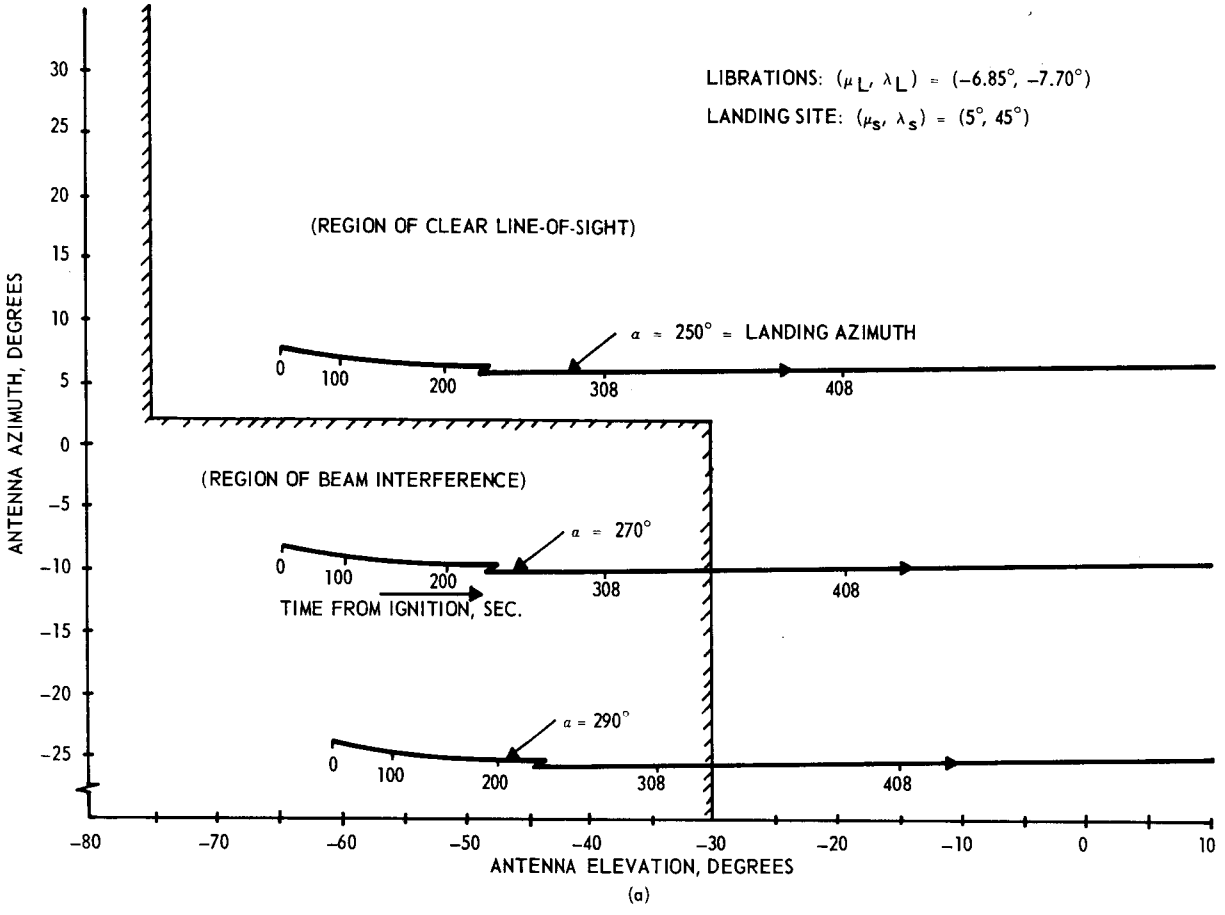

(a)

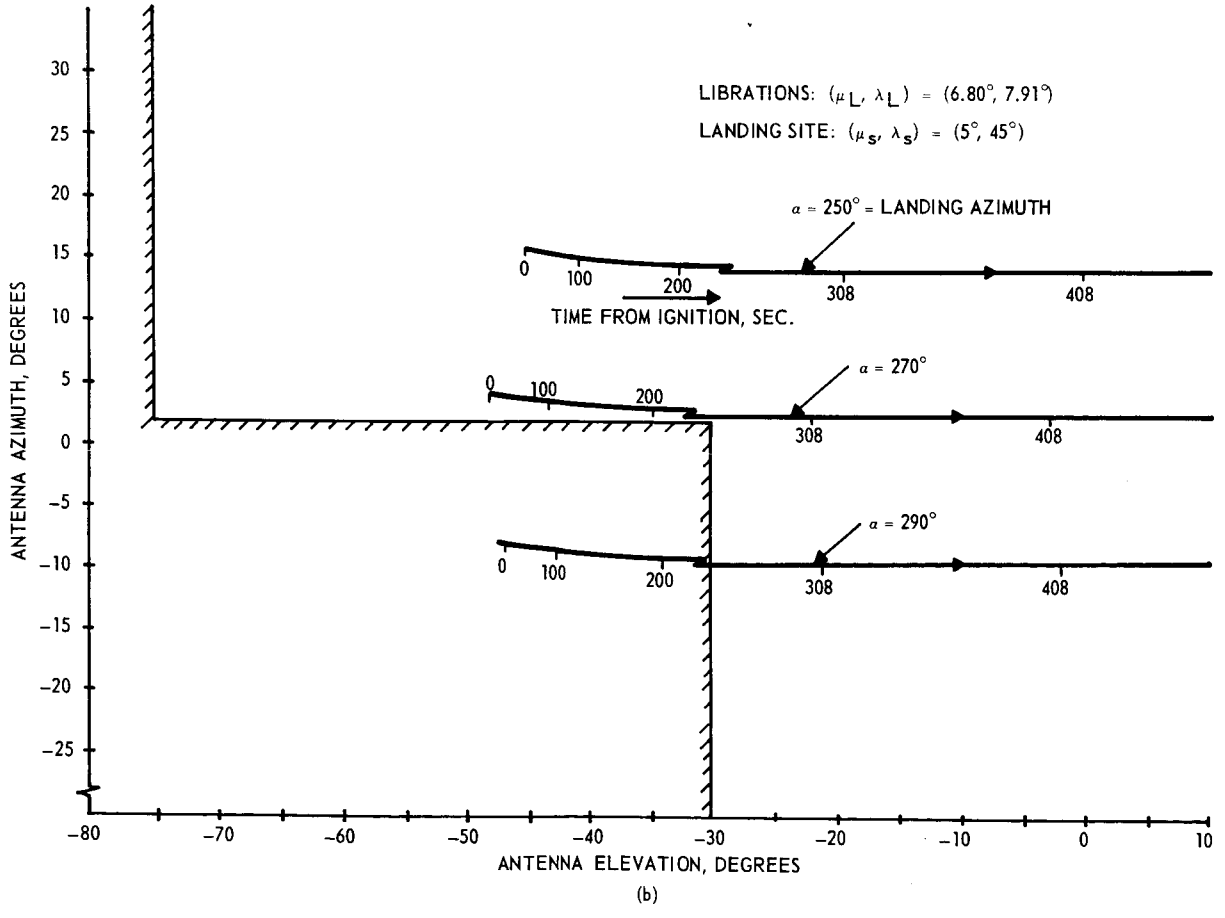

(b)

UNCORRECTED S-BAND ANTENNA ANGLE LOCUS DURING POWERED DESCENT

FIGURE (26)

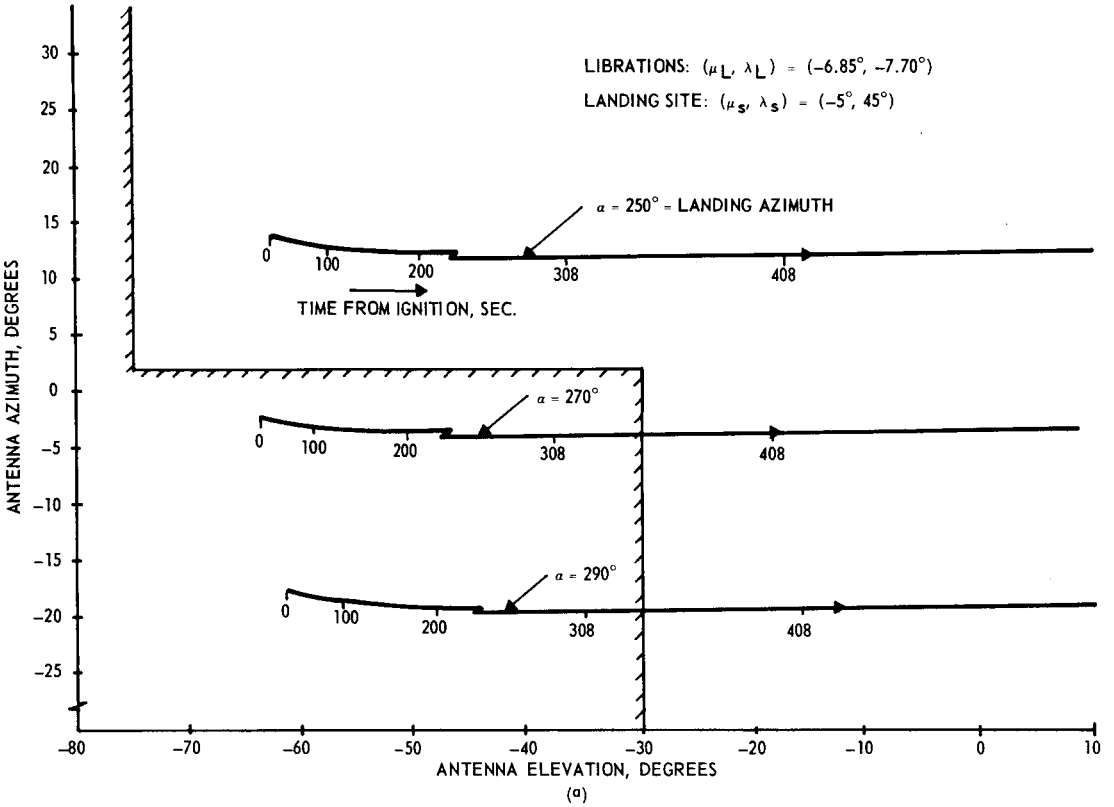

(a)

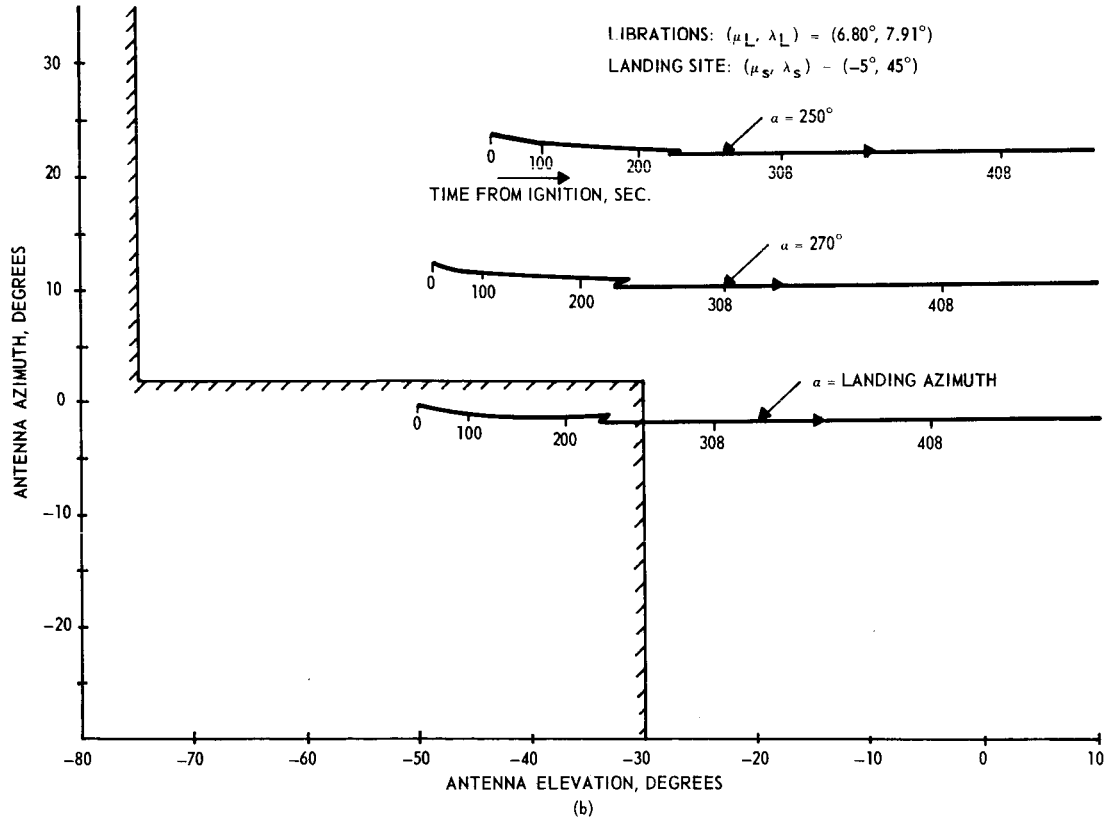

(b)

UNCORRECTED S-BAND ANTENNA ANGLE LOCUS DURING POWERED DESCENT

FIGURE (27)

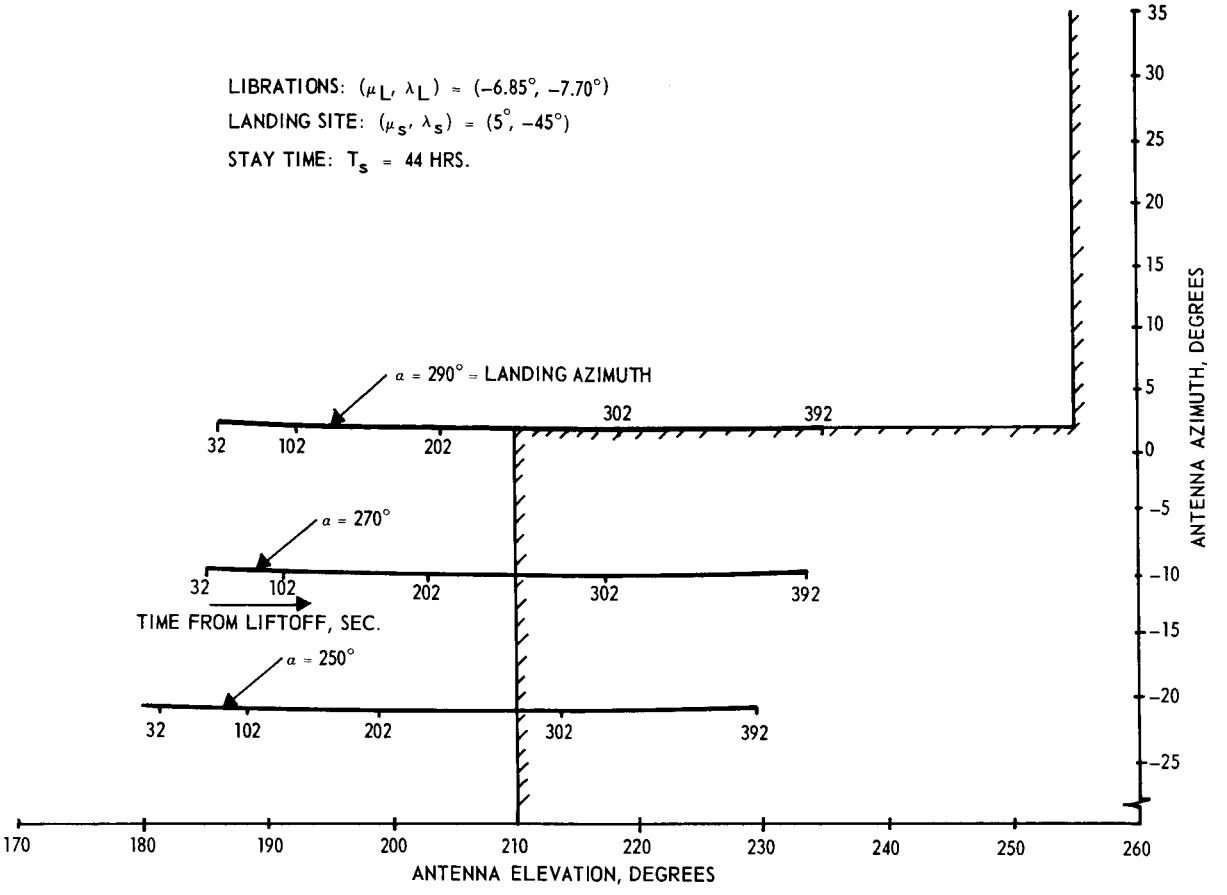

(a)

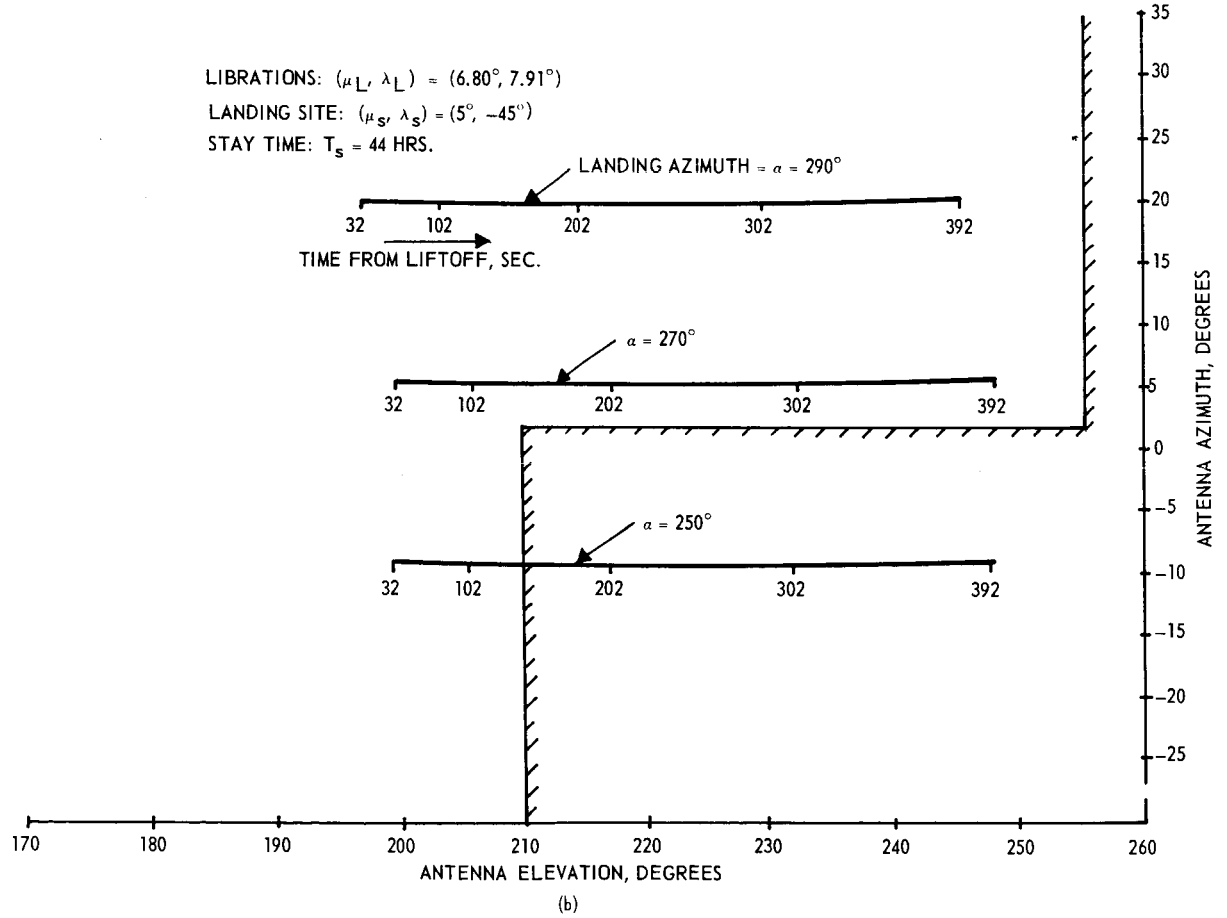

(b)

UNCORRECTED S-BAND ANTENNA ANGLE LOCUS DURING LM POWERED ASCENT

FIGURE (28)

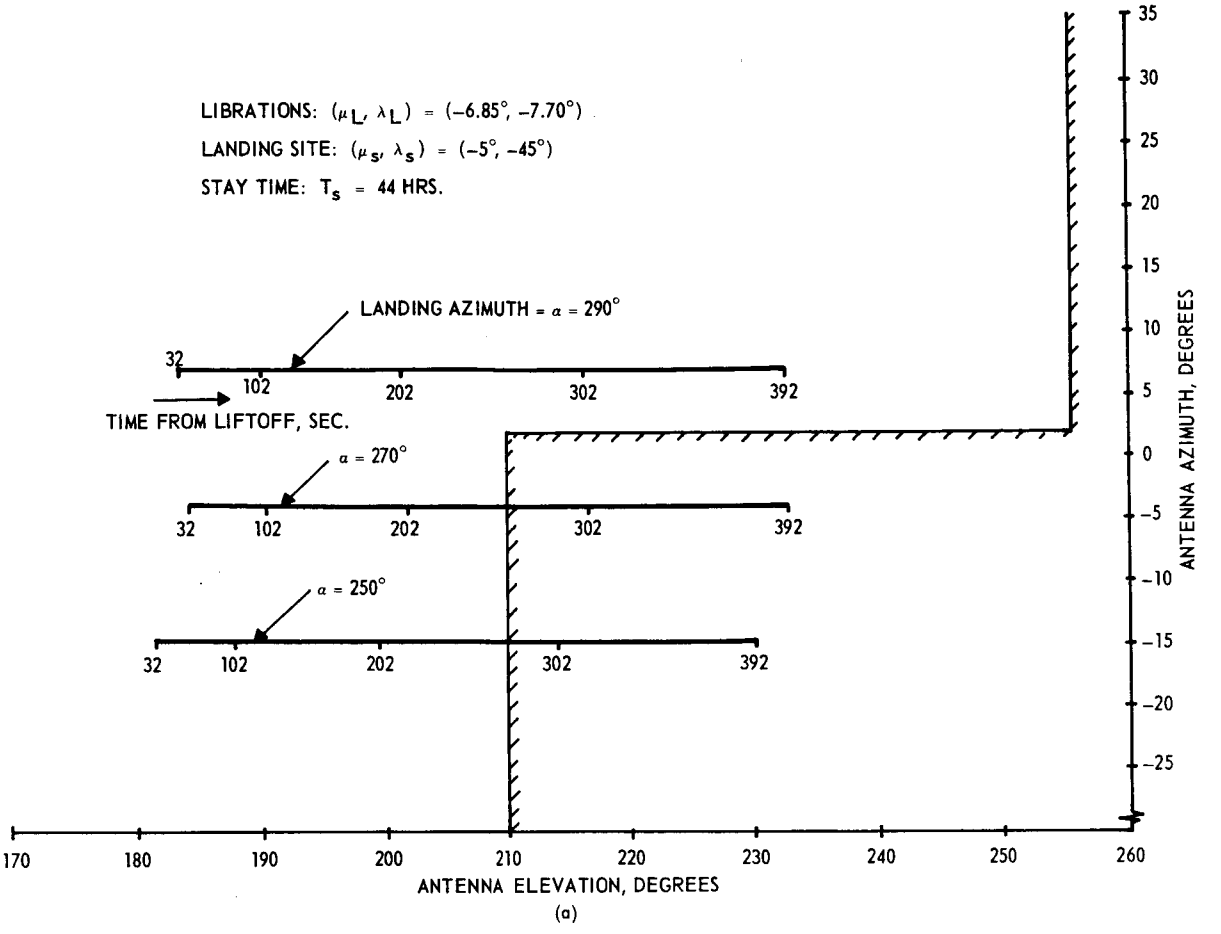

(a)

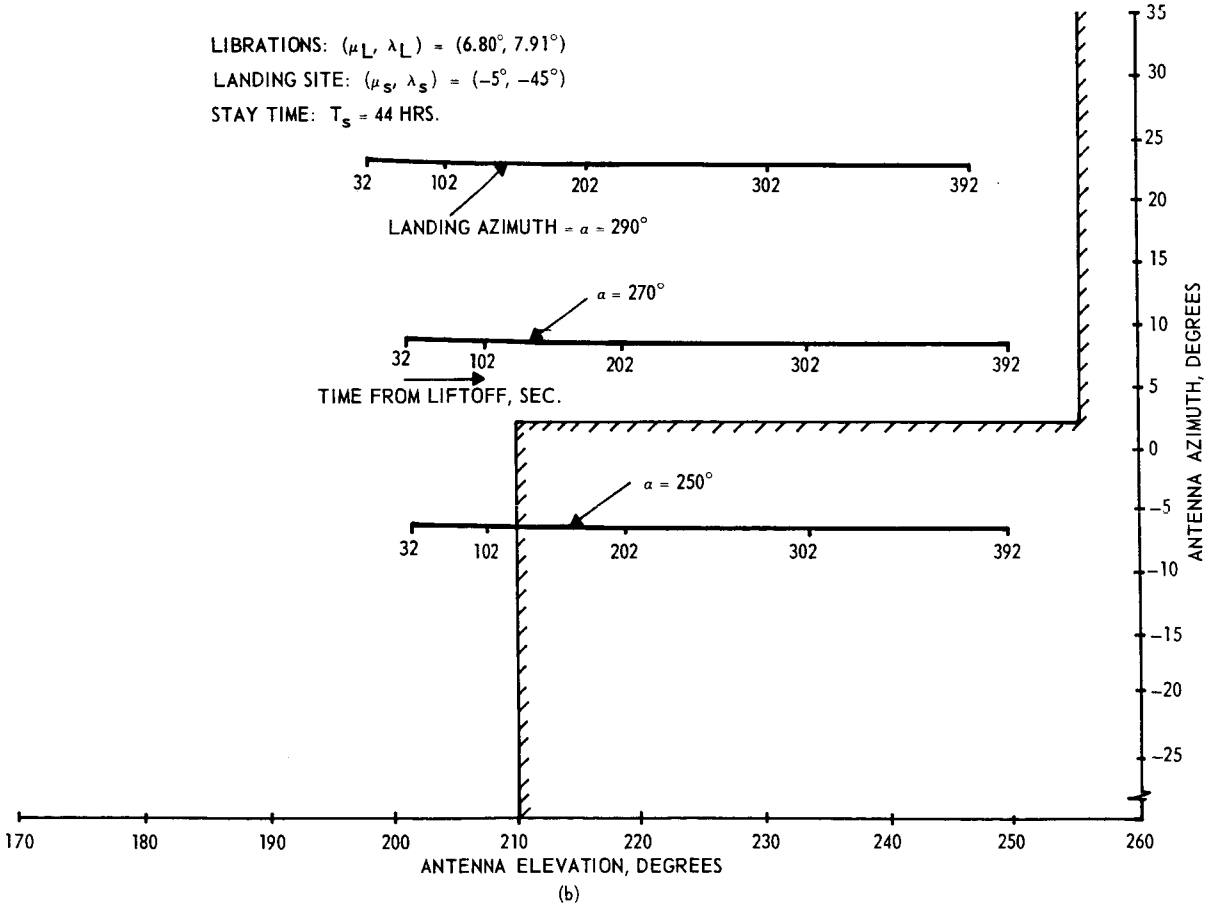

(b)

UNCORRECTED S-BAND ANTENNA ANGLE LOCUS DURING POWERED ASCENT

FIGURE (29)

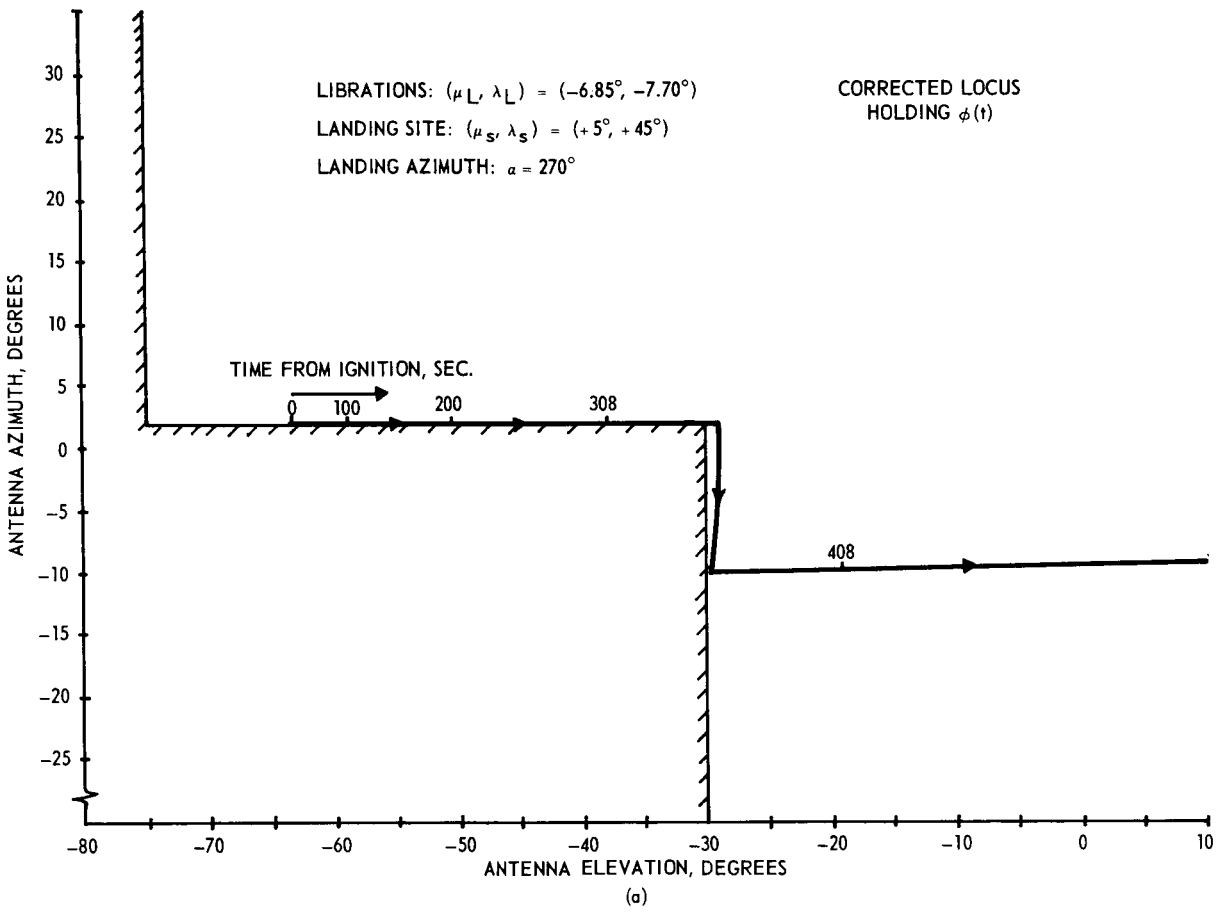

(a)

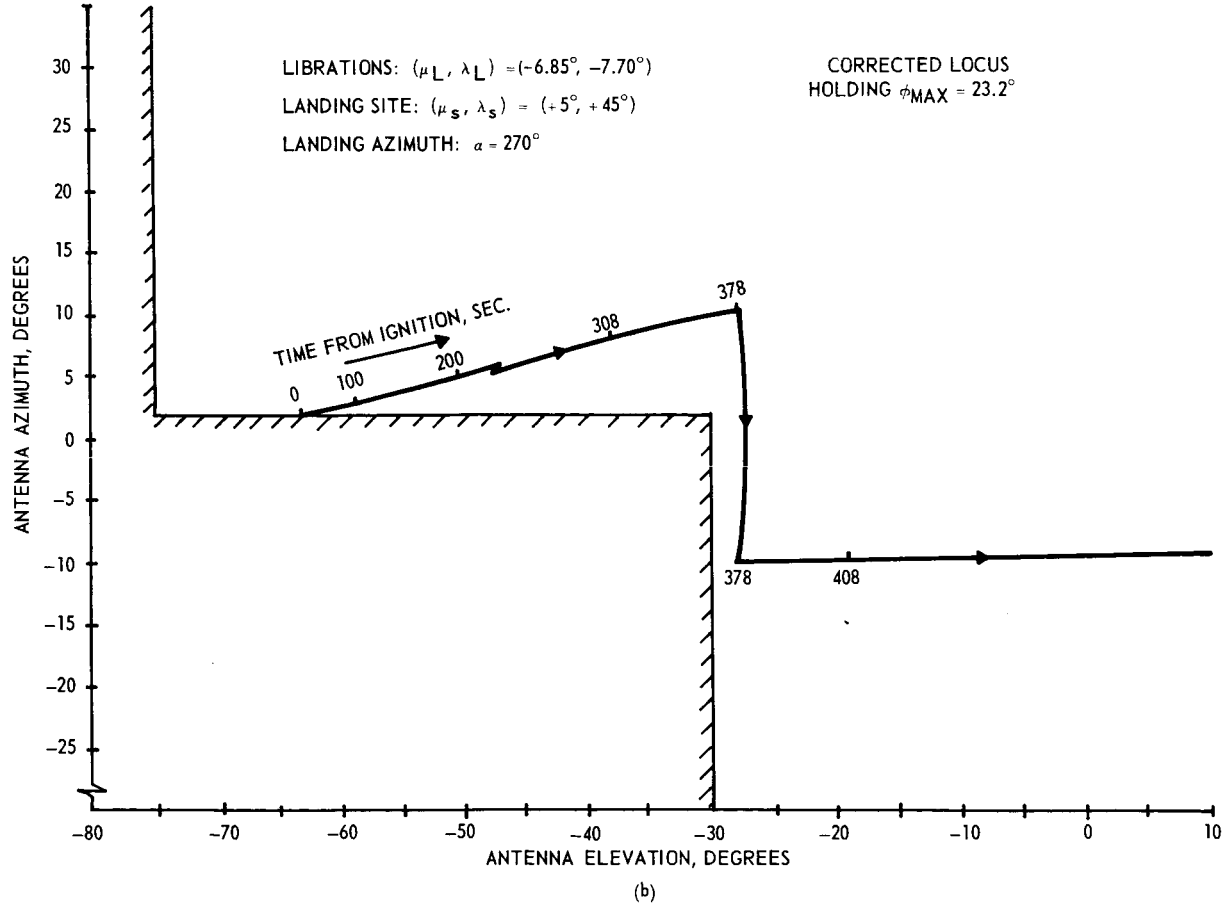

(b)

CORRECTED S-BAND ANTENNA ANGLE LOCUS DURING POWERED DESCENT

FIGURE (30)

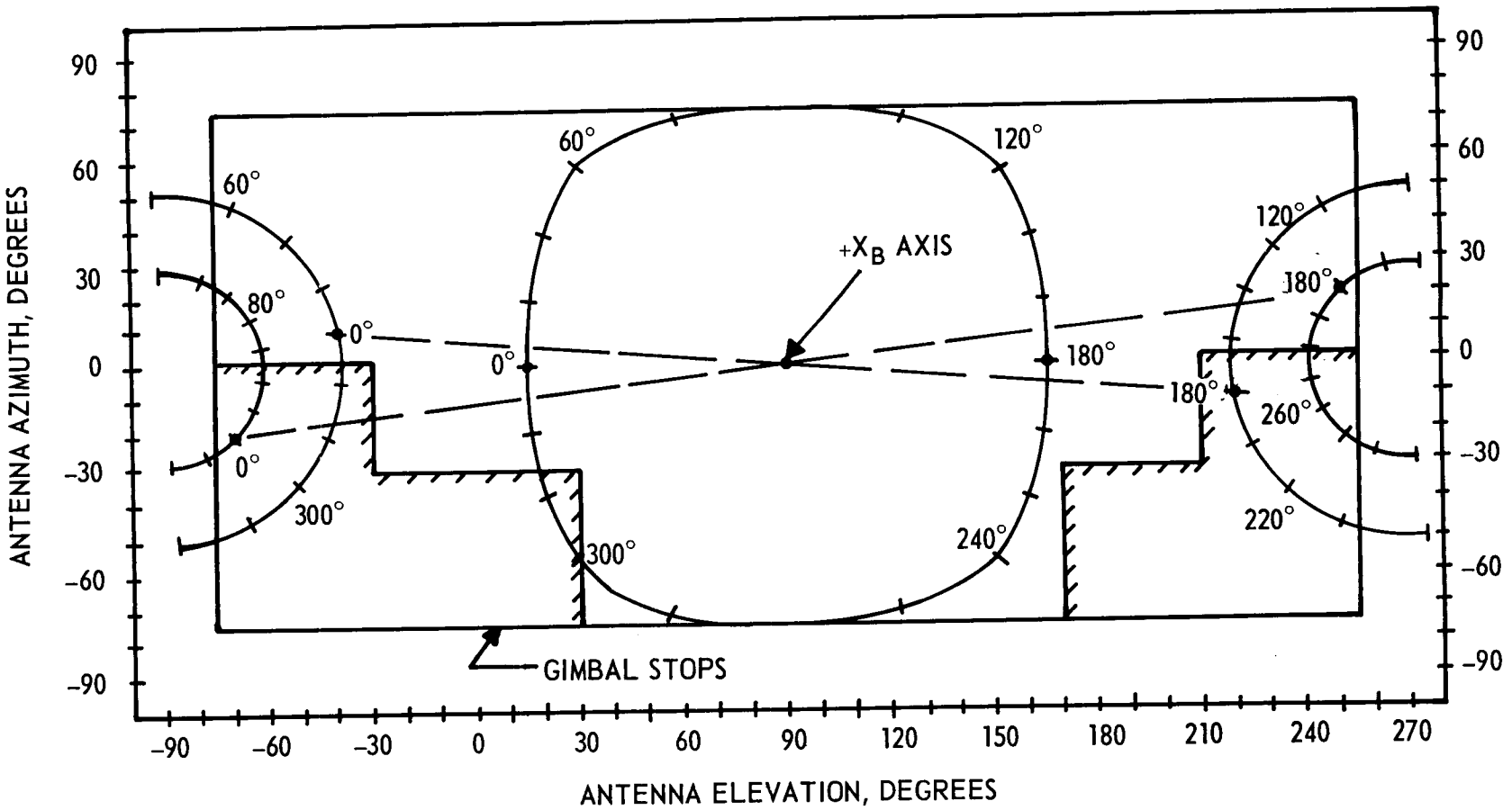

ANTENNA ANGLE YAW LOCI (STATIC LM)

FIGURE (31)

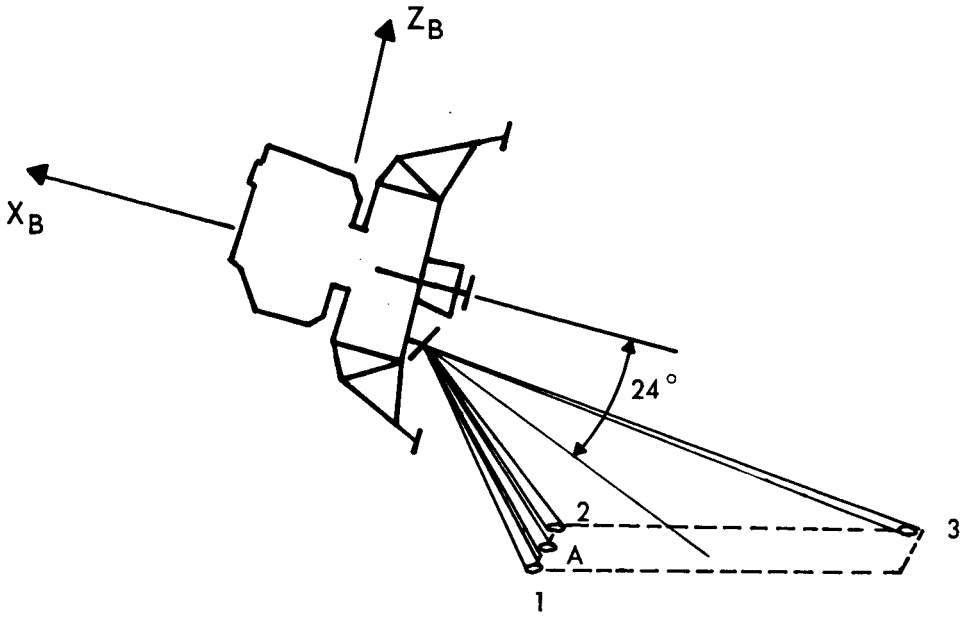

POSITION NO. 1

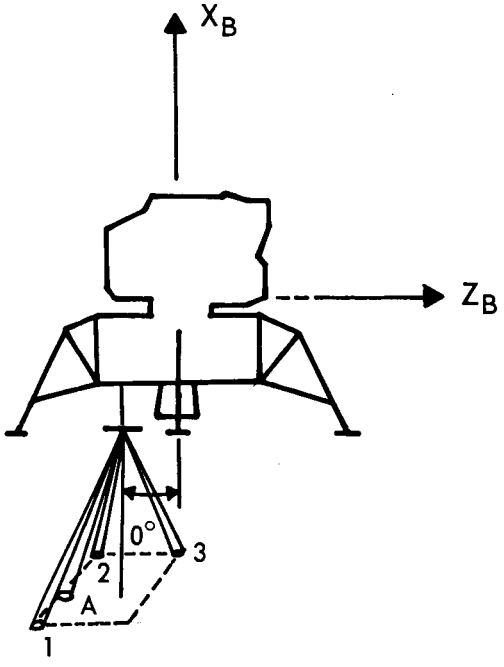

LANDING RADAR BEAM CONFIGURATION

FIGURE (32)

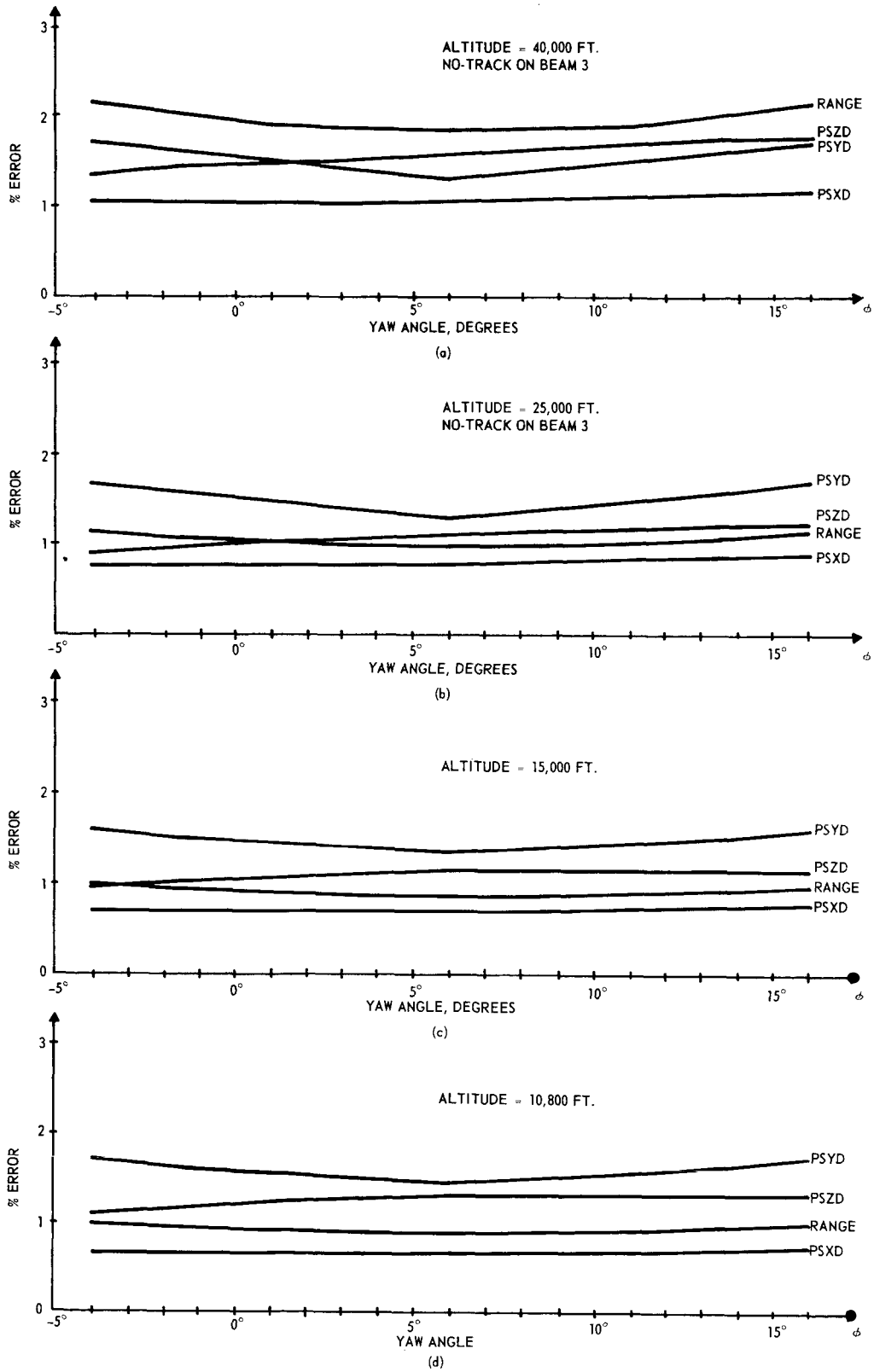

NOTE: PSXD, PSYD, & PSZD ARE VELOCITY RELATED QUANTITIES
RANGE IS MEASURED ALONG THE ALTIMETER BEAM

UPDATE ERRORS DUE TO YAWING (% OF TOTAL RANGE OR VELOCITY)

FIGURE (33)

YAW REQUIRED AT LR INTERFACE ALTITUDE (30,000 ft.)
LIBRATIONS: $(\mu_L, \lambda_L) = (-6.85°, -7.70°)$

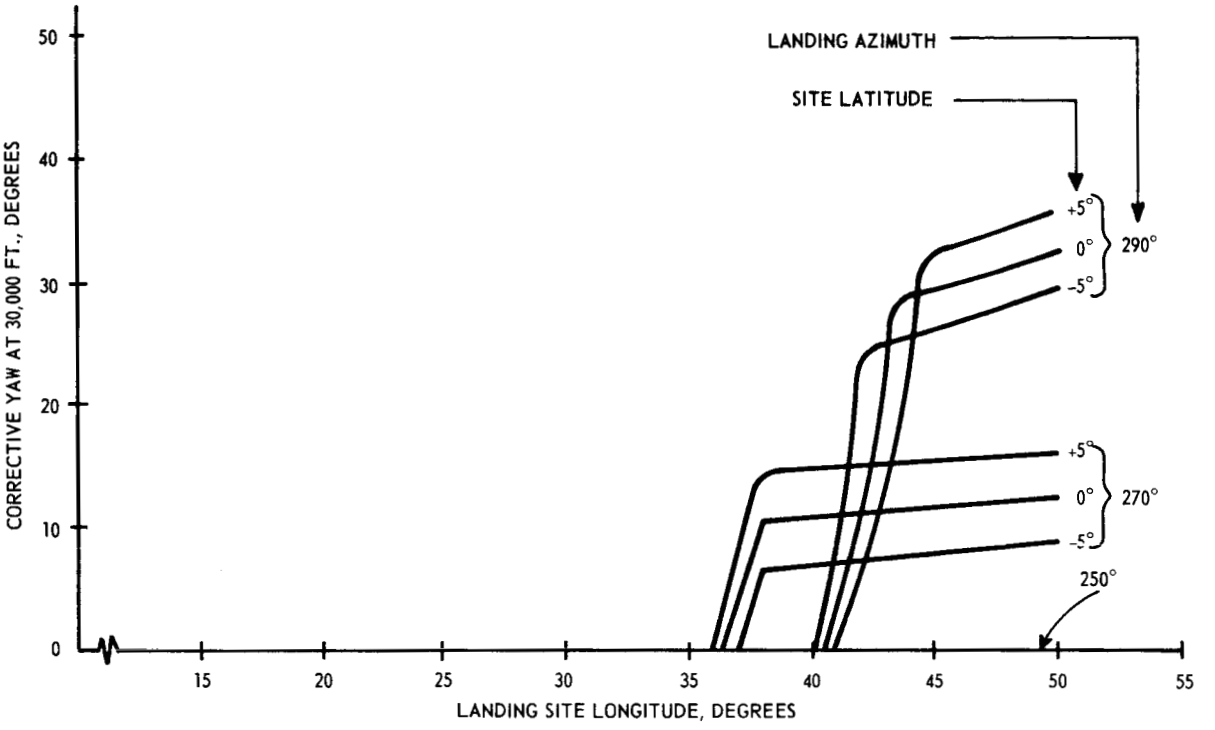

FIGURE (34)

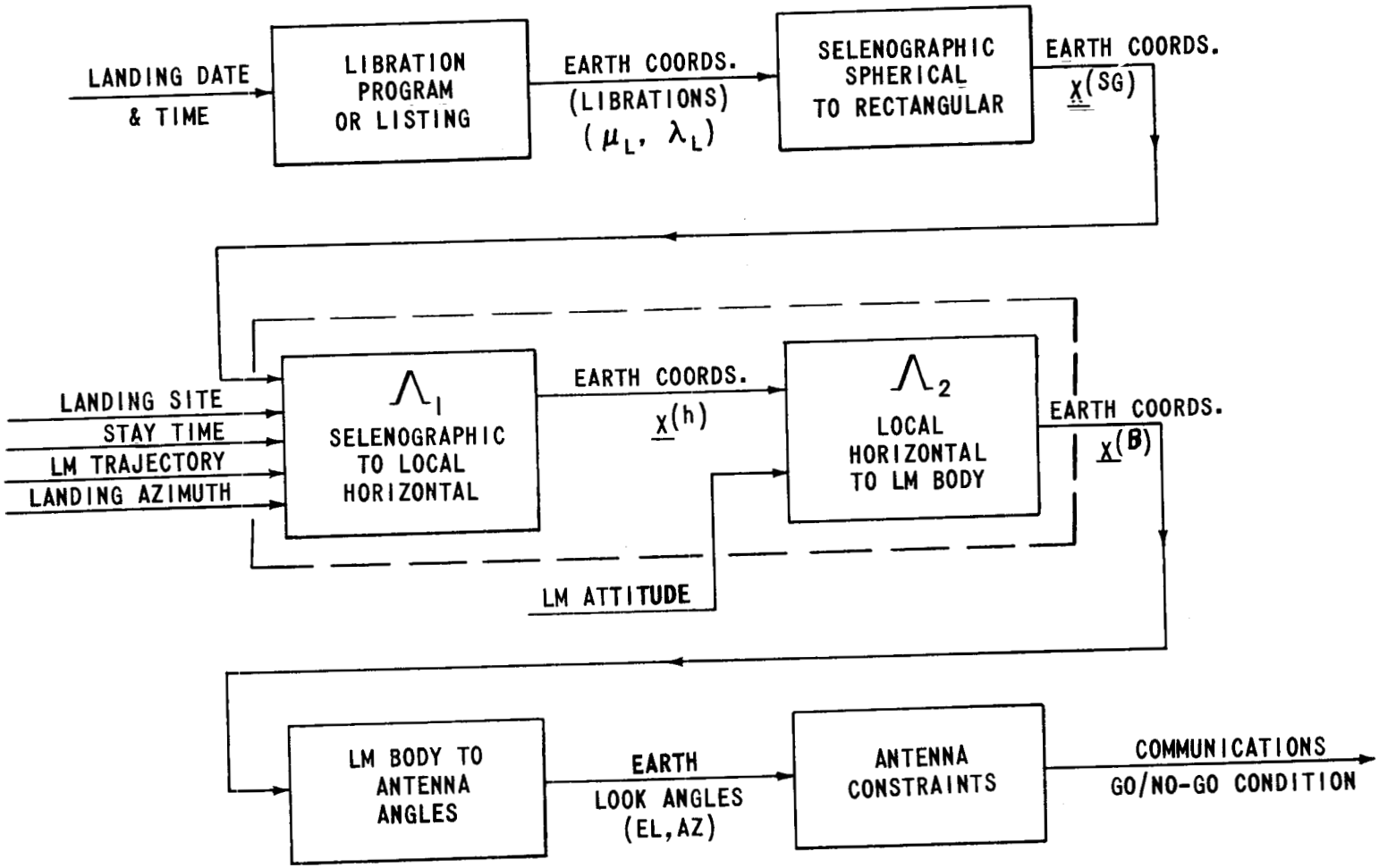

TRANSFORMATION SEQUENCE FOR COMMUNICATIONS SIMULATION

FIGURE (A-1)

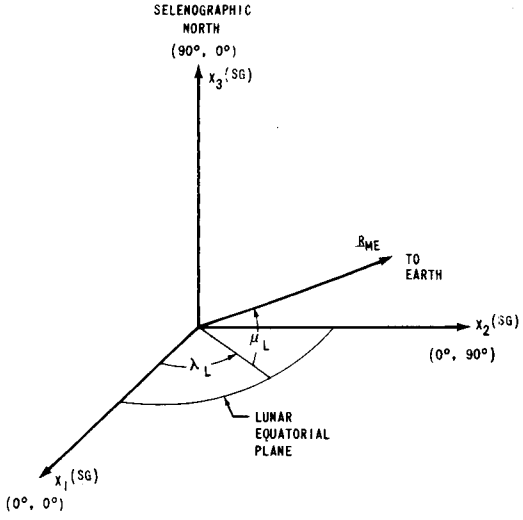

LUNAR LIBRATIONS

(a)

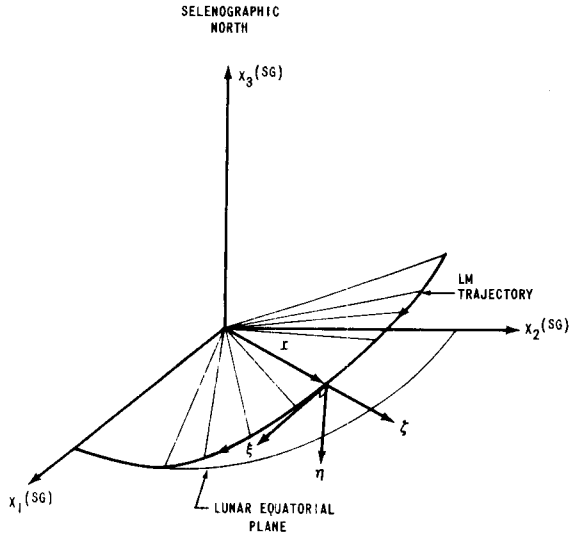

LOCAL HORIZONTAL - LOCAL VERTICAL REFERENCE SYSTEM (ξ, η, ζ)

(b)

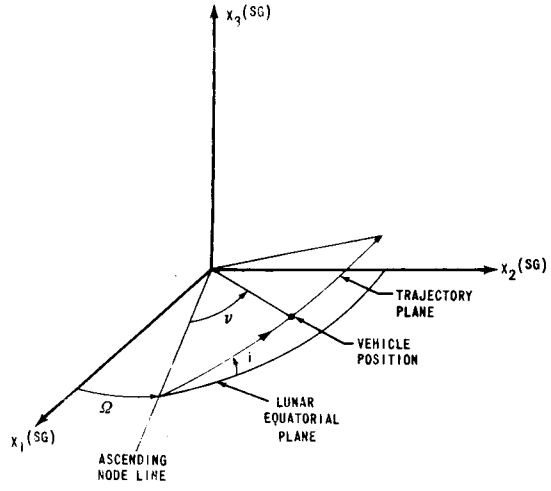

RIGHT ASCENSION - DECLINATION SYSTEM

(c)

COORDINATE SYSTEM DEFINITIONS

FIGURE (A-2)

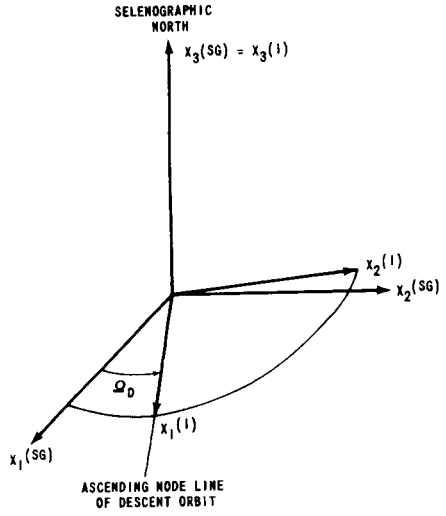

$$A = \begin{bmatrix} \cos(\Omega_D) & \sin(\Omega_D) & 0 \\ -\sin(\Omega_D) & \cos(\Omega_D) & 0 \\ 0 & 0 & 1 \end{bmatrix}$$

(a)

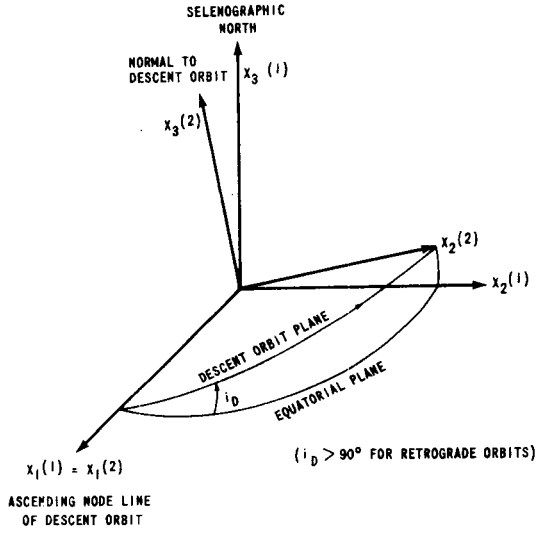

$$B = \begin{bmatrix} 1 & 0 & 0 \\ 0 & \cos(i_D) & \sin(i_D) \\ 0 & -\sin(i_D) & \cos(i_D) \end{bmatrix}$$

(b)

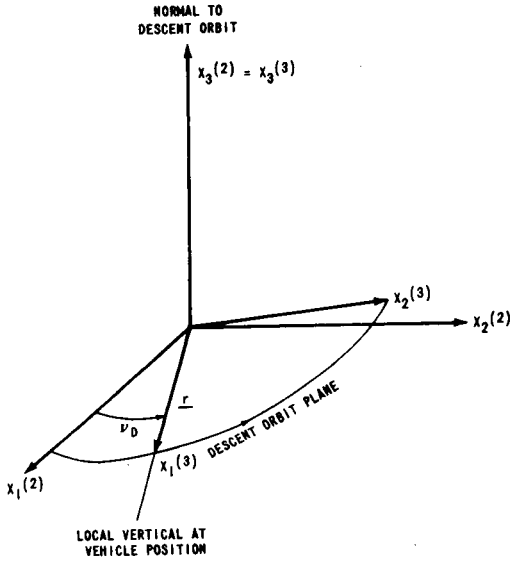

$$C = \begin{bmatrix} \cos(\nu_D) & \sin(\nu_D) & 0 \\ -\sin(\nu_D) & \cos(\nu_D) & 0 \\ 0 & 0 & 1 \end{bmatrix}$$

(c)

DESCENT ORBIT TRANSFORMATIONS

FIGURE (A-3)

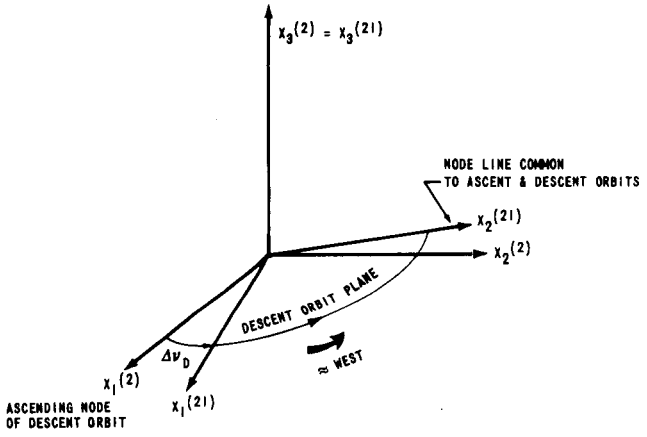

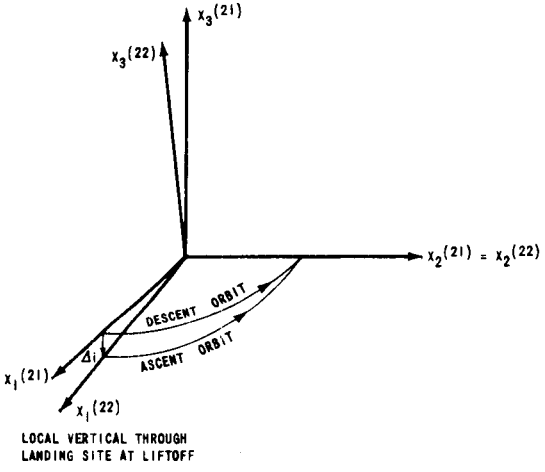

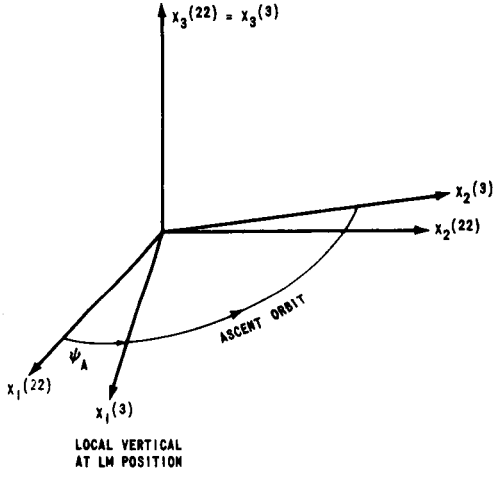

$$C_1 = \begin{bmatrix} \cos(\Delta\nu_D) & \sin(\Delta\nu_D) & 0 \\ -\sin(\Delta\nu_D) & \cos(\Delta\nu_D) & 0 \\ 0 & 0 & 1 \end{bmatrix} \qquad (a)$$

$$C_2 = \begin{bmatrix} \cos(\Delta i) & 0 & -\sin(\Delta i) \\ 0 & 1 & 0 \\ \sin(\Delta i) & 0 & \cos(\Delta i) \end{bmatrix} \qquad (b)$$

$$C_3 = \begin{bmatrix} \cos(\psi_A) & \sin(\psi_A) & 0 \\ -\sin(\psi_A) & \cos(\psi_A) & 0 \\ 0 & 0 & 1 \end{bmatrix} \qquad (c)$$

ASCENT ORBIT TRANSFORMATIONS

FIGURE (A-4)

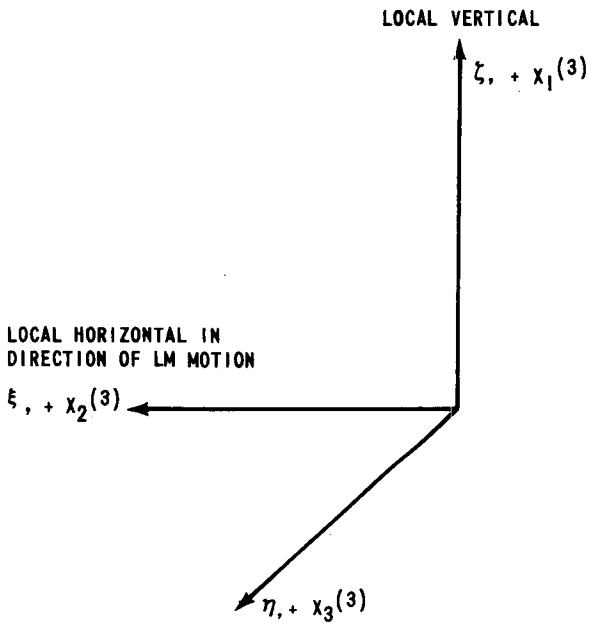

$$\xi = + X_2^{(3)})$$
$$\eta = + X_3^{(3)}$$
$$\zeta = + X_1^{(3)}$$

$$D = \begin{bmatrix} 0 & 1 & 0 \\ 0 & 0 & 1 \\ 1 & 0 & 0 \end{bmatrix}$$

LOCAL HORIZONTAL SYSTEM

(b)

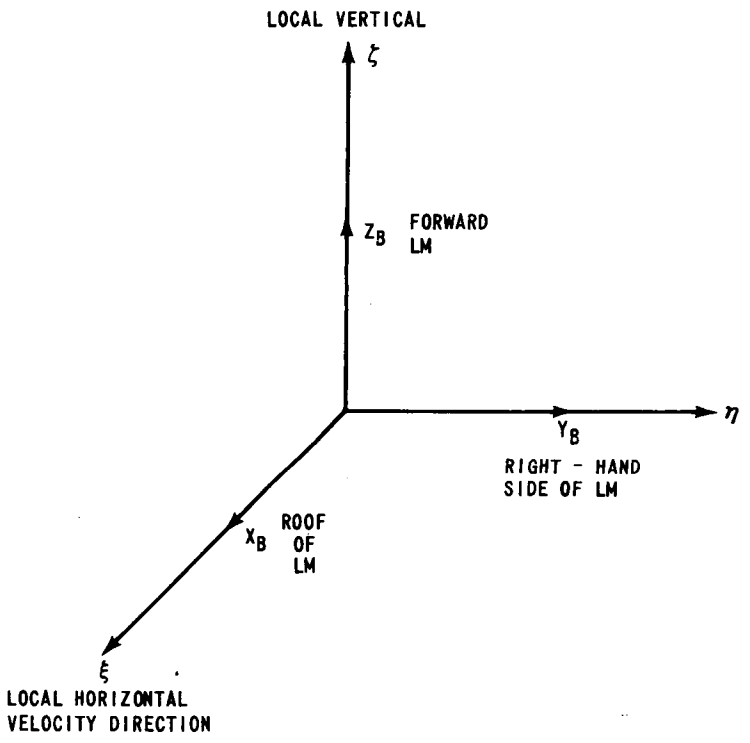

LM INITIAL ATTITUDE

(a)

FIGURE (A-5)

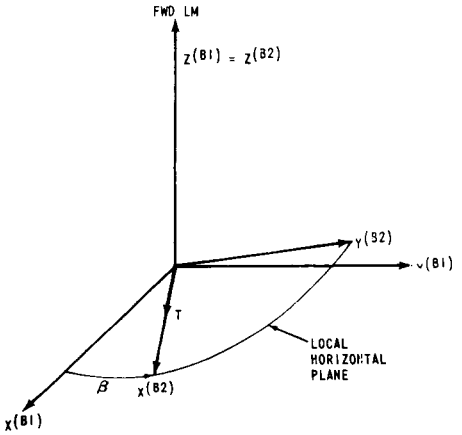

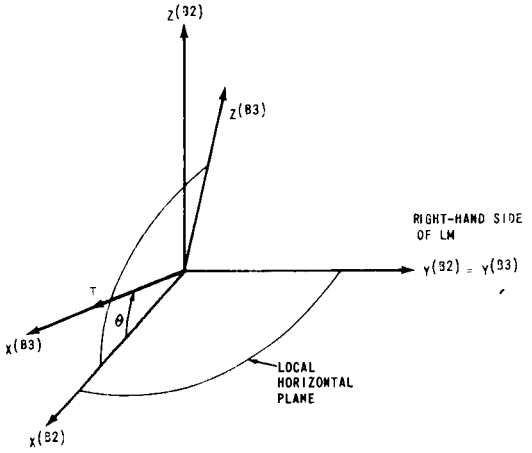

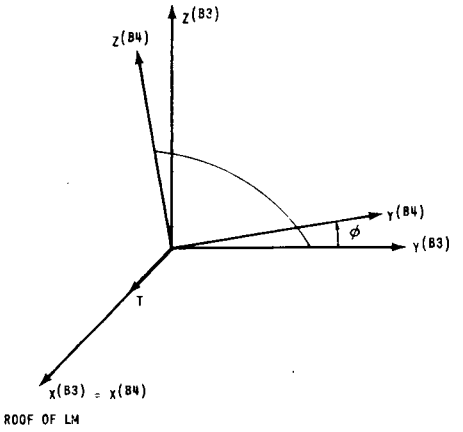

$$E = \begin{bmatrix} \cos\beta & \sin\beta & 0 \\ -\sin\beta & \cos\beta & 0 \\ 0 & 0 & 1 \end{bmatrix}$$

(a)

$$F = \begin{bmatrix} \cos\theta & 0 & \sin\theta \\ 0 & 1 & 0 \\ -\sin\theta & 0 & \cos\theta \end{bmatrix}$$

(b)

$$G = \begin{bmatrix} 1 & 0 & 0 \\ 0 & \cos\phi & \sin\phi \\ 0 & -\sin\phi & \cos\phi \end{bmatrix}$$

(c)

LM THRUST ATTITUDE TRANSFORMATIONS

FIGURE (A-6)

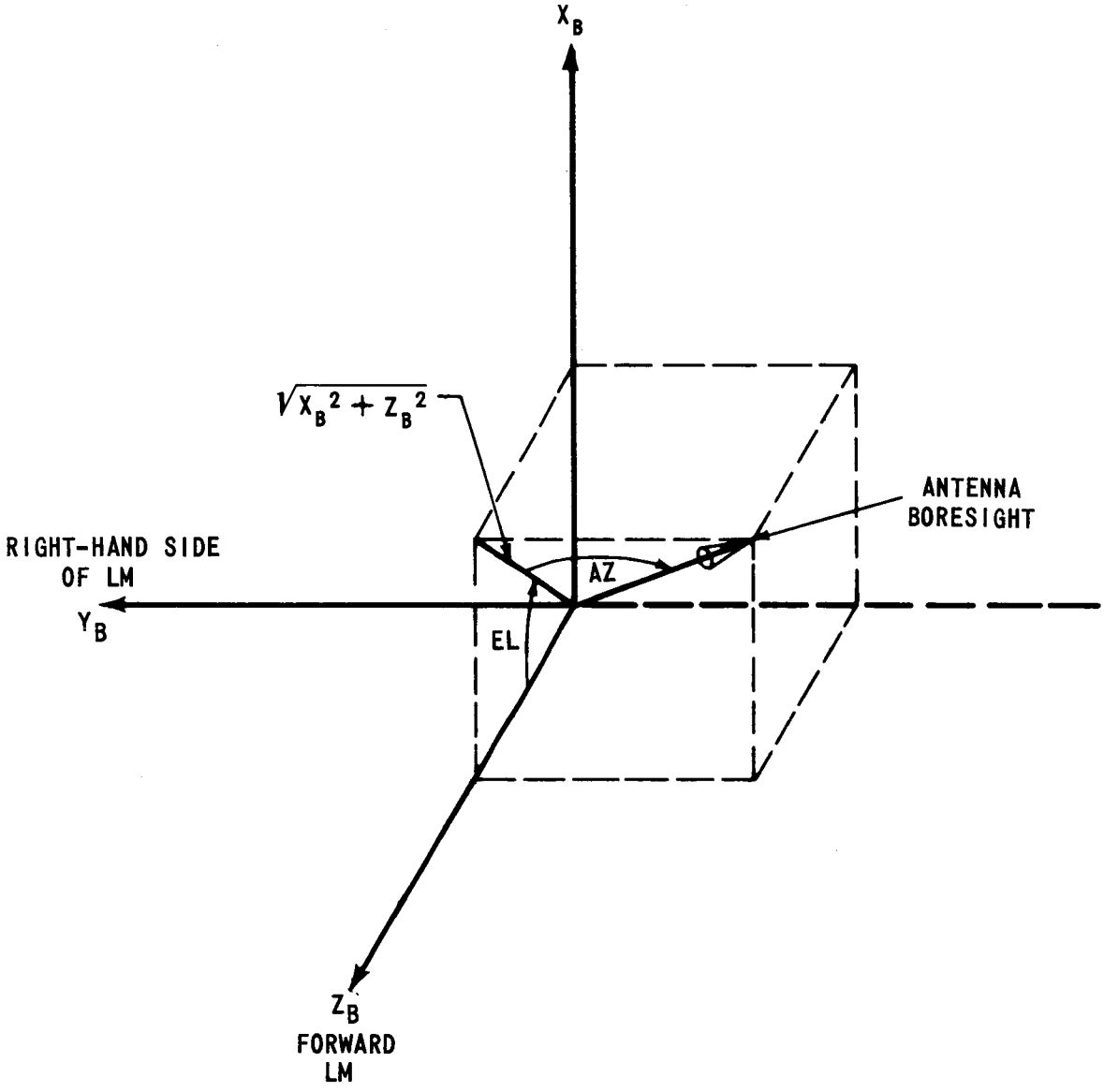

$$EL = TAN^{-1} \left(\frac{X_B}{Z_B}\right)$$

$$AZ = TAN^{-1} \left[\frac{Y_B}{\sqrt{X_B^2 + Z_B^2}}\right]$$

TRANSFORMATION TO ANTENNA ANGLES

FIGURE (A-7)

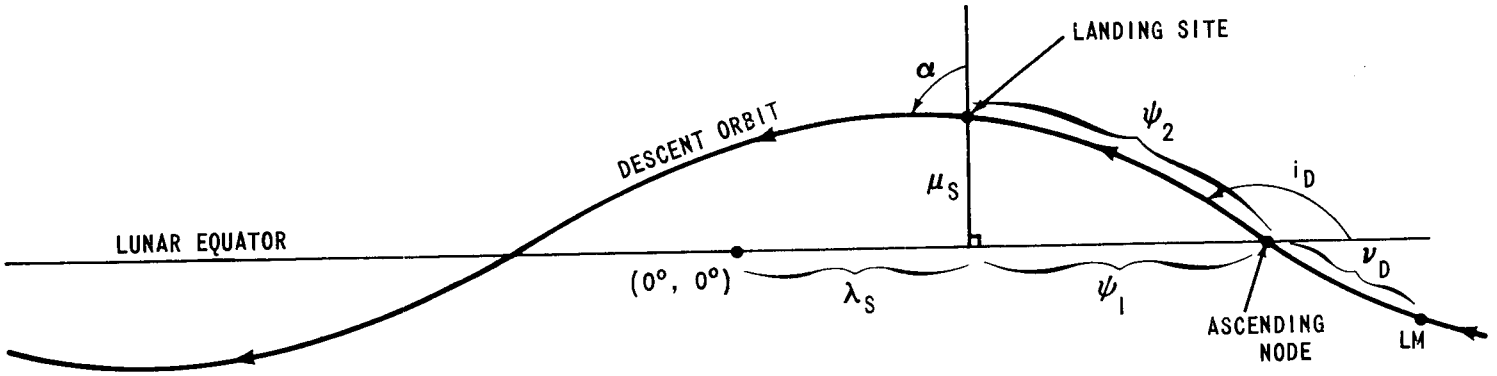

LUNAR ORBIT TRACK FOR: $\alpha > 270°$, $\mu_S > 0°$, $\lambda_S > 0°$

FIGURE (B-1)

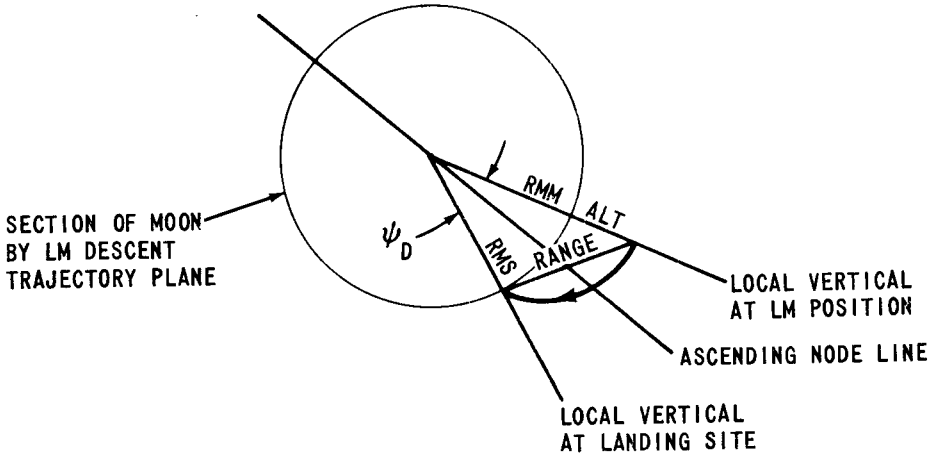

DESCENT RANGE ANGLE

FIGURE (B-2)

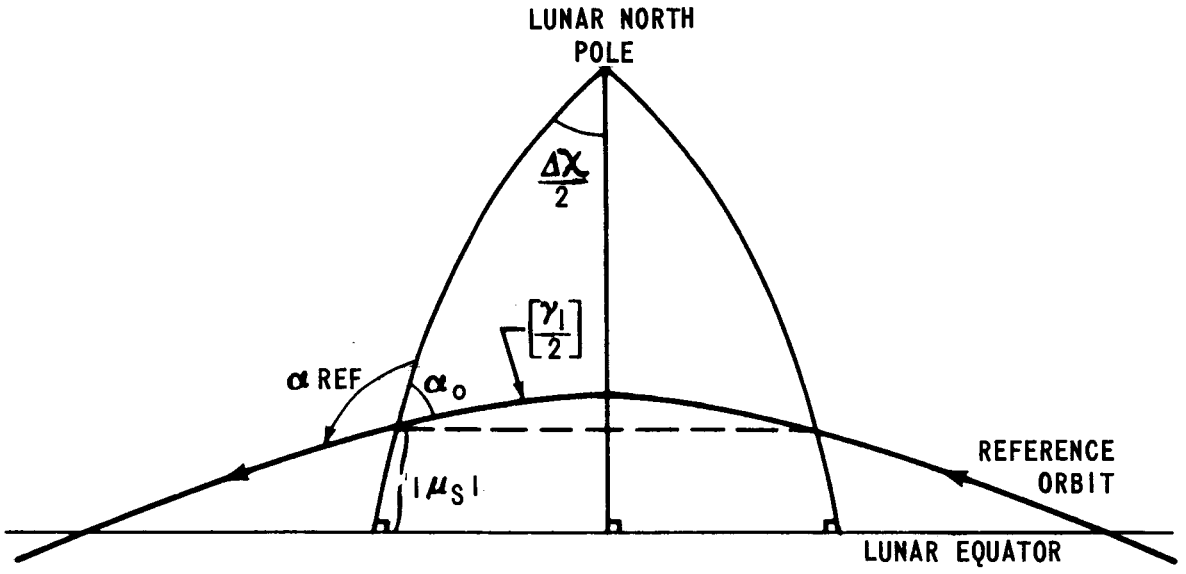

REFERENCE ORBIT GEOMETRY

FIGURE (B-3)

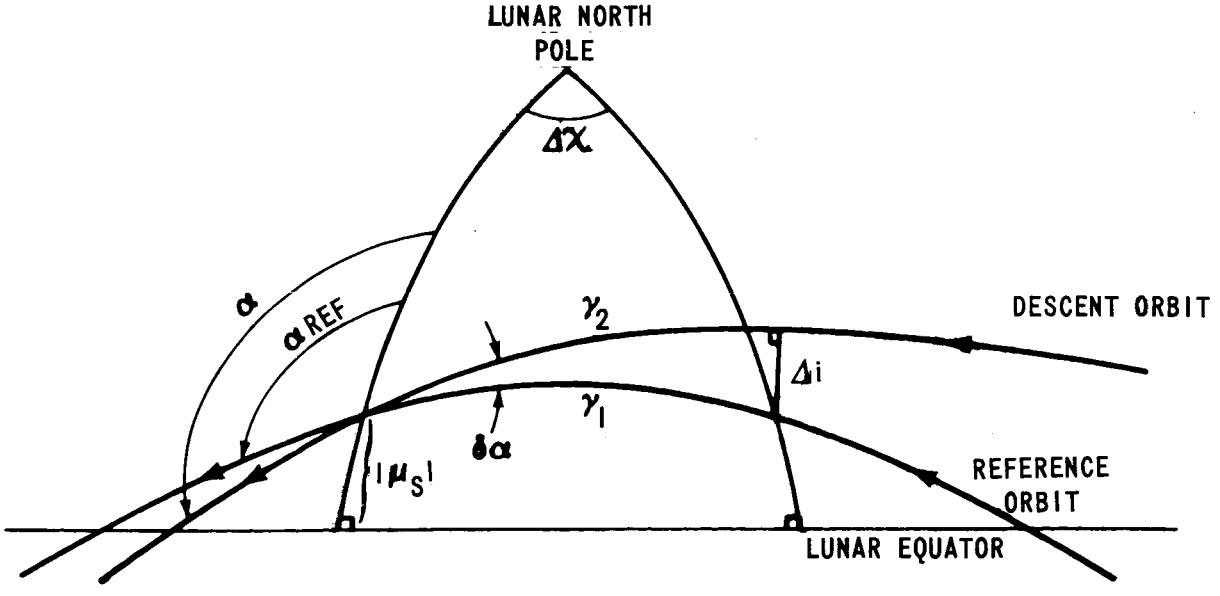

DESCENT ORBIT GEOMETRY

FIGURE (B-4)

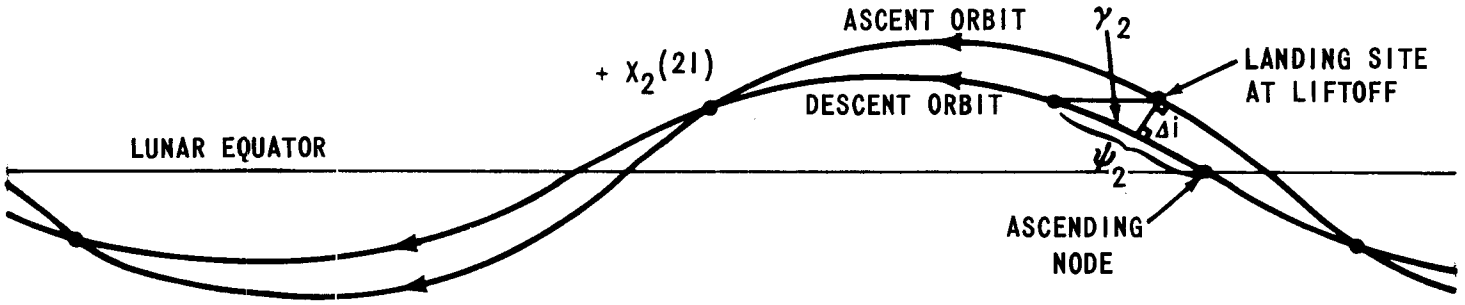

DESCENT AND ASCENT ORBIT TRACKS

FIGURE (B-5)

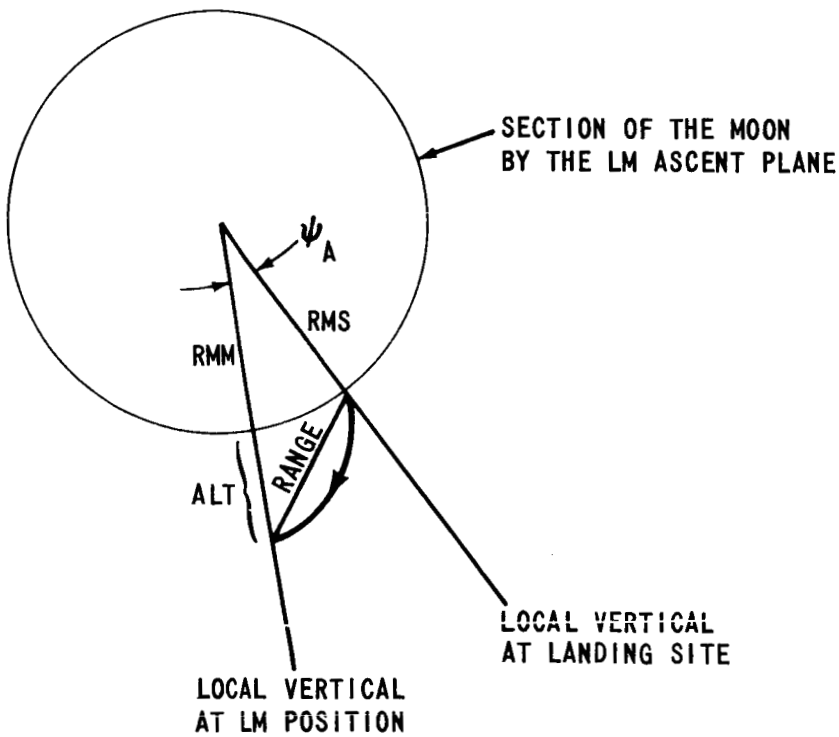

ASCENT RANGE ANGLE

FIGURE (B-6)

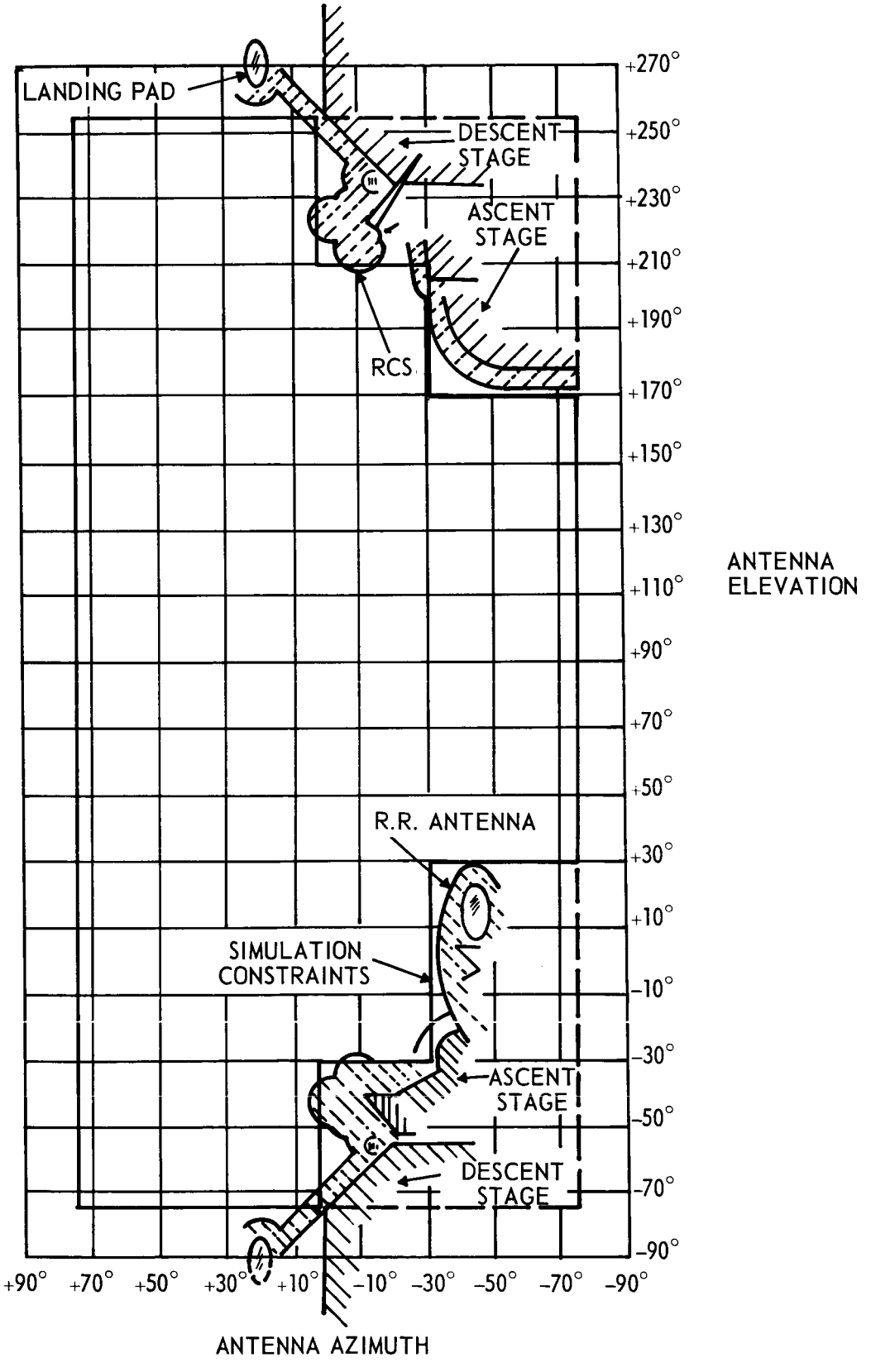

S-BAND STEERABLE ANTENNA COVERAGE

FIGURE (C-1)

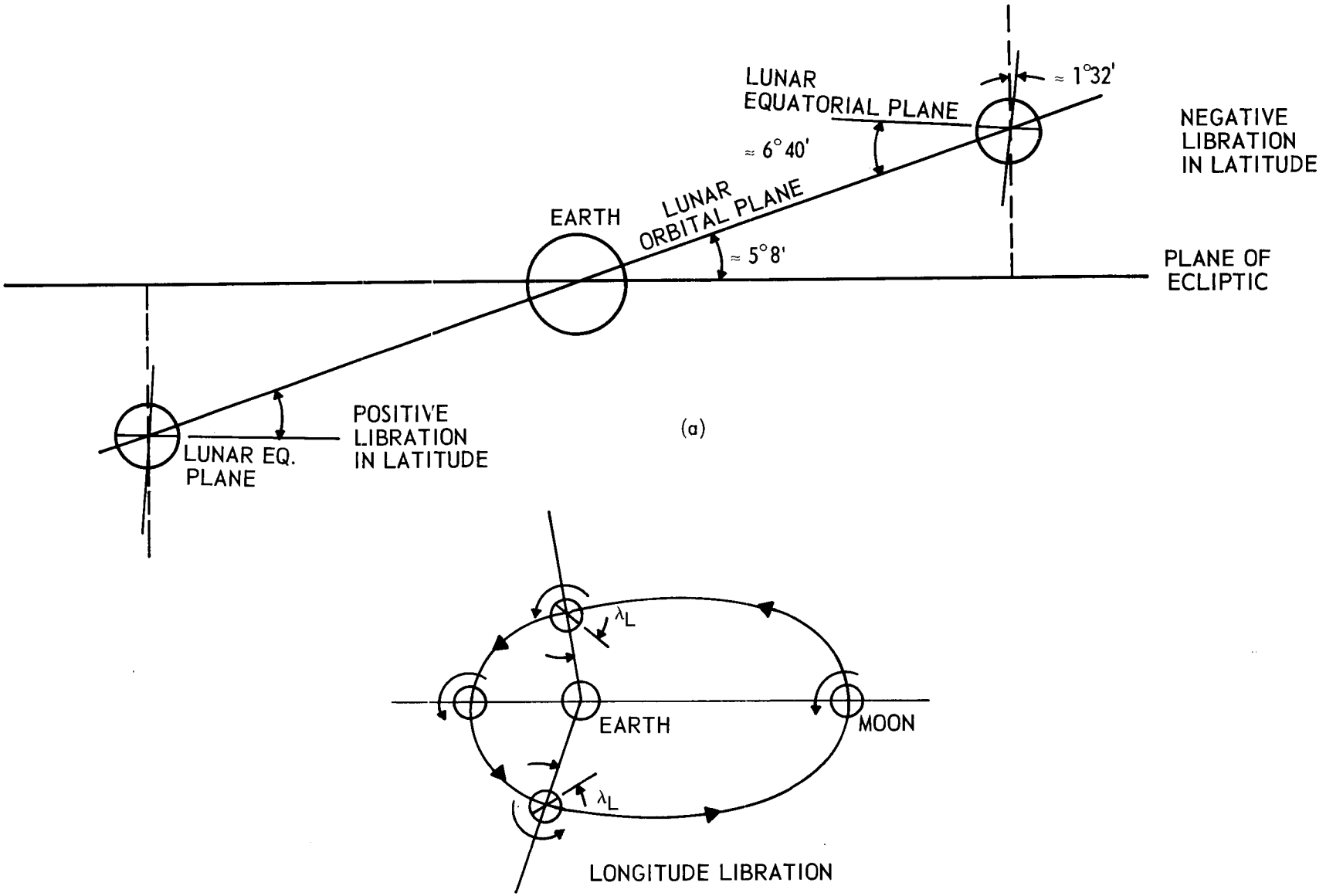

LUNAR OPTICAL LIBRATIONS

FIGURE (D-1)

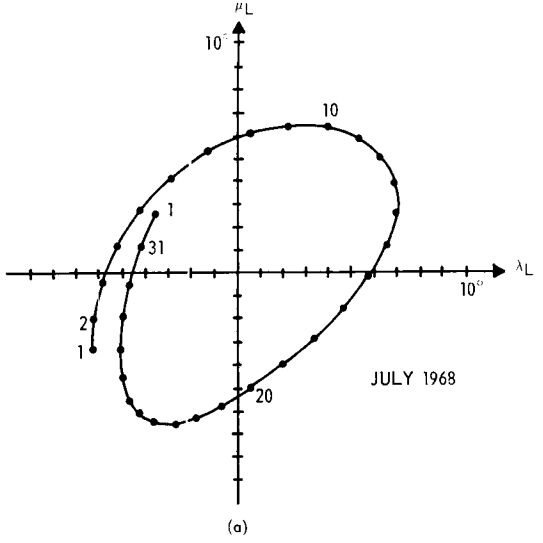

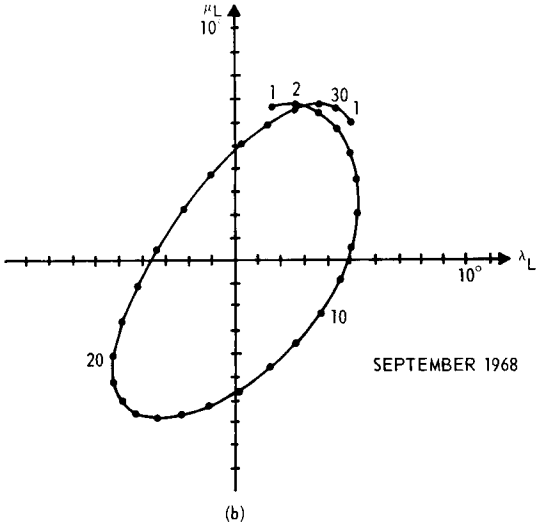

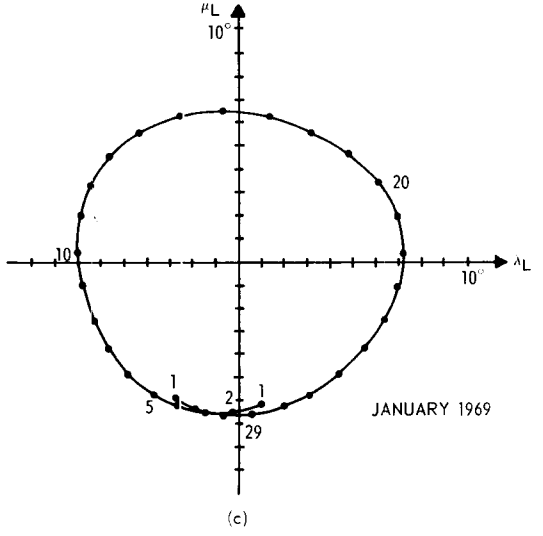

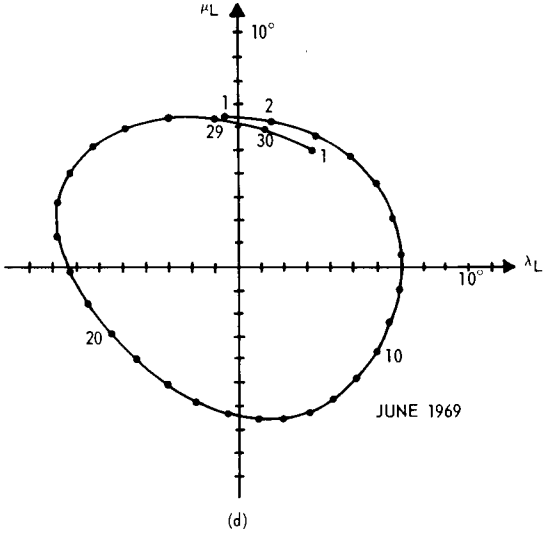

LUNAR LIBRATION LOCI

FIGURE (D-2)